From sperm selection to embryo development:

New insights into key assisted reproductive technologies in the horse

Muhammad Umair

2023

Thesis layout and cover design: M. Umair
ISNB: 978-94-6483-375-1
DOI: htttps://doi.org/10.33540/1924

From sperm selection to embryo development:

New insights into key assisted reproductive technologies in the horse

Van spermaselectie tot embryo-ontwikkeling: Nieuwe inzichten in geassisteerde voortplantings-technologieën bij het paard
(met een samenvatting in het Nederlands)

Proefschrift

ter verkrijging van de graad van doctor aan de
Universiteit Utrecht
op gezag van de
rector magnificus, prof.dr. H.R.B.M. Kummeling,
ingevolge het besluit van het college voor promoties
in het openbaar te verdedigen op

woensdag 27 september 2023 des ochtends te 10.15 uur

door

Muhammad Umair

geboren op 14 augustus 1990
te Muzaffargarh, Pakistan

Promotor:
Prof. dr. T.A.E. Stout

Copromotoren:
Dr. A.N.J. Claes
Dr. M. de Ruijter - Villani

Dit proefschrift werd (mede) mogelijk gemaakt met financiële steun van The Punjab Educational Endowment Fund (PEEF), Punjab, Pakistan.

Contents

Chapter 1

General introduction

The range of assisted reproductive technologies (ARTs) available to the horse breeding industry has expanded markedly in recent years. Artificial insemination (AI), embryo transfer (ET) and *in vitro* embryo production (IVEP) are all now available to many branches of the breeding industry. Nevertheless, optimization of the newer ARTs is required to meet the increasing demands of horse owners. AI is still the most widely used ART in equine breeding programs, having largely replaced natural mating in sports horses in Western Europe during the 1980-90s. In the Netherlands, since the early 90s, over 90% of all Warmblood mares bred annually are artificially inseminated, compared to <5% in the late 1970s [1]. The many benefits of AI over natural mating explain this rapid increase over 20 years, these include; reducing the risk of transmission of bacterial (e.g. *Taylorella equigenitalis*, the contagious equine metritis organism [2]) or viral (e.g. equine viral arteritis) venereal diseases by preventing genital contact of the breeding stallion with mares, increased selection for genetically superior stallions by insemination of multiple (5-10) mares with a single ejaculate, and the relative ease of (international) exchange of genetic material by transport of semen rather than live animals. AI also prevents transmission of diseases passed via animal-to-animal contact, for example, *Streptococcus equi equi* (the bacterium causing 'strangles') or equine herpes virus 1 [3], and provides the opportunity to monitor semen quality by examining a sample of each ejaculate using light microscopy and other laboratory techniques [4]. Equine AI can be performed with fresh, cooled-stored, and frozen semen. Fresh semen can only be used to inseminate mares at the same stud farm or within a short geographical distance, since the semen cannot be transported or stored for prolonged periods without compromising the fertilizing ability of the spermatozoa, particularly if the bulk of the seminal plasma is not removed. To allow longer storage in the liquid state, semen can be cooled to 5°C, preferably after removal of most of the seminal plasma by centrifugation (600 g for 15-20 minutes), and diluting in a semen extender. Lowering the temperature slows down sperm metabolism and prevents the growth of microbes. Cooled semen is commonly used within 24 to 48 h of collection without marked adverse effects on semen quality or fertility. Although spermatozoa gradually lose fertilizing capacity during prolonged storage, semen can be stored for longer durations (up to 96 h) at 5 °C. If this is insufficient for the required transport, cryopreservation can be used to store stallion semen indefinitely. This enables the transport of a stallion's genetic material worldwide, allows semen collection and AI to be temporally independent, and enables the banking of valuable genetic material in case of the death of a valuable stallion. Import and export of cryopreserved (frozen) semen can be a useful alternative to transport of live animals to promote genetic diversity in a previously restricted horse

population.

In the same way that AI can be used to increase the selection intensity on the male side of a breeding program, ET can be used to increase the contribution of genetically superior mares. Embryos can be recovered by lavaging the uterus of valuable donor mares 6-9 days after ovulation, and transferred non-surgically to a synchronized recipient mare. Using ET, multiple foals per year can be obtained from genetically valuable mares. *In vivo* derived (IVD) embryos can be transferred fresh, chilled for up to 24 h or cryopreserved for long term storage and transport. In 2020, more than 26,000 IVD embryos were recorded to have been transferred fresh or after cooled transport, compared to only 96 after cryopreservation (IETS annual report 2020, [5]). While these figures are probably gross underestimates of the total ET market, the marked difference between the numbers of fresh and frozen IVD embryos transferred shows that the potential of embryo cryopreservation has not been fully exploited despite several potential benefits, such as; more efficient use of recipient mares, collecting embryos out of the physiological breeding season, easier international transport and obtaining embryos from competing mares in breaks from heavy training.

In vitro embryo production (IVEP) is performed by conventional *in vitro* fertilization (IVF) or intracytoplasmic sperm injection (ICSI) in a number of species. In this respect, protocols for conventional IVF are well established for the mouse, cow, pig, and man. However, IVF has proven extremely challenging in horses and, despite many attempts, until very recently only two foals were reported to have been produced by IVF, in 1991 [6] and 1992 [7]. Failure of conventional IVF in the horse is thought to be due to the inability to adequately capacitate stallion sperm so that they can bind to and then penetrate the zona pellucida of the oocyte [6,8]. Recently, Felix et al [9] were successful in achieving equine IVF by incubating raw or diluted semen in a PHE (penicillamine, hypo-taurine and epinephrine) based fertilization medium for a prolonged period (22 h) before co-incubation with oocytes. However, at present this new equine IVF procedure only appears to work with freshly collected semen, and needs optimization for clinical and commercial purposes, which are more likely to use cooled or cryopreserved semen. As a result of the poor success of conventional IVF, ICSI is currently the method of choice for fertilizing horse oocytes recovered by transvaginal ultrasound guided follicle aspiration, or by manual scraping of ovarian follicles post-mortem. Cryopreserved semen is most commonly used for ICSI because it allows greater flexibility of planning for the ICSI procedure and uses only a small portion of the semen straw; the rest of the straw can be stored such that there is no need for semen to be transported for every ICSI procedure,

frozen semen can also be used from desirable stallions that are no longer alive.

IVP equine embryos are classified as a blastocyst once they begin to expand and a trophoblast layer starts to become visible [10]. The time it takes IVP embryos to reach the blastocyst stage varies from 6 to 12 days or more post-ICSI [11]. Since slow development is an indicator of poor quality, only day 6-9 IVP embryos are usually used commercially [12], although later embryos may be transferred if the mare is already dead or does not produce many embryos. Blastocyst formation runs in parallel with the first segregation event among the previously totipotent blastomeres, differentiation of trophectoderm cells from the pluripotent Inner Cell Mass (ICM) cells. This is closely followed by a second segregation of the ICM cells into primitive endoderm and epiblast, such that an expanded blastocyst is composed of three distinct cell types. Little is known about how and whether cell lineage segregation differs between *in vivo* and *in vitro* equine embryos. Studying cell lineage segregation in the *in vitro* equine embryo may help to explain their lower developmental competence and help to optimize *in vitro* embryo culture protocols.

Sperm selection

In the horse breeding industry, sub-fertile stallions are often maintained in a breeding program because stallion selection is based primarily on pedigree and athletic performance rather than fertility [13]. In cases of poor sperm quality, sperm selection techniques can be useful for improving the breeding performance of stallions with marginal fertility. Sperm selection techniques (Figure 1) described include swim up (SU, Figure 1 A), density gradient centrifugation (DGC, Figure 1 B), glass wool filtration (GWF, , Figure 1 C), microfluidic selection (MF, Figure 1 D), fluorescence activated cell sorting (FACS, Figure 1 E), magnetic activated cell sorting (MACS, Figure 1 F) and zeta potential selection (ZPS, Figure 1 G) [14].

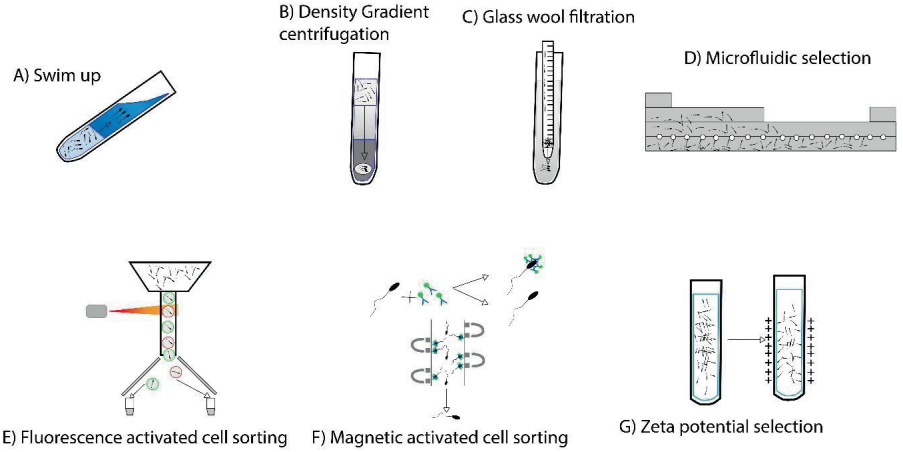

Figure 1. Sperm selection techniques. *A) Swim up, B) Density gradient centrifugation, C) Glass wool filtration, D) Microfluidic selection, E) Fluorescence activated cell sorting, F) Magnetic activated cell sorting, G) Zeta potential selection. Adapted from [14].*

DGC is most commonly used to process the semen of sub-fertile stallions because of the ease of use and low cost. Similarly, SU is commonly used in an ICSI/IVF situation because it is easy, cheap and only a few sperm are required for a fertilization attempt. Limited data is available on the use of MF (based on rheo-, chemo-, and thermotactic behaviours of viable spermatozoa) in equine ARTs, and the technology is costly compared to SU and DGC. In addition, although MF like SU preferentially selects motile, morphologically normal sperm cells with intact DNA, it can only be used in an IVEP situation due to the low number of sperm recovered. In contrast, DGC can be used both for AI and IVEP because it can readily be scaled up to process and yield larger sperm numbers. Single- or double-layer DGC (continuous or discontinuous DGC, respectively) can be used to process a semen sample [15–17]. Although the use of Percoll for DGC is now prohibited in human clinics due to the endotoxic effects of the Polyvinylpyrrolidone (PVP)-coated silica particles (associated with cytoplasmic fragmentation and reduced embryo development) [18–22], it is still the most common colloid used in many animal breeding industries, including equine ART. EquiPure ™ is a Percoll substitute used in equine reproduction that has similar sperm selection principles to Percoll and aims to enrich the population of motile, morphologically normal spermatozoa with intact DNA by separating spermatozoa of similar density into a pellet. However, in the pellet, the spermatozoa are tightly packed and at risk of coming into contact with reactive oxygen species (ROS), and debris. Moreover, high centrifugal forces have been reported to increase ROS generation in spermatozoa, where ROS are known to induce DNA damage, a non-compensable defect that can compromise embryo quality, blastocyst rates, implantation rates and pregnancy outcomes. Therefore, DGC methods have been modified to avoid collection of the desired sperm fraction in the pellet and to minimize the generation of ROS. Opti-prep ™ (60 % Iodixanol, density) is another colloid that was originally developed as an X-ray contrast medium and has been thoroughly evaluated by clinical trials for safe *in vivo* use. It was initially used as a dense cushion to prevent spermatozoa forming a tightly packed pellet in the bottom of the centrifuge tube. A double layer Opti-prep ™ DGC was also used to try to select the viable sperm population from stallion ejaculates. However, low sperm recovery (33%) from the ejaculates of stallions with normal semen quality parameters was an issue, which was proposed to be due to the density of the Opti-prep ™ solutions used as the top and bottom layers [23]. For similar reasons, a modified DGC method was developed for bull semen, in which the raw

bull semen was first diluted with 60% iodixanol that was then layered between a top and bottom layer of Opti-prep ™; this resulted in three sperm populations with distinct differences in quality [24]. This particular approach to Opti-prep ™ separation has not been described for stallion semen, and it is not known whether processing stallion semen with Opti-prep ™ at high centrifugal forces (1000 g, 20 minutes) would result in generation of ROS. Sperm selection techniques are often used to process semen samples of sub-fertile stallions prior to semen storage or artificial insemination and, in these situations, minimal loss of good quality spermatozoa is an important consideration.

Semen storage and sperm metabolism

In horse breeding, semen storage for limited (up to 72 h at 5 °C, standard storage temperature for stallion spermatozoa) or for indefinite periods (cryopreservation) is performed to facilitate transport of semen. Indeed, around 90% of Standardbred and Hanoverian mares are inseminated with chilled/cooled or cryopreserved semen [1,25]. Cooling of semen reduces the sperm metabolism by up to 93% [26] as extended spermatozoa (diluted in a semen extender) are cooled down to 4-5 °C [27,28], while sperm metabolism is reduced to extremely low levels after cryopreservation [29]. Equine spermatozoa can produce ATP through oxidative phosphorylation (OXPHOS) as well as through the glycolytic pathway. Although OXPHOS is more efficient than glycolysis for ATP generation, spermatozoa from man and rodents rely on glycolysis for ATP production [30]. By contrast, stallion spermatozoa generate ATP primarily via the OXPHOS [31,32] pathway, which occurs in the mitochondria. This reliance of stallion spermatozoa on OXPHOS for energy production leads to the production of reactive oxygen species (ROS) as a by-product [33] and, following the exhaustion of the antioxidant reserves within the sperm cell, ROS (Superoxide and hydrogen peroxide; reduced form of superoxide) accumulation results in an increased production of metabolic by-products, and accumulation of ROS together with cytotoxic lipid aldehydes (acrolein, 4-hydroxynonenal and malondialdehyde) which can induce extensive lipid peroxidation, DNA damage and thereby accelerated cell death [34]. On the other hand, ROS play an important role in sperm capacitation [35] such that completely blocking ROS generation is undesirable.

Semen storage and sperm capacitation

To fertilize an oocyte, a spermatozoon must undergo a physiological maturation process (capacitation, Figure 2) in the female reproductive tract [36,37]. Spermatozoa have also been proposed to undergo capacitation-like changes (e.g. an increase in plasma membrane fluidity and a rise in the free intra-cellular Ca^{2+} concentration) as a result of semen processing and

storge (for example cryopreservation [38–41]). These capacitation like-changes would

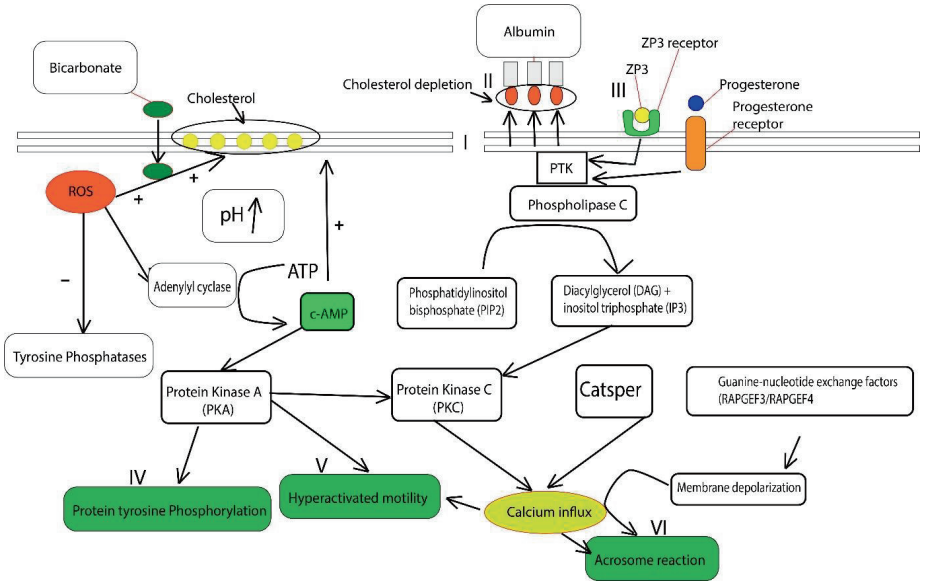

Figure 2. Mechanisms that contribute to sperm capacitation, with a focus on the horse. *The following changes take place in spermatozoa during capacitation: (I) an increase in membrane fluidity; (II) cholesterol depletion; (III) accumulation of lipid raft receptors; (IV) an increase in protein tyrosine phosphorylation; (V) hyperactivated motility; and (VI) the acrosome reaction. PTK stands for protein tyrosine kinase; ROS stands for reactive oxygen species; ZP3-receptor stands for ZP protein 3-receptor;+ stands for activation; - stands for inhibition. Adapted from [187].*

impact sperm function and, therefore, reduce fertilizing capacity *in vivo* [42]. Nevertheless, it is not yet known whether or to what extent capacitation like-changes or aging-related changes occur during prolonged cooled storage (up to 96 h) of stallion spermatozoa at 5 °C.

During capacitation, the spermatozoon undergoes a series of changes that include an increase in plasma membrane fluidity and depletion of cholesterol from the plasma membrane, which allows formation of so-called ‘lipid rafts’ in which specific proteins and receptors aggregate; capacitation results in the sperm acquiring hyperactivated motility and the ability to undergo the acrosome reaction (Figure 2).

Changes in the plasma membrane

A spermatozoon has a highly polarized morphology with a heterogenic surface that can be divided into four surface membrane domains; the apical ridge, and the pre-equatorial, equatorial and post-equatorial regions, respectively. These domains play specific roles in fertilization; the apical ridge contributes to zona pellucida binding (rabbit [43]); both the apical ridge and the pre-equatorial region participate in the acrosome reaction, and the equatorial surface region

first initiates oolemma binding before participating in fertilization fusion. The area of the sperm head where these maturational events occur, i.e. the sperm plasma membrane including the lipid rafts (microdomains), covers the acrosomal cap and plays a key role in the dynamics of sperm capacitation [44].

Depletion of cholesterol

One of the essential steps in sperm capacitation, is phospholipid redistribution in the lipid bilayer over the sperm head surface. Bicarbonate (HCO_3^-), soluble adenylyl cyclase and cAMP (Cyclic adenosine 3′,5′-monophosphate) facilitate an increase in plasma membrane fluidity (detectable via an increase in merocyanine 540 uptake, [45,46]) leading to a redistribution of cholesterol from the equatorial region to the apical part of the sperm plasma membrane, accompanied by retrograde movement of seminolipids (pig) [47,48].

In vitro, the extraction of cholesterol from the sperm membrane is achieved by delivery of free cholesterol to the hydrophobic pocket of albumin molecules by active cholesterol transporters, and is aided by oxidation of membrane sterols [49,50]. In bull spermatozoa, ROS production is a key step in oxysterol formation [51], and the more hydrophilic nature of oxysterols compared to native cholesterol allows them to more easily move through the plasma membrane and bind to sterol-accepter molecules like albumin. The unique ability of albumin to scavenge hydrophilic oxidation products and facilitate cholesterol extraction makes it an important component of a sperm capacitating medium [52]. Nevertheless, standard capacitating conditions (i.e., media including Ca^{2+}, HCO^{3-} and bovine serum albumin) are insufficient to remove cholesterol from the stallion sperm plasma membrane. This apparent difference in the regulation of plasma membrane cholesterol depletion during stallion sperm capacitation suggests a species-specific difference.

Lipid raft aggregation

Following the increase in membrane fluidity and cholesterol depletion, porcine spermatozoa undergo redistribution of the laterally segregated molecules, and aggregation of lipid-ordered microdomains at the apical ridge area of the sperm head [52]. A capacitation-dependent change is shown by the proteins and lipids that make up these microdomains, and is typified by higher proportions of cholesterol, sphingomyelin, gangliosides and phospholipids with saturated long- chain acyl groups and lipid-modified proteins like GPI-anchored proteins [53,54]. Furthermore, lipid raft specific markers (caveolin-1 and flotillin-1, [54]) accumulate, together with functional zona pellucida-binding protein complexes, in these microdomains. In man, the microdomains contain proteins (angiotensin-converting enzyme and protein disulphide

isomerase A6) capable of interacting with heat shock protein A2, which in turn plays a key role in sperm surface remodeling during capacitation and oocyte recognition [55]. In pigs, primary binding between capacitated spermatozoa and the zona pellucida is regulated by key proteins including isoforms of AQN-3 (spermadhesin), P47 (porcine homologue of SED-1), fertilin β and peroxiredoxin 5 [56]. Nevertheless, it has not been confirmed whether these proteins are located in the microdomains.

Hyperactivated motility

To understand the phenomenon of hyperactivated motility, understanding of normal sperm motility is important. Sperm motility is influenced by cytoplasmic pH, and there is a slight variation in pH requirement among species for maximizing the percentage of motile sperm; de-membranated bull sperm (pH 7.0 to 8.1, [57]), man (pH 7.8, [58]) and ram (pH 7.5 to 8.0, [59]). In comparison, stallion spermatozoa show maximum motility at pH 7.0 [60]. At the appropriate cytoplasmic pH, symmetrical flagellar movement is achieved, resulting in progressive motility. This involves the activation of dynein ATPases on phosphorylated dynein molecules, and their interaction with Ca^{2+} leads to the sliding of the adjacent outer axonemal doublet microtubules [61], with the sperm tail bending as a result of the force generated after the doublets slide along one another [62]. Moreover, an asynchronous phosphorylation and dephosphorylation of dynein arms along the entire axonemal length produces a flagellar waveform [63]. Mammalian sperm motility is initiated and maintained through ATP, Ca^{2+} and HCO^{3-} driven cAMP-dependent phosphorylation of the flagellar proteins [64,65,57]. Both Ca^{2+} and HCO^{3-} directly regulate soluble adenylyl cyclase, resulting in cAMP generation and protein kinase A activation (Figure 2) [66,67]. The serine/threonine kinase, protein kinase A, is an important downstream target of cAMP in the sperm flagellum [68]; protein kinase A is activated by phosphorylation and triggers downstream phosphorylation of tyrosine kinase which has targets located primarily in the sperm tail [69,70]. On the other hand, calcineurin (calmodulin-dependent protein serine/threonine phosphatase) induces the dephosphorylation of dynein, which is essential to balance the cAMP-driven serine/threonine kinases in the sperm tail. The sperm motility status is dictated by the resulting net phosphorylation [71]. Spermatozoa are non-motile when serine/threonine phosphatase is active, while increased motility correlates with the activity of serine/threonine kinase [72,73].

After attaining hyperactive motility, spermatozoa detach from their binding site on the oviductal epithelium and leave the oviductal ‘sperm reservoir’ [74]. Next, the spermatozoa migrate through the viscous luminal fluids of the oviduct to penetrate first the cumulus matrix

and then the zona pellucida of a mature oocyte to fuse with the oolemma [75,76]. Hyperactive spermatozoa of many species show a highly asymmetrical and high-amplitude flagellar beating pattern (whip-like motion of the sperm tail), manifesting as a circular, figure of eight or zigzag movement pattern *in vitro* [77,78]. Cytosolic influx of Ca^{2+} into the sperm tail is associated with the onset and maintenance of hyperactivated motility [79,80]. An increase in the intra-cellular Ca^{2+} concentration from ~50nM to 400nM changed progressive sperm movement into hyperactive motility in de-membranated bull spermatozoa [57]. On the other hand, an inverse relationship was observed between hyperactive motility and cytoplasmic Ca^{2+} concentration in stallion sperm cells [60]. Loux et al [81] showed that de-membranated stallion spermatozoa did not acquire hyperactive motility by increasing the external Ca^{2+} concentration at any pH. However, intact sperm cells showed hyperactive motility and an increase in cytoplasmic Ca^{2+} in response to cytoplasmic alkalinization (intracellular rise from pH 7.1 to 7.3-7.4). *In vitro*, hyperactive motility can be induced and retained for several hours in mouse spermatozoa by exposure to Ca^{2+} ionophores (A23187 or ionomycin) [82,83]. Conversely, stallion spermatozoa become immotile and lose membrane integrity within 1h of exposure to Ca^{2+} ionophore [84,85]. In contrast to other mammalian species, stallion spermatozoa depend on mitochondrial ATP, which may underlie the adverse effects of Ca^{2+} ionophores on motility and membrane integrity. In this respect, mitochondrial failure and initiation of cell death can result from an excessive Ca^{2+} concentration in the mitochondria [86]. Furthermore, inhibition of mitochondrial ATPase activity by Ca^{2+} ionophores uncouples oxidative phosphorylation [87,88]. Since Ca^{2+} ionophores and other inhibitors which inhibit oxidative phosphorylation lead to a decrease in mitochondrial ATP generation (loss of sperm motility and membrane integrity), it is challenging to design a capacitation induction protocol for successful equine *in vitro* fertilization, where sperm motility and membrane integrity need to be maintained for hours. Although an intra-cellular Ca^{2+} rise and initiation of asymmetrical flagellar beating can be triggered in mouse spermatozoa using pharmacological agents (caffeine [89], thimerosal [89,90] and thapsigagrin [89,91]), it is not yet known whether similar molecules can reliably affect cytoplasmic Ca^{2+} concentration and induce hyperactive motility in stallion spermatozoa.

Acrosome reaction

During mammalian fertilization, the Ca^{2+}-dependent release of acrosomal contents is essential because it enables the sperm cell to penetrate the acellular glycoprotein coat (zona pellucida) of the mature oocyte to enable fusion with the oolemma [77]. *In vivo*, the acrosome reaction

occurs at the site of fertilization, and involves a multipoint membrane fusion event between the sperm plasma membrane and the outer acrosomal membrane [92], leading to the production of mixed vesicles consisting of both plasma membrane and outer acrosomal membrane. The remaining unfused acrosomal membrane segments, which include the outer acrosomal equatorial area and the sperm plasma membrane where they join the inner acrosomal membrane covering the apical part of the nucleus, function as the new sperm plasma membrane surface [93,94]. A hairpin-like structure in this re-designed outer sperm membrane is integral to oolemma binding leading to gamete fusion and subsequent oocyte activation [77]. In porcine spermatozoa, the fusion of the sperm plasma membrane and the outer acrosomal membrane is facilitated by soluble N-ethylmaleimide-SNARE protein interactions, via the formation of a trans ternary-soluble N-ethylmaleimide-sensitive factor attachment receptor protein during capacitation. Syntaxin 1B and VAMP 3 (plasma membrane), and SNAP 23 (outer acrosomal membrane) are the key factors involved in this process [95]. The conversion to *cis*-soluble N- ethylmaleimide-SNARE complexes requires the entry of Ca^{2+} (*in vivo* following ZP-binding; *in vitro* via exposure to Ca^{2+} ionophore) and is critical to acrosomal exocytosis and zona pellucida penetration [96]. In the mouse, zona pellucida glycoprotein 3 (ZP3, present on the mature oocyte) is one of the main triggers to the acrosome reaction in capacitated spermatozoa [77,97,98]. However, induction of the acrosome reaction and passage of spermatozoa through the ZP has also been reported following contact of murine sperm with the intercellular matrix of the cumulus cell complex [99,100]. While capacitated acrosome-intact spermatozoa initiate zona binding in most other mammals, including the horse [77], a low incidence of acrosome reaction was shown by stallion spermatozoa after 1 h of zona pellucida binding *in vitro* [42,101,102]. In horse spermatozoa, progesterone (present in cumulus cell secretions and follicular fluid) has been proposed to play a role in inducing the acrosome reaction (Figure 2) [103–105]. The progesterone-induced acrosome reaction was proposed to proceed in a protein kinase C and protein tyrosine kinase-dependent manner [106] (similar to the zona pellucida mediated acrosome reaction) rather than via protein kinase A [107]. In this respect, it has been shown that activation of sperm protein tyrosine kinase linked to phospholipase C generates diacylglycerol from phosphatidylinositol-biphosphate to stimulate protein kinase C (Figure 2). However, it is not yet known how the production of diacylglycerol leads to the acrosome reaction. On the other hand, *in vitro* induction of the acrosome reaction in stallion spermatozoa by HCO_3^- is supported by a protein kinase A, rather than protein tyrosine kinase and protein kinase C,

dependent pathway (Figure 2) [106], indicating that HCO_3^- and progesterone induce the acrosome reaction via distinct pathways. In short, factors shown to trigger acrosomal exocytosis *in vitro* (Ca^{2+} ionophore and HCO_3^-) may do so via non-physiological pathways [85].

Equine embryo cryopreservation

Cryopreserving equine embryos is useful in case of temporary unavailability or shortage of synchronized recipient mares. It also provides flexibility by enabling transfer of an embryo at a desired time of the year, irrespective of when the embryo was produced, and enables intercontinental shipping of embryos. Although early-stage equine embryos (day 6-7 morulae or early blastocysts) less than 300 µm in diameter (Figure 3 A) result in acceptable pregnancy rates after freezing and thawing [108], larger embryos (>300 µm, Figure 3 B) historically yielded pregnancy rates below 25%. Embryo size (specifically surface area to volume ratio) and the presence of the acellular blastocyst capsule around expanded equine embryos were thought to be the main reasons for their poor freezability (Figure 3 B) [109].

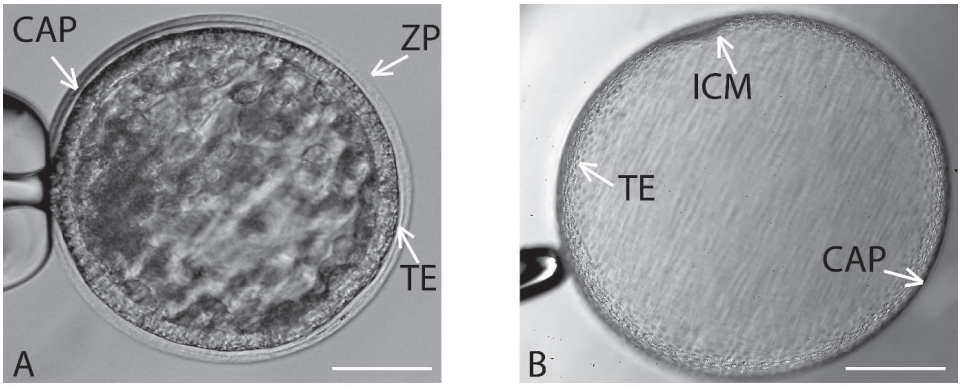

Figure 3. In vivo derived horse blastocysts. *A) <300 µm early blastocyst: small blastocoel cavity, thin zona pellucida (ZP) and capsule between trophectoderm and ZP, B) >550 µm expanded blastocyst: large blastocoel cavity, only the capsule is present around trophectoderm. ZP; Zona pellucida, CAP; Capsule, TE; Trophectoderm, ICM; Inner cell mass. Scale bar= 50 µm (A) and 150 µm (B).*

The capsule is an acellular glycoprotein coat composed of mucin-like glycoproteins that develops around the embryo immediately after it enters the uterus (day 6.5 post-ovulation) [110]. Capsule thickness and dry-weight increase until around day 18 [111], after which this tertiary embryo coat begins to attenuate, such that it loses continuity between days 21 and 23, and has disappeared completely by day 28-30 [112]. It has been proposed that the capsule impedes the diffusion of cryoprotectants into the embryo leading to a higher risk of

intracellular ice crystal formation during cryopreservation. This is presumably why thinning the capsule by trypsin treatment prior to freezing improved embryo survival rates [113], and reduced damage to the embryonic cytoskeleton [114]. In addition, the large volume of blastocoel fluid and lower surface area to volume ratio have been proposed to hinder successful cryoprotectant diffusion. In this respect, cryo-survival of large equine blastocysts markedly improves after puncturing, with or without aspiration of blastocoel fluid [115,116].

Cryopreservation techniques

Equine embryos have been cryopreserved by two major techniques, vitrification and slow- freezing.

Vitrification

Vitrification involves ultra-fast freezing, which leads to an instantaneous transition from the liquid phase (of both the intra- and extra-cellular fluids) to a solid glass-like state (solidification) without ice crystal formation. To achieve solidification, a high concentration of cryoprotectants (around 4-5 times higher than for slow-freezing) and a very rapid reduction in temperature (direct immersion in liquid nitrogen) are required [117]. A cooling rate of approximately 2500 °C/min can, for example, be achieved by plunging a 0.25 mL straw directly into liquid nitrogen. Even higher freezing rates (around 20,000 C/min) can be achieved by ensuring that the embryo is in a small droplet (<1 μL) in an open system (open-pulled straw [118–120] or hemi straw [121]), cryotop or cryo-loop [119]); the rapid cooling rate ensures quicker passage through the critical cryoinjury zones, and a decrease in the concentration of cryoprotectants needed. In comparison to slow-freezing, vitrification is simpler, faster, and less expensive, with equilibration and freezing combined requiring <15 min and no need for expensive equipment [122,123]. The major drawback of vitrification is the higher concentrations of the cryoprotectants, which can be toxic/detrimental to the embryo. Ensuring that immersion of the embryo in the various solutions and, in particular the final solution with the highest concentration of cryoprotectants, does not exceed the recommended durations is crucial to success. Therefore, experience in handling and not losing track of the embryo in the very dense final solution is critical for successful vitrification [124].

Slow-freezing

During slow-freezing (also known as controlled-rate freezing), embryos are exposed to the cryoprotectants in a stepwise manner (gradually) prior to controlled-rate cooling in stages. The typical cryoprotectant used to slow-freeze horse embryos is glycerol (10%), which is

introduced via 2-4 solutions of increasing concentration of cryoprotectant, to allow the embryo to equilibrate. There have, however, been concerns that cellular ultrastructural and metabolic damage to slow-frozen embryos was due more to the exposure to glycerol than the freezing process *per se* [125–127]. These findings led to studies to examine the use of other cryoprotectants with lower molecular weights (DMSO, ethylene glycol, 1,2 propanediol [126] and methanol [128]) which would be expected to penetrate more easily through the capsule and into the embryonic cells [126] [124]). However, ethylene glycol [126] and methanol [128], although relatively non-toxic, were reported to have poor and inconsistent cryoprotective abilities compared to glycerol. On the other hand, promising pregnancy rates have been reported with ethylene glycol (64%) [129].

Ice crystal formation and dehydration are twin threats that an embryo has to face during slow-freezing. As cooling progresses, solutes are left behind by gradual extracellular ice crystal formation, which increases the osmolarity of the remaining extracellular fluid. The flow of water out of the cells (non-frozen intracellular fluid) required to balance the intracellular and extracellular solute concentrations causes cellular dehydration. Therefore, defining an optimal cooling rate is critical, since overly rapid cooling will lead to lethal intracellular ice formation [130], whereas overly slow cooling will damage cells due to severe dehydration and solute toxicity. This explains why a programmable freezing machine is required to successfully slow-freeze embryos, which increases the start-up costs significantly, and why seeding of the straws is required at -6 to -7 °C. The aim of seeding is to avoid supercooling (cooling to below the normal freezing point without ice formation) by initiating coordinated ice crystal formation in the extracellular fluid. The long pre-freezing equilibration (around 40 minutes) and freezing process (1.5 to 2 h) make slow-freezing a time-consuming technique.

In vitro embryo production

In the horse, ICSI is the method of choice for *in vitro* embryo production because conventional IVF is not established as a commercially viable clinical procedure. There are, however, differences in speed of development, viability, and morphological appearance and quality between IVP blastocysts and *in vivo* flushed/derived (IVD) blastocysts. Previously, it has been shown that the pregnancy rate is lower (75%) for frozen-thawed IVP equine blastocysts than fresh IVD blastocysts (85-90%) [131]. Moreover, IVP equine blastocysts have a lower number of cells than IVD blastocysts [132], higher rates of apoptosis [133] and aneuploidy [134], and more a poorly discernible ICM and cytoskeleton structure [132], indicating lower quality than IVD blastocysts and, potentially, delayed or altered specification of the ICM (an

important event during pre-implantation embryo development) in IVP equine blastocysts.

Pre-implantation embryo development

Early embryo development begins with the production of a diploid zygote, following the fusion of the maternal (oocyte) and paternal (spermatozoon) gametes at fertilization (Figure 4). The zygote is a totipotent single cell which then undergoes a number of cell lineage specification events as development progresses, to produce all the cell types in the future organism, including all of the extra-embryonic structures.

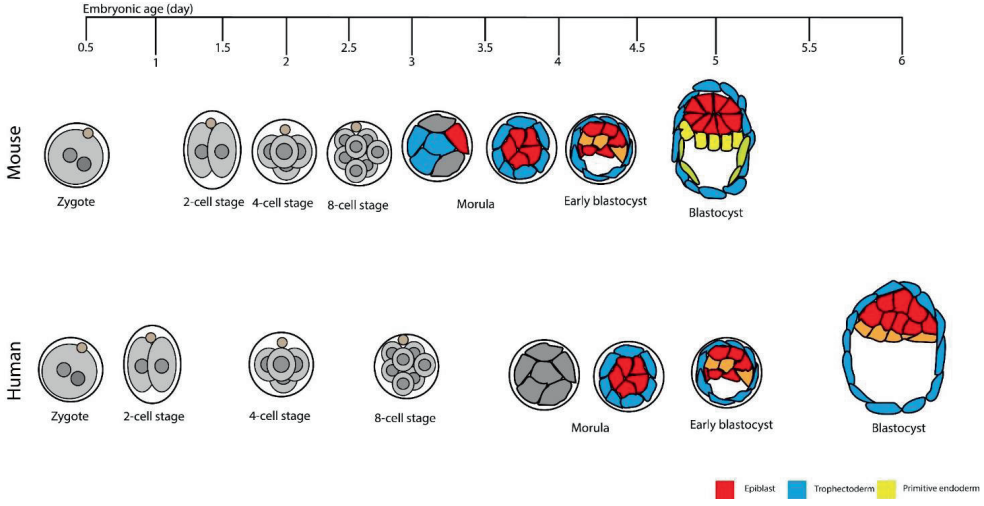

Figure 4. Preimplantation development of mouse versus human embryo from zygote to the blastocyst stage. *The first cell lineage decision occurs during the compacted morula stage, and the second cell lineage decision is completed at the blastocyst stage [188].*

First cell lineage segregation

Before embryonic genome activation, somewhere between the 2 (rodents) and 4-8-cell stage (ungulates including the horse [135], and primates), the embryo depends on maternal transcripts and proteins for the events involved in cell division [136]. During the very early developmental stages, the blastomeres are morphologically homogeneous, until the outer cells of the embryo begin to polarize, at about the 8-cell stage in the mouse (Figure 4). In the mouse, the outer polar cells then commit to a trophectoderm (TE) lineage, and the inner apolar cells to inner cell mass (ICM) (Figure 4) [137–139]. In the murine outer polar cells, formation of an apical domain triggers a transcriptional network including Hippo/YAP signaling and TEAD4 activation, which downregulates SOX-2 (pluripotency factor) and upregulates CDX-2, from around the morula stage [140–142]. Following the activation of CDX-2, a further pluipotency-associated

transcription factor OCT4 is downregulated [141,143] and other TE markers (GATA-3, Eomes or Elf5) [144] begin to be expressed; this marks the first cell lineage segregation event during blastocyst formation. Subsequently, the TE contributes exclusively to placental structures, whereas the ICM gives rise to both the embryo proper and extra-embryonic structures. In non-rodent mammals, however, there are differences in the temporal expression profiles of the critical transcription factors, and in the roles they play in directing cell differentiation. Despite the expression of TE-specific genes (CDX-2, GATA-3 and TEAD-4) in the TE of blastocysts from various species (cow [145–147], pig [148,149] and man [147,150,151]), notable differences have been observed in the timing of their expression and apparent function, compared to rodents. In the mouse [141], CDX-2 is ubiquitously expressed in presumptive TE cells before the blastocyst stage, compared to expression in scattered cells in pig [152] and cow embryos [153,154]. In addition, co-expression of CDX-2 and OCT-4 has been observed in the TE until the late blastocyst stage in human [155], porcine [152], and bovine embryos [153], in marked contrast to the mutually exclusive expression observed in murine blastocysts [141]. In murine blastocysts, OCT-4 expression is repressed by CDX-2 [143], whereas downregulation of CDX-2 has no effect on OCT-4 expression in bovine embryos [153,156]. In this respect, OCT-4 repression in murine TE is mediated by an essential OCT-4 region, -CR4-, which is absent in the bovine OCT-4 promotor [153]. Absence of OCT-4 has also been associated with qualitatively different developmental abnormalities in rodents compared to non-rodent mammals. OCT-4 knockout (KO) mouse embryos reach the blastocyst stage with impaired primitive endoderm specification (PE), whereas blastocyst formation is compromised and CDX-2 expression reduced in cattle [157] and human [158,159] OCT-4 KO morulae.

Apparently, the role of other transcription factors in the differentiation of TE and ICM differs between mouse and non-rodent mammals. Absence of TEAD4, the upstream regulator of the TE genes CDX-2 and EOMES, appears to have no effect on TE specification in non-rodent mammals, since blastocyst formation is not impaired by its downregulation in the cow [160,161]. By contrast, ablation of TEAD4 abolished blastocyst formation in the mouse [162,163]. Moreover, blastocyst stage cow [145,156,164], pig [148] and human [151] embryos do not express transcription factors downstream of TEAD4, such as EOMES and ELF5. Although, the role of these genes has yet to be investigated by specific gene ablation experiments in ungulates, these observations clearly suggest that TE specification is regulated by a different transcriptional network in ungulates than it is in the mouse.

Second lineage segregation

During the second cell lineage segregation, the ICM differentiates into the pluripotent epiblast (EPI) and the primitive endoderm (PE) (Figure 4). In murine embryos, different hypoblast markers are expressed sequentially at different embryonic stages; GATA-6, PDGFRα, SOX-17 and GATA-4 are expressed at the 8-cell, 16-cell, 32-cell, and 64-cell stages respectively [165,166]. Indeed, while cells of the early ICM (D 3.5) co-express both EPI (OCT-4, SOX-2 and NANOG) and PE (GATA-6, SOX-17 and PDGFRα) proteins, by D 4.5 the cells express either EPI or PE markers in a mutually exclusive fashion [165,167]. Although the temporal expression pattern of the various cell lineage markers has yet to be examined in detail for most domestic mammals, broad similarities in the gene network regulating the second lineage segregation have been observed across those mammals examined [168]. For example, epiblast markers are co-expressed with GATA-6, PDGFRα and SOX-17 in bipotent ICM cells, and become restricted to the PE in later blastocysts in pigs [148], cattle [145] and man [151]. Nevertheless, important differences have been found between rodent and non-rodent species. In mouse morulae, the EPI marker NANOG is co-expressed with the PE marker GATA-6 in all cells of the initial ICM, whereas the division of the late ICM into EPI and PE depends upon mutual repression of the opposing transcription factor [165,169]. However, this might not be a strict prerequisite in all mammals, since the expression of GATA-6 has been observed in all cell lineages within primate, porcine, and bovine blastocysts, only becoming restricted to the PE in later developmental stages [145,148,151,170–172]. On the other hand, morulae of human, pig and cow embryos do not express NANOG [148,154,173,174]. After designation, the PE forms an epithelium which stays in contact with the blastocoel cavity, and later covers the inner embryonic surface in primates and ungulates [175].

Embryo quality and lineage specific markers

Despite attempts to optimize ARTs, and marked improvements over time, the efficiency of *in vitro* embryo production systems is lower than desired, and *in vitro* produced embryos differ significantly from *in vivo* derived (IVD) embryos [176]. In cattle, *in vitro* embryo production is well established, but pregnancy rates after transfer to a recipient cow are 10-40% lower than after transfer of IVD embryos [177–180]. In addition, most of the pregnancy failures (80%) after the transfer of IVP embryos occur early in gestation, before day 40. IVP bovine embryos appear to suffer from a higher incidence of defects in embryonic lineage specification (particularly the EPI) after embryo transfer. In cattle, early pregnancy loss (before D 40) has been estimated at 80% following the transfer of IVP embryos. Similarly, a higher incidence of early pregnancy loss has been reported after the transfer of IVP equine embryos (16-20% before D 60 of gestation) [181,182].

Assessment of embryo quality is important for the improvement of IVEP techniques, and to direct modification of current IVEP protocols. Although *in vivo* development of IVP embryos following transfer would be the ultimate indicator of embryo quality, it has two major drawbacks: 1) cost, such studies are laborious and involve experimental animals, 2) intrinsic variabilities in uterine receptivity among recipients [183,184]. Generally, both human and farm animal embryos are selected for transfer on the basis of their morphology [185], since this is a non-invasive technique and transfer of better-quality grade embryos results in higher pregnancy rates [183,184]. However, while a grading system is well established for equine IVD embryos, grading IVP horse embryos is much more challenging and, as yet, there is no universally accepted morphological grading system. On the other hand, it has been shown that the speed of *in vitro* equine embryo development has an influence on likelihood of pregnancy (higher pregnancy rates after the transfer of IVP embryos that reached the blastocyst stage before D9 compared to on or after D9) [12]. The effect of developmental speed on pregnancy rate presumably relates to differences in embryo quality but, to date, it is not clear exactly which quality parameters are impacted [170]. One other surprising effect of equine IVEP is a markedly elevated incidence of monozygotic (monochorionic, diallantoic) twins [186] which presumably results from division of the ICM into two separate cell clusters, or formation of a more diffuse ICM in which 2 primitive streaks are able to develop. Both the higher incidence of monozygotic twins and the lower pregnancy rates and embryo quality of IVP compared to flushed embryos, could be related to inadequate or aberrant cell lineage segregation during the first 2 specification events. To better investigate possible differences in the timing and spatial distribution of cell lineage segregation in IVP equine embryos compared to *in vivo* derived (IVD) embryos it is imperative to use markers (e.g. CDX-2, SOX-2, and GATA-6) for each of the three cell lineages (TE, EPI and PE) simultaneously.

Scope of this thesis

The aim of this thesis is to optimize a number of the principal limiting steps in the most important ARTs including sperm selection, prolonged liquid *in vitro* semen storage, embryo cryopreservation and *in vitro* embryo production. In **chapter 2**, a modified flotation density gradient centrifugation (DGC) technique (double layer) was developed using Opti-prep ™ (a colloid solution) to process the semen of sub-fertile stallions with a high DNA fragmentation index (a non-compensable sperm defect). In **chapter 3**, multiparametric flow cytometry was used to investigate whether increasing ROS and ROS-induced damage in viable, acrosome-intact stallion sperm or disturbed normal cell homeostasis (plasma membrane fluidity and

regulation of intra-cellular Ca^{2+} concentration) are the major factors compromising quality of stallion semen during prolonged storage in the liquid form (96 h at 5 °C). In **chapter 4**, the question of whether slow-freezing of punctured and collapsed *in vivo* expanded blastocysts is more or less damaging than vitrification was investigated. Previously, slow-freezing has proven to cause less damage than vitrification to small equine embryos; surprisingly, to date only vitrification has been tested and validated as a method for successfully cryopreserving large blastocysts after puncture with or without blastocyst fluid aspiration to reduce their volume. In **chapter 5**, the influence of embryo type (IVD versus IVP embryos) and developmental stage (early *in vivo* blastocysts versus *in vivo* blastocysts), speed of *in vitro* development (fast versus slow development) and culture system (*in vitro* and *in vivo*) on cell lineage segregation and allocation in equine embryos was investigated, to determine whether aberrant patterns of lineage segregation may explain reduced developmental competence, a more restricted window of recipient mare synchrony tolerance, and a higher incidence of monozygotic twin formation. Finally, in **chapter 6**, the results of these studies are summarized and discussed, along with new perspectives for further research.

References

1. Aurich J, Aurich C. Developments in European horse breeding and consequences for veterinarians in equine reproduction. Reprod Domest Anim 2006;41:275–9.
2. Schulman ML, May CE, Keys B, Guthrie AJ. Contagious equine metritis: artificial reproduction changes the epidemiologic paradigm. Vet Microbiol 2013;167:2–8.
3. Samper JC, Tibary A. Disease transmission in horses. Theriogenology 2006;66:551–9.
4. Varner DD. Developments in stallion semen evaluation. Theriogenology 2008;70:448–62. https://doi.org/10.1016/j.theriogenology.2008.04.023.
5. Viana J. 2018 Statistics of embryo production and transfer in domestic farm animals. Embryo Technol Newsl 2019;36:17.
6. Palmer E, Bezard J, Magistrini M, Duchamp G. In vitro fertilization in the horse. A retrospective study. J Reprod Fertil Suppl 1991;44:375–84.
7. Bézard J. In vitro fertilization in the mare. Rec Med Vet 1992;168:993–1003.
8. Leemans B, Gadella BM, Stout TA, De Schauwer C, Nelis H, Hoogewijs M, et al. Why doesn't conventional IVF work in the horse? The equine oviduct as a microenvironment for capacitation/fertilization. Reproduction 2016;152:R233–45.
9. Felix MR, Turner RM, Dobbie T, Hinrichs K. Successful in vitro fertilization in the horse: production of blastocysts and birth of foals after prolonged sperm incubation for

capacitation. Biol Reprod 2022;107:1551–64.

10. Morris LHA. The development of in vitro embryo production in the horse. Equine Vet J 2018;50:712–20. https://doi.org/10.1111/evj.12839.
11. Stout TAE. Clinical Application of in Vitro Embryo Production in the Horse. J Equine Vet Sci 2020;89:103011. https://doi.org/10.1016/j.jevs.2020.103011.
12. Ducheyne KD, Rizzo M, Cuervo-Arango J, Claes A, Daels PF, Stout TAE, et al. In vitro production of horse embryos predisposes to micronucleus formation, whereas time to blastocyst formation affects likelihood of pregnancy. Reprod Fertil Dev 2019;31:1830. https://doi.org/10.1071/RD19227.
13. Colenbrander B, Gadella B, Stout T. The predictive value of semen analysis in the evaluation of stallion fertility. Reprod Domest Anim 2003;38:305–11.
14. Orsolini MF, Meyers SA, Dini P. An Update on Semen Physiology, Technologies, and Selection Techniques for the Advancement of In Vitro Equine Embryo Production: Section II. Animals 2021;11:3319. https://doi.org/10.3390/ani11113319.
15. Bolton V, Braude P. Preparation of human spermatozoa for in vitro fertilization by isopycnic centrifugation on self-generating density gradients. Arch Androl 1984;13:167–76.
16. Pousette Å, Åkerlöf E, Rosenborg L, Fredricsson B. Increase in progressive motility and improved morphology of human spermatozoa following their migration through Percoll gradients. Int J Androl 1986;9:1–13.
17. Henkel RR, Schill W-B. Sperm preparation for ART. Reprod Biol Endocrinol 2003;1:1–22.
18. Arcidiacono A, Walt H, Campana A, Balerna M. The use of Percoll gradients for the preparation of subpopulations of human spermatozoa. Int J Androl 1983;6:433–45.
19. Fishel S, Jackson P, Webster J, Faratian B. Endotoxins in culture medium for human in vitro fertilization. Fertil Steril 1988;49:108–11.
20. De Vos A, Nagy Z, Van de Velde H, Joris H, Bocken G, Van Steirteghem A. Percoll gradient centrifugation can be omitted in sperm preparation for intracytoplasmic sperm injection. Hum Reprod Oxf Engl 1997;12:1980–4.
21. Strehler E, Baccetti B, Sterzik K, Capitani S, Collodel G, De Santo M, et al. Detrimental effects of polyvinylpyrrolidone on the ultrastructure of spermatozoa (Notulae seminologicae 13). Hum Reprod Oxf Engl 1998;13:120–3.
22. Söderlund B, Lundin K. The use of silane-coated silica particles for density gradient centrifugation in in-vitro fertilization. Hum Reprod 2000;15:857–60.

23. Stuhtmann G, Oldenhof H, Peters P, Klewitz J, Martinsson G, Sieme H. Iodixanol density gradient centrifugation for selecting stallion sperm for cold storage and cryopreservation. Anim Reprod Sci 2012;133:184–90.
24. Beer-Ljubić B, Aladrović J, Marenjak TS, Majić-Balić I, Laškaj R, Milinković-Tur S. Biochemical properties of bull spermatozoa separated in iodixanol density solution. Res Vet Sci 2012;92:292– 4.
25. Nath L, Anderson G, McKinnon A. Reproductive efficiency of Thoroughbred and Standardbred horses in north-east Victoria. Aust Vet J 2010;88:169–75.
26. Graham J. Principles of cooled semen. Equine Reprod 2011;2:1308–15.
27. Varner DD, Blanchard TL, Love CL, Garcia M, Kenney RM. Effects of cooling rate and storage temperature on equine spermatozoal motility parameters. Theriogenology 1988;29:1043–54.
28. Moran D, Jasko D, Squires E, Amann R. Determination of temperature and cooling rate which induce cold shock in stallion spermatozoa. Theriogenology 1992;38:999–1012.
29. Clulow J, Gibb Z. Liquid storage of stallion spermatozoa–past, present and future. Anim Reprod Sci 2022:107088.
30. Storey BT. Mammalian sperm metabolism: oxygen and sugar, friend and foe. Int J Dev Biol 2008;52:427–37. https://doi.org/10.1387/ijdb.072522bs.
31. Morrell JM, Johannisson A, Dalin A-M, Hammar L, Sandebert T, Rodriguez-Martinez H. Sperm morphology and chromatin integrity in Swedish warmblood stallions and their relationship to pregnancy rates. Acta Vet Scand 2008;50:2. https://doi.org/10.1186/1751-0147-50-2.
32. Gibb Z, Lambourne SR, Aitken RJ. The Paradoxical Relationship Between Stallion Fertility and Oxidative Stress1. Biol Reprod 2014;91:77, 1–10. https://doi.org/10.1095/biolreprod.114.118539.
33. Halliwell B, Gutteridge JMC. Free Radicals in Biology and Medicine. Oxford University Press; 2015. https://doi.org/10.1093/acprof:oso/9780198717478.001.0001.
34. Gibb Z, Lambourne SR, Curry BJ, Hall SE, Aitken RJ. Aldehyde Dehydrogenase Plays a Pivotal Role in the Maintenance of Stallion Sperm Motility1. Biol Reprod 2016;94. https://doi.org/10.1095/biolreprod.116.140509.
35. Baumber J, Sabeur K, Vo A, Ball BA. Reactive oxygen species promote tyrosine phosphorylation and capacitation in equine spermatozoa. Theriogenology 2003;60:1239–47. https://doi.org/10.1016/S0093-691X(03)00144-4.
36. Austin C. Observations on the Penetration of the Sperm into the Mammalian Egg. Aust J

Biol Sci 1951;4:581. https://doi.org/10.1071/BI9510581.

37. Chang MC. Fertilizing Capacity of Spermatozoa deposited into the Fallopian Tubes. Nature 1951;168:697–8. https://doi.org/10.1038/168697b0.
38. Ortega-Ferrusola C, Anel-Lopez L, Martin-Munoz P, Ortiz-Rodriguez J, Gil M, Alvarez M, et al. Computational flow cytometry reveals that cryopreservation induces spermptosis but subpopulations of spermatozoa may experience capacitation-like changes. Reproduction 2017;153:293–304.
39. Bergqvist A, Johannisson A, Bäckgren L, Dalin A, Rodriguez-Martinez H, Morrell J. Single Layer Centrifugation of Stallion Spermatozoa through Androcoll^{TM}-E does not Adversely Affect their Capacitation-Like Status, as Measured by CTC Staining. Reprod Domest Anim 2011;46:e74–8.
40. Leahy T, Gadella B. Capacitation and capacitation-like sperm surface changes induced by handling boar semen. Reprod Domest Anim 2011;46:7–13.
41. Cormier N, Bailey JL. A differential mechanism is involved during heparin-and cryopreservation- induced capacitation of bovine spermatozoa. Biol Reprod 2003;69:177–85.
42. Meyers SA, Liu IK, Overstreet JW, Vadas S, Drobnis EZ. Zona pellucida binding and zona-induced acrosome reactions in horse spermatozoa: comparisons between fertile and subfertile stallions. Theriogenology 1996;46:1277–88.
43. O'Rand MG, Fisher SJ. Localization of zona pellucida binding sites on rabbit spermatozoa and induction of the acrosome reaction by solubilized zonae. Dev Biol 1987;119:551–9. https://doi.org/10.1016/0012-1606(87)90058-3.
44. Gadella BM, Tsai P, Boerke A, Brewis IA. Sperm head membrane reorganisation during capacitation. Int J Dev Biol 2008;52:473–80. https://doi.org/10.1387/ijdb.082583bg.
45. Gadella BM, Harrison RA. The capacitating agent bicarbonate induces protein kinase A-dependent changes in phospholipid transbilayer behavior in the sperm plasma membrane. Development 2000;127:2407–20. https://doi.org/10.1242/dev.127.11.2407.
46. Gadella BM, Harrison RAP. Capacitation Induces Cyclic Adenosine 3′,5′-Monophosphate- Dependent, but Apoptosis-Unrelated, Exposure of Aminophospholipids at the Apical Head Plasma Membrane of Boar Sperm Cells1. Biol Reprod 2002;67:340–50. https://doi.org/10.1095/biolreprod67.1.340.
47. Gadella BM, Gadella TW, Colenbrander B, van Golde LM, Lopes-Cardozo M. Visualization and quantification of glycolipid polarity dynamics in the plasma membrane of the mammalian spermatozoon. J Cell Sci 1994;107:2151–63.

https://doi.org/10.1242/jcs.107.8.2151.

48. Gadella BM, Lopes-Cardozo M, van Golde LM, Colenbrander B, Gadella TW. Glycolipid migration from the apical to the equatorial subdomains of the sperm head plasma membrane precedes the acrosome reaction. Evidence for a primary capacitation event in boar spermatozoa. J Cell Sci 1995;108:935–46. https://doi.org/10.1242/jcs.108.3.935.
49. Boerke A, Brouwers JF, Olkkonen VM, van de Lest CHA, Sostaric E, Schoevers EJ, et al. Involvement of Bicarbonate-Induced Radical Signaling in Oxysterol Formation and Sterol Depletion of Capacitating Mammalian Sperm During In Vitro Fertilization1. Biol Reprod 2013;88. https://doi.org/10.1095/biolreprod.112.101253.
50. Flesch FM, Brouwers JFHM, Nievelstein PFEM, Verkleij AJ, van Golde LMG, Colenbrander B, et al. Bicarbonate stimulated phospholipid scrambling induces cholesterol redistribution and enables cholesterol depletion in the sperm plasma membrane. J Cell Sci 2001;114:3543–55. https://doi.org/10.1242/jcs.114.19.3543.
51. Brouwers JF, Boerke A, Silva PFN, Garcia-Gil N, van Gestel RA, Helms JB, et al. Mass Spectrometric Detection of Cholesterol Oxidation in Bovine Sperm1. Biol Reprod 2011;85:128–36. https://doi.org/10.1095/biolreprod.111.091207.
52. Boerke A, Tsai PS, Garcia-Gil N, Brewis IA, Gadella BM. Capacitation-dependent reorganization of microdomains in the apical sperm head plasma membrane: Functional relationship with zona binding and the zona-induced acrosome reaction. Theriogenology 2008;70:1188–96. https://doi.org/10.1016/j.theriogenology.2008.06.021.
53. Simons K, Toomre D. Lipid rafts and signal transduction. Nat Rev Mol Cell Biol 2000;1:31–9. https://doi.org/10.1038/35036052.
54. van Gestel RA, Brewis IA, Ashton PR, Helms JB, Brouwers JF, Gadella BM. Capacitation- dependent concentration of lipid rafts in the apical ridge head area of porcine sperm cells. MHR Basic Sci Reprod Med 2005;11:583–90. https://doi.org/10.1093/molehr/gah200.
55. Bromfield EG, McLaughlin EA, Aitken RJ, Nixon B. Heat Shock Protein member A2 forms a stable complex with angiotensin converting enzyme and protein disulfide isomerase A6 in human spermatozoa. Mol Hum Reprod 2016;22:93–109. https://doi.org/10.1093/molehr/gav073.
56. van Gestel RA, Brewis IA, Ashton PR, Brouwers JF, Gadella BM. Multiple proteins present in purified porcine sperm apical plasma membranes interact with the zona pellucida of the oocyte. MHR Basic Sci Reprod Med 2007;13:445–54. https://doi.org/10.1093/molehr/gam030.

57. Ho H-C, Granish KA, Suarez SS. Hyperactivated Motility of Bull Sperm Is Triggered at the Axoneme by Ca2+ and Not cAMP. Dev Biol 2002;250:208–17. https://doi.org/10.1006/dbio.2002.0797.

58. Giroux-Widemann V, Jouannet P, Pignot-Paintrand I, Feneux D. Effects of pH on the reactivation of human spermatozoa demembranated with triton X-100. Mol Reprod Dev 1991;29:157–62. https://doi.org/10.1002/mrd.1080290211.

59. Ishijima S, Witman GB. Flagellar movement of intact and demembranated, reactivated ram spermatozoa. Cell Motil Cytoskeleton 1987;8:375–91. https://doi.org/10.1002/cm.970080410.

60. Loux SC, Macías-Garcia B, González-Fernández L, Canesin HD, Varner DD, Hinrichs K. Regulation of Axonemal Motility in Demembranated Equine Sperm1. Biol Reprod 2014;91:152, 1–16. https://doi.org/10.1095/biolreprod.114.122804.

61. Shingyoji C, Murakami A, Takahashi K. Local reactivation of Triton-extracted flagella by iontophoretic application of ATP. Nature 1977;265:269–70. https://doi.org/10.1038/265269a0.

62. Tash JS. Protein phosphorylation: The second messenger signal transducer of flagellar motility. Cell Motil Cytoskeleton 1989;14:332–9. https://doi.org/10.1002/cm.970140303.

63. Wargo MJ, Smith EF. Asymmetry of the central apparatus defines the location of active microtubule sliding in *Chlamydomonas* flagella. Proc Natl Acad Sci 2003;100:137–42. https://doi.org/10.1073/pnas.0135800100.

64. Tash JS, Means AR. Cyclic Adenosine 3′,5′ Monophosphate, Calcium and Protein Phosphorylation in Flagellar Motility. Biol Reprod 1983;28:75–104. https://doi.org/10.1095/biolreprod28.1.75.

65. White DR, Aitken RJ. Relationship between calcium, cyclic AMP, ATP, and intracellular pH and the capacity of hamster spermatozoa to express hyperactivated motility. Gamete Res 1989;22:163–77. https://doi.org/10.1002/mrd.1120220205.

66. Liguori L, Rambotti MG, Bellezza I, Minelli A. Electron Microscopic Cytochemistry of Adenylyl Cyclase Activity in Mouse Spermatozoa. J Histochem Cytochem 2004;52:833–6. https://doi.org/10.1369/jhc.3B6141.2004.

67. Hess KC, Jones BH, Marquez B, Chen Y, Ord TS, Kamenetsky M, et al. The "Soluble" Adenylyl Cyclase in Sperm Mediates Multiple Signaling Events Required for Fertilization. Dev Cell 2005;9:249–59. https://doi.org/10.1016/j.devcel.2005.06.007.

68. Visconti PE, Johnson LR, Oyaski M, Fornés M, Moss SB, Gerton GL, et al. Regulation,

Localization, and Anchoring of Protein Kinase A Subunits during Mouse Sperm Capacitation. Dev Biol 1997;192:351–63. https://doi.org/10.1006/dbio.1997.8768.

69. Si Y, Olds-Clarke P. Evidence for the Involvement of Calmodulin in Mouse Sperm Capacitation1. Biol Reprod 2000;62:1231–9. https://doi.org/10.1095/biolreprod62.5.1231.
70. Leclerc P, de Lamirande E, Gagnon C. Cyclic Adenosine 3′,5′monophosphate-Dependent Regulation of Protein Tyrosine Phosphorylation in Relation to Human Sperm Capacitation and Motility1. Biol Reprod 1996;55:684–92. https://doi.org/10.1095/biolreprod55.3.684.
71. TASH JS, BRACHO GE. Regulation of sperm motility: emerging evidence for a major role for protein phosphatases. J Androl 1994;15:505–9.
72. Vijayaraghavan S, Stephens DT, Trautman K, Smith GD, Khatra B, da Cruz e Silva EF, et al. Sperm motility development in the epididymis is associated with decreased glycogen synthase kinase-3 and protein phosphatase 1 activity. Biol Reprod 1996;54:709–18.
73. Smith GD, Wolf DP, Trautman KC, da Cruz e Silva EF, Greengard P, Vijayaraghavan S. Primate sperm contain protein phosphatase 1, a biochemical mediator of motility. Biol Reprod 1996;54:719–27.
74. Suarez SS, Pacey A. Sperm transport in the female reproductive tract. Hum Reprod Update 2006;12:23–37.
75. Demott RP, Suarez SS. Hyperactivated sperm progress in the mouse oviduct. Biol Reprod 1992;46:779–85.
76. Stauss CR, Votta TJ, Suarez SS. Sperm motility hyperactivation facilitates penetration of the hamster zona pellucida. Biol Reprod 1995;53:1280–5.
77. Yanagimachi R. Mammalian fertilization. In ‘The Physiology of Reproduction’.(Eds E. Knobil and JD Neill.) pp. 189–318 1994.
78. Ishijima S, Mohri H, Overstreet JW, Yudin AI. Hyperactivation of monkey spermatozoa is triggered by Ca2+ and completed by cAMP. Mol Reprod Dev 2006;73:1129–39.
79. Suarez SS, Varosi SM, Dai X. Intracellular calcium increases with hyperactivation in intact, moving hamster sperm and oscillates with the flagellar beat cycle. Proc Natl Acad Sci 1993;90:4660–4.
80. Suarez SS. Control of hyperactivation in sperm. Hum Reprod Update 2008;14:647–57.
81. Loux SC, Crawford KR, Ing NH, González-Fernández L, Macías-García B, Love CC, et al. CatSper and the relationship of hyperactivated motility to intracellular calcium and pH kinetics in equine sperm. Biol Reprod 2013;89:123–1.

82. Suarez SS, Vincenti L, Ceglia MW. Hyperactivated motility induced in mouse sperm by calcium ionophore A23187 is reversible. J Exp Zool 1987;244:331–6.
83. Tateno H, Krapf D, Hino T, Sánchez-Cárdenas C, Darszon A, Yanagimachi R, et al. Ca2+ ionophore A23187 can make mouse spermatozoa capable of fertilizing in vitro without activation of cAMP- dependent phosphorylation pathways. Proc Natl Acad Sci 2013;110:18543–8.
84. Christensen P, Whitfield C, Parkinson T. In vitro induction of acrosome reactions in stallion spermatozoa by heparin and A23187. Theriogenology 1996;45:1201–10.
85. Rathi R, Colenbrander B, Bevers MM, Gadella BM. Evaluation of in vitro capacitation of stallion spermatozoa. Biol Reprod 2001;65:462–70.
86. Contreras L, Drago I, Zampese E, Pozzan T. Mitochondria: the calcium connection. Biochim Biophys Acta BBA-Bioenerg 2010;1797:607–18.
87. Humes HD, Weinberg JM. Ionophore A23187 induced reductions in toad urinary bladder epithelial cell oxidative phosphorylation and viability. Pflüg Arch 1980;388:217–20.
88. Krumschnabel G, Schwarzbaum PJ, Wieser W. Energetics of trout hepatocytes during A23187- induced disruption of Ca2+ homeostasis. Comp Biochem Physiol C Pharmacol Toxicol Endocrinol 1999;124:187–95.
89. Ho H-C, Suarez SS. An inositol 1, 4, 5-trisphosphate receptor-gated intracellular Ca2+ store is involved in regulating sperm hyperactivated motility. Biol Reprod 2001;65:1606–15.
90. Marquez B, Suarez SS. Different signaling pathways in bovine sperm regulate capacitation and hyperactivation. Biol Reprod 2004;70:1626–33.
91. Ho H-C, Suarez SS. Characterization of the intracellular calcium store at the base of the sperm flagellum that regulates hyperactivated motility. Biol Reprod 2003;68:1590–6.
92. Tsai P-SJ, Brewis IA, van Maaren J, Gadella BM. Involvement of complexin 2 in docking, locking and unlocking of different SNARE complexes during sperm capacitation and induced acrosomal exocytosis. PLoS One 2012;7:e32603.
93. Kim K-S, Gerton GL. Differential release of soluble and matrix components: evidence for intermediate states of secretion during spontaneous acrosomal exocytosis in mouse sperm☆. Dev Biol 2003;264:141–52.
94. Vjugina U, Evans JP. New insights into the molecular basis of mammalian sperm-egg membrane interactions. Front Biosci-Landmark 2008;13:462–76.
95. Tsai P-S, Garcia-Gil N, Van Haeften T, Gadella BM. How pig sperm prepares to fertilize:

stable acrosome docking to the plasma membrane. PloS One 2010;5:e11204.Roggero CM, De Blas GA, Dai H, Tomes CN, Rizo J, Mayorga LS. Complexin/synaptotagmin interplay controls acrosomal exocytosis. J Biol Chem 2007;282:26335–43.

96. Bleil JD, Wassarman PM. Identification of a ZP3-binding protein on acrosome-intact mouse sperm by photoaffinity crosslinking. Proc Natl Acad Sci 1990;87:5563–7.

97. Arnoult C, Cardullo RA, Lemos JR, Florman HM. Activation of mouse sperm T-type Ca2+ channels by adhesion to the egg zona pellucida. Proc Natl Acad Sci 1996;93:13004–9.

98. Inoue N, Satouh Y, Ikawa M, Okabe M, Yanagimachi R. Acrosome-reacted mouse spermatozoa recovered from the perivitelline space can fertilize other eggs. Proc Natl Acad Sci 2011;108:20008–11.

99. Jin M, Fujiwara E, Kakiuchi Y, Okabe M, Satouh Y, Baba SA, et al. Most fertilizing mouse spermatozoa begin their acrosome reaction before contact with the zona pellucida during in vitro fertilization. Proc Natl Acad Sci 2011;108:4892–6.

100. Ellington J, Ball B, Yang X. Binding of stallion spermatozoa to the equine zona pellucida after coculture with oviductal epithelial cells. Reproduction 1993;98:203–8.

101. Cheng F, Fazeli A, Voorhout WF, Marks A, Bevers MM, Colenbrander B. Use of peanutagglutinin to assess the acrosomal status and the zona pellucida-induced acrosome reaction in stallion spermatozoa. J Androl 1996;17:674–82.

102. Saaranen M, Calvo L, Dennison L, Banks S, Bustillo M, Dorfmann A, et al. Andrology: Acrosome reaction inducing activity in follicular fluid correlates with progesterone concentration but not with oocyte maturity or fertilizability. Hum Reprod 1993;8:1448–54.

103.Cheng F, Fazeli A, Voorhout W, Tremoleda J, Bevers M, Colenbrander B. Progesterone in mare follicular fluid induces the acrosome reaction in stallion spermatozoa and enhances in vitro binding to the zona pellucida. Int J Androl 1998;21:57–66.

104. Lange-Consiglio A, Cremonesi F. 163 Hyperactivation of stallion sperm in follicular fluid for in vitro fertilization of equine oocytes. Reprod Fertil Dev 2011;24:193–4.

105. Rathi R, Colenbrander B, Stout T, Bevers M, Gadella B. Progesterone induces acrosome reaction in stallion spermatozoa via a protein tyrosine kinase dependent pathway. Mol Reprod Dev Inc Gamete Res 2003;64:120–8.

106. Breitbart H, Naor Z. Protein kinases in mammalian sperm capacitation and the acrosome reaction. Rev Reprod 1999;4:151–9.

107. Stout TA. Cryopreservation of equine embryos: current state-of-the-art. Reprod Domest Anim 2012;47:84–9.

108. Bruyas J, Sanson J, Battut I, Fiéni F, Tainturier D. Comparison of the cryoprotectant properties of glycerol and ethylene glycol for early (day 6) equine embryos. J Reprod Fertil Suppl 2000:549– 60.
109. Flood PF, Betteridge KJ, Diocee MS. Transmission electron microscopy of horse embryos 3-16 days after ovulation. J Reprod Fertil Suppl 1982;32:319–27.
110. Oriol JG, Betteridge KJ, Clarke AJ, Sharom FJ. Mucin-like glycoproteins in the equine embryonic capsule. Mol Reprod Dev 1993;34:255–65. https://doi.org/10.1002/mrd.1080340305.
111. Stout TAE, Meadows S, Allen WR. Stage-specific formation of the equine blastocyst capsule is instrumental to hatching and to embryonic survival in vivo. Anim Reprod Sci 2005;87:269–81. https://doi.org/10.1016/j.anireprosci.2004.11.009.
112. Comparison of pregnancy rates for days 7–8 equine embryos frozen in glycerol with or without previous enzymatic treatment of their capsule. Theriogenology 2002;58:721–3. https://doi.org/10.1016/S0093-691X(02)00891-9.
113. Tharasanit T, Colenbrander B, Stout TAE. Effect of cryopreservation on the cellular integrity of equine embryos. Reproduction 2005;129:789–98. https://doi.org/10.1530/rep.1.00622.
114. Choi YH, Velez IC, Riera FL, Roldán JE, Hartman DL, Bliss SB, et al. Successful cryopreservation of expanded equine blastocysts. Theriogenology 2011;76:143–52. https://doi.org/10.1016/j.theriogenology.2011.01.028.
115. Wilsher S, Rigali F, Couto G, Camargo S, Allen WR. Vitrification of equine expanded blastocysts following puncture with or without aspiration of the blastocoele fluid. Equine Vet J 2019;51:500–5. https://doi.org/10.1111/evj.13039.
116. Liebermann J, Nawroth F, Isachenko V, Isachenko E, Rahimi G, Tucker MJ. Potential Importance of Vitrification in Reproductive Medicine. Biol Reprod 2002;67:1671–80. https://doi.org/10.1095/biolreprod.102.006833.
117. Vajta G, Holm P, Kuwayama M, Booth PJ, Jacobsen H, Greve T, et al. Open pulled straw (OPS) vitrification: A new way to reduce cryoinjuries of bovine ova and embryos. Mol Reprod Dev 1998;51:53–8. https://doi.org/10.1002/(SICI)1098-2795(199809)51:1<53::AID-MRD6>3.0.CO;2- V.
118. Oberstein N, O'Donovan MK, Bruemmer JE, Seidel GE, Carnevale EM, Squires EL. Cryopreservation of equine embryos by open pulled straw, cryoloop, or conventional slow cooling methods. Theriogenology 2001;55:607–13. https://doi.org/10.1016/S0093-691X(01)00429-0.

119. Moussa M, Bersinger I, Doligez P, Guignot F, Duchamp G, Vidament M, et al. In vitro comparisons of two cryopreservation techniques for equine embryos: Slow-cooling and open pulled straw (OPS) vitrification. Theriogenology 2005;64:1619–32. https://doi.org/10.1016/j.theriogenology.2005.04.001.
120. Herrera C. Vitrification of Equine In Vivo-Derived Embryos After Blastocoel Aspiration. In: Wolkers WF, Oldenhof H, editors. Cryopreserv. Free.-Dry. Protoc., vol. 2180, New York, NY: Springer US; 2021, p. 517–22. https://doi.org/10.1007/978-1-0716-0783-1_25.
121. Eldridge-Panuska WD, Caracciolo di Brienza V, Seidel GE, Squires EL, Carnevale EM. Establishment of pregnancies after serial dilution or direct transfer by vitrified equine embryos. Theriogenology 2005;63:1308–19 . https://doi.org/10.1016/j.theriogenology.2004.06.015.
122. Carnevale EM. Vitrification of Equine Embryos. Vet Clin North Am Equine Pract 2006;22:831–41. https://doi.org/10.1016/j.cveq.2006.08.003.
123. McKinnon AO, Squires EL, Vaala WE, Varner DD. Equine reproduction. John Wiley & Sons; 2011.
124. Wilson JM, Caceci T, Potter GD, Kraemer DC. Ultrastructure of cryopreserved horse embryos. J Reprod Fertil Suppl 1987;35:405–17.
125. Bruyas J-F, Battut I, Pol J-M, Botrel C, Fieni F, Tainturier D. Quantitative Analysis of Morphological Modifications of Day 6.5 Horse Embryos after Treatment with Four Cryoprotectants: Differential Effects on Inner Cell Mass and Trophoblast Cells1. Biol Reprod 1995;52:329–39 . https://doi.org/10.1093/biolreprod/52.monograph_series1.329.
126. Rieger D, Bruyas JF, Lagneaux D, Bézard J, Palmer E. The effect of cryopreservation on the metabolic activity of day-6.5 horse embryos. J Reprod Fertil Suppl 1991;44:411–7.
127. Bass LD, Denniston DJ, Maclellan LJ, McCue PM, Seidel GE, Squires EL. Methanol as a cryoprotectant for equine embryos. Theriogenology 2004;62:1153–9 . https://doi.org/10.1016/j.theriogenology.2003.12.026.
128. Hochi S, Maruyama K, Oguri N. Direct transfer of equine blastocysts frozen-thawed in the presence of ethylene glycol and sucrose. Theriogenology 1996;46:1217–24. https://doi.org/10.1016/S0093-691X(96)00292-0.
129. Mazur P. The role of intracellular freezing in the death of cells cooled at supraoptimal rates. Cryobiology 1977;14:251–72. https://doi.org/10.1016/0011-2240(77)90175-4.
130. Cuervo-Arango J, Claes AN, Stout TAE. In vitro-produced horse embryos exhibit a very

narrow window of acceptable recipient mare uterine synchrony compared with in vivo-derived embryos. Reprod Fertil Dev 2019;31:1904. https://doi.org/10.1071/RD19294.

131. Tremoleda JL, Stout TAE, Lagutina I, Lazzari G, Bevers MM, Colenbrander B, et al. Effects of In Vitro Production on Horse Embryo Morphology, Cytoskeletal Characteristics, and Blastocyst Capsule Formation. Biol Reprod 2003;69:1895–906. https://doi.org/10.1095/biolreprod.103.018515.
132. Pomar FJR, Teerds KJ, Kidson A, Colenbrander B, Tharasanit T, Aguilar B, et al. Differences in the incidence of apoptosis between in vivo and in vitro produced blastocysts of farm animal species: a comparative study. Theriogenology 2005;63:2254–68. https://doi.org/10.1016/j.theriogenology.2004.10.015.
133. Rambags BPB, Krijtenburg PJ, Drie HF van, Lazzari G, Galli C, Pearson PL, et al. Numerical chromosomal abnormalities in equine embryos produced in vivo and in vitro. Mol Reprod Dev 2005;72:77–87. https://doi.org/10.1002/mrd.20302.
134. Goszczynski DE, Tinetti PS, Choi YH, Hinrichs K, Ross PJ. Genome activation in equine in vitro– produced embryos. Biol Reprod 2022;106:66–82 . https://doi.org/10.1093/biolre/ioab173.
135. Piliszek A, Madeja ZE. Pre-implantation Development of Domestic Animals. Curr. Top. Dev. Biol., vol. 128, Elsevier; 2018, p. 267–94 . https://doi.org/10.1016/bs.ctdb.2017.11.005.
136. Korotkevich E, Niwayama R, Courtois A, Friese S, Berger N, Buchholz F, et al. The Apical Domain Is Required and Sufficient for the First Lineage Segregation in the Mouse Embryo. Dev Cell 2017;40:235-247.e7. https://doi.org/10.1016/j.devcel.2017.01.006.
137. Maître J-L, Turlier H, Illukkumbura R, Eismann B, Niwayama R, Nédélec F, et al. Asymmetric division of contractile domains couples cell positioning and fate specification. Nature 2016;536:344–8. https://doi.org/10.1038/nature18958.
138. Artus J, Hue I, Acloque H. Preimplantation development in ungulates: a 'ménage à quatre'scenario. Reproduction 2020;159:R151–72. https://doi.org/10.1530/REP-19-0348.
139. Wicklow E, Blij S, Frum T, Hirate Y, Lang RA, Sasaki H, et al. HIPPO Pathway Members Restrict SOX2 to the Inner Cell Mass Where It Promotes ICM Fates in the Mouse Blastocyst. PLoS Genet 2014;10:e1004618. https://doi.org/10.1371/journal.pgen.1004618.
140. Strumpf D, Mao C-A, Yamanaka Y, Ralston A, Chawengsaksophak K, Beck F, et al. Cdx2 is required for correct cell fate specification and differentiation of trophectoderm in

the mouse blastocyst. Development 2005;132:2093–102. https://doi.org/10.1242/dev.01801.

141. Hirate Y, Hirahara S, Inoue K, Suzuki A, Alarcon VB, Akimoto K, et al. Polarity-Dependent Distribution of Angiomotin Localizes Hippo Signaling in Preimplantation Embryos. Curr Biol 2013;23:1181–94. https://doi.org/10.1016/j.cub.2013.05.014.
142. Niwa H, Toyooka Y, Shimosato D, Strumpf D, Takahashi K, Yagi R, et al. Interaction between Oct3/4 and Cdx2 Determines Trophectoderm Differentiation. Cell 2005;123:917–29. https://doi.org/10.1016/j.cell.2005.08.040.
143. Ng RK, Dean W, Dawson C, Lucifero D, Madeja Z, Reik W, et al. Epigenetic restriction of embryonic cell lineage fate by methylation of Elf5. Nat Cell Biol 2008;10:1280–90. https://doi.org/10.1038/ncb1786.
144. Wei Q, Zhong L, Zhang S, Mu H, Xiang J, Yue L, et al. Bovine lineage specification revealed by single-cell gene expression analysis from zygote to blastocyst†. Biol Reprod 2017;97:5–17. https://doi.org/10.1093/biolre/iox071.
145. Negrón-Pérez VM, Zhang Y, Hansen PJ. Single-cell gene expression of the bovine blastocyst. Reproduction 2017;154:627–44. https://doi.org/10.1530/REP-17-0345.
146. Gerri C, McCarthy A, Alanis-Lobato G, Demtschenko A, Bruneau A, Loubersac S, et al. Initiation of a conserved trophectoderm program in human, cow and mouse embryos. Nature 2020;587:443–7. https://doi.org/10.1038/s41586-020-2759-x.
147. Ramos-Ibeas P, Sang F, Zhu Q, Tang WWC, Withey S, Klisch D, et al. Pluripotency and X chromosome dynamics revealed in pig pre-gastrulating embryos by single cell analysis. Nat Commun 2019;10:500. https://doi.org/10.1038/s41467-019-08387-8.
148. Kong Q, Yang X, Zhang H, Liu S, Zhao J, Zhang J, et al. Lineage specification and pluripotency revealed by transcriptome analysis from oocyte to blastocyst in pig. FASEB J 2020;34:691–705. https://doi.org/10.1096/fj.201901818RR.
149. Niakan KK, Eggan K. Analysis of human embryos from zygote to blastocyst reveals distinct gene expression patterns relative to the mouse. Dev Biol 2013;375:54–64. https://doi.org/10.1016/j.ydbio.2012.12.008.
150. Blakeley P, Fogarty NME, del Valle I, Wamaitha SE, Hu TX, Elder K, et al. Defining the three cell lineages of the human blastocyst by single-cell RNA-seq. Development 2015:dev.123547. https://doi.org/10.1242/dev.123547.
151. Bou G, Liu S, Sun M, Zhu J, Xue B, Guo J, et al. CDX2 is essential for cell proliferation and polarity in porcine blastocysts. Development 2017:dev.141085. https://doi.org/10.1242/dev.141085.

152. Berg DK, Smith CS, Pearton DJ, Wells DN, Broadhurst R, Donnison M, et al. Trophectoderm Lineage Determination in Cattle. Dev Cell 2011;20:244–55. https://doi.org/10.1016/j.devcel.2011.01.003.
153. Kuijk EW, Du Puy L, Van Tol HTA, Oei CHY, Haagsman HP, Colenbrander B, et al. Differences in early lineage segregation between mammals. Dev Dyn 2008;237:918–27. https://doi.org/10.1002/dvdy.21480.
154. Cauffman G, Van de Velde H, Liebaers I, Van Steirteghem A. Oct-4 mRNA and protein expression during human preimplantation development. MHR Basic Sci Reprod Med 2004;11:173–81. https://doi.org/10.1093/molehr/gah155.
155. Goissis MD, Cibelli JB. Functional characterization of CDX2 during bovine preimplantation development in vitro: *C DX2* K NOCKDOWN IN B OVINE E MBRYOS. Mol Reprod Dev 2014;81:962–70. https://doi.org/10.1002/mrd.22415.
156. Daigneault BW, Rajput S, Smith GW, Ross PJ. Embryonic POU5F1 is Required for Expanded Bovine Blastocyst Formation. Sci Rep 2018;8:7753. https://doi.org/10.1038/s41598-018-25964-x.
157. Fogarty NME, McCarthy A, Snijders KE, Powell BE, Kubikova N, Blakeley P, et al. Genome editing reveals a role for OCT4 in human embryogenesis. Nature 2017;550:67–73. https://doi.org/10.1038/nature24033.
158. Stamatiadis P, Boel A, Cosemans G, Popovic M, Bekaert B, Guggilla R, et al. Comparative analysis of mouse and human preimplantation development following *POU5F1* CRISPR/Cas9 targeting reveals interspecies differences. Hum Reprod 2021;36:1242–52. https://doi.org/10.1093/humrep/deab027.
159. Sakurai N, Takahashi K, Emura N, Hashizume T, Sawai K. Effects of downregulating TEAD4 transcripts by RNA interference on early development of bovine embryos. J Reprod Dev 2017;63:135–42. https://doi.org/10.1262/jrd.2016-130.
160. Akizawa H, Kobayashi K, Bai H, Takahashi M, Kagawa S, Nagatomo H, et al. Reciprocal regulation of TEAD4 and CCN2 for the trophectoderm development of the bovine blastocyst. Reproduction 2018;155:563–71. https://doi.org/10.1530/REP-18-0043.
161. Nishioka N, Yamamoto S, Kiyonari H, Sato H, Sawada A, Ota M, et al. Tead4 is required for specification of trophectoderm in pre-implantation mouse embryos. Mech Dev 2008;125:270–83. https://doi.org/10.1016/j.mod.2007.11.002.
162. Yagi R, Kohn MJ, Karavanova I, Kaneko KJ, Vullhorst D, DePamphilis ML, et al. Transcription factor TEAD4 specifies the trophectoderm lineage at the beginning of

mammalian development. Development 2007;134:3827–36. https://doi.org/10.1242/dev.010223.

163. Degrelle SA, Campion E, Cabau C, Piumi F, Reinaud P, Richard C, et al. Molecular evidence for a critical period in mural trophoblast development in bovine blastocysts. Dev Biol 2005;288:448–60. https://doi.org/10.1016/j.ydbio.2005.09.043.
164. Plusa B, Piliszek A, Frankenberg S, Artus J, Hadjantonakis A-K. Distinct sequential cell behaviours direct primitive endoderm formation in the mouse blastocyst. Development 2008;135:3081–91. https://doi.org/10.1242/dev.021519.
165. Artus J, Piliszek A, Hadjantonakis A-K. The primitive endoderm lineage of the mouse blastocyst: Sequential transcription factor activation and regulation of differentiation by Sox17. Dev Biol 2011;350:393–404. https://doi.org/10.1016/j.ydbio.2010.12.007.
166. Chazaud C, Yamanaka Y. Lineage specification in the mouse preimplantation embryo. Development 2016;143:1063–74. https://doi.org/10.1242/dev.128314.
167. Frankenberg SR, de Barros FRO, Rossant J, Renfree MB. The mammalian blastocyst. WIREs Dev Biol 2016;5:210–32. https://doi.org/10.1002/wdev.220.
168. Bessonnard S, De Mot L, Gonze D, Barriol M, Dennis C, Goldbeter A, et al. Gata6, Nanog and Erk signaling control cell fate in the inner cell mass through a tristable regulatory network. Dev Camb Engl 2014;141:3637–48. https://doi.org/10.1242/dev.109678.
169. Petropoulos S, Edsgärd D, Reinius B, Deng Q, Panula SP, Codeluppi S, et al. Single-Cell RNA- Seq Reveals Lineage and X Chromosome Dynamics in Human Preimplantation Embryos. Cell 2016;165:1012–26. https://doi.org/10.1016/j.cell.2016.03.023.
170. Nakamura T, Okamoto I, Sasaki K, Yabuta Y, Iwatani C, Tsuchiya H, et al. A developmental coordinate of pluripotency among mice, monkeys and humans. Nature 2016;537:57–62. https://doi.org/10.1038/nature19096.
171. Stirparo GG, Boroviak T, Guo G, Nichols J, Smith A, Bertone P. Integrated analysis of single- cell embryo data yields a unified transcriptome signature for the human preimplantation epiblast. Development 2018:dev.158501. https://doi.org/10.1242/dev.158501.
172. Kuijk EW, van Tol LTA, Van de Velde H, Wubbolts R, Welling M, Geijsen N, et al. The roles of FGF and MAP kinase signaling in the segregation of the epiblast and hypoblast cell lineages in bovine and human embryos. Development 2012;139:871–82. https://doi.org/10.1242/dev.071688.
173. Cauffman G, De Rycke M, Sermon K, Liebaers I, Van de Velde H. Markers that define

stemness in ESC are unable to identify the totipotent cells in human preimplantation embryos. Hum Reprod 2009;24:63–70. https://doi.org/10.1093/humrep/den351.

174. Ramos-Ibeas P, Lamas-Toranzo I, Martínez-Moro Á, de Frutos C, Quiroga AC, Zurita E, et al. Embryonic disc formation following post-hatching bovine embryo development in vitro. Reproduction 2020;160:579–89. https://doi.org/10.1530/REP-20-0243.
175. Ramos-Ibeas P, Heras S, Gómez-Redondo I, Planells B, Fernández-González R, Pericuesta E, et al. Embryo responses to stress induced by assisted reproductive technologies. Mol Reprod Dev 2019;86:1292–306. https://doi.org/10.1002/mrd.23119.
176. Santos JEP, Thatcher WW, Chebel RC, Cerri RLA, Galvão KN. The effect of embryonic death rates in cattle on the efficacy of estrus synchronization programs. Anim Reprod Sci 2004;82– 83:513–35. https://doi.org/10.1016/j.anireprosci.2004.04.015.
177. Lucy MC. Reproductive Loss in High-Producing Dairy Cattle: Where Will It End? J Dairy Sci 2001;84:1277–93. https://doi.org/10.3168/jds.S0022-0302(01)70158-0.
178. Wiltbank MC, Baez GM, Garcia-Guerra A, Toledo MZ, Monteiro PLJ, Melo LF, et al. Pivotal periods for pregnancy loss during the first trimester of gestation in lactating dairy cows. Theriogenology 2016;86:239–53. https://doi.org/10.1016/j.theriogenology.2016.04.037.
179. Pohler KG, Green JA, Geary TW, Peres RFG, Pereira MHC, Vasconcelos JLM, et al. Predicting Embryo Presence and Viability. In: Geisert RD, Bazer FW, editors. Regul. Implant. Establ. Pregnancy Mamm., vol. 216, Cham: Springer International Publishing; 2015, p. 253–70. https://doi.org/10.1007/978-3-319-15856-3_13.
180. Hinrichs K, Choi YH, Love CC, Spacek S. Use of in vitro maturation of oocytes, intracytoplasmic sperm injection and in vitro culture to the blastocyst stage in a commercial equine assisted reproduction program. J Equine Vet Sci 2014;34:176. https://doi.org/10.1016/j.jevs.2013.10.129.
181. Claes A, Cuervo-Arango J, Broek J, Galli C, Colleoni S, Lazzari G, et al. Factors affecting the likelihood of pregnancy and embryonic loss after transfer of cryopreserved in vitro produced equine embryos. Equine Vet J 2019;51:446–50. https://doi.org/10.1111/evj.13028.
182. Estrada-Cortés E, Ortiz WG, Chebel RC, Jannaman EA, Moss JI, de Castro FC, et al. Embryo and cow factors affecting pregnancy per embryo transfer for multiple-service, lactating Holstein recipients. Transl Anim Sci 2019;3:60–5. https://doi.org/10.1093/tas/txz009.
183. Geary TW, Burns GW, Moraes JGN, Moss JI, Denicol AC, Dobbs KB, et al.

Identification of Beef Heifers with Superior Uterine Capacity for Pregnancy. Biol Reprod 2016;95:47–47. https://doi.org/10.1095/biolreprod.116.141390.

184. Stringfellow DA, Seidel SM. Manual of the international embryo transfer society. The Society; 1998.

185. Dijkstra A, Cuervo-Arango J, Stout TAE, Claes A. Monozygotic multiple pregnancies after transfer of single in vitro produced equine embryos. Equine Vet J 2020;52:258–61. https://doi.org/10.1111/evj.13146.

186. Leemans B, Stout TAE, De Schauwer C, Heras S, Nelis H, Hoogewijs M, et al. Update on mammalian sperm capacitation: how much does the horse differ from other species? Reproduction 2019;157:R181–97. https://doi.org/10.1530/REP-18-0541.

187. Molè MA, Weberling A, Zernicka-Goetz M. Comparative analysis of human and mouse development: From zygote to pre-gastrulation. Curr. Top. Dev. Biol., vol. 136, Elsevier; 2020, p. 113–38. https://doi.org/10.1016/bs.ctdb.2019.10.002.

Chapter 2

A Modified Flotation Density Gradient Centrifugation Technique Improves the Semen Quality of Stallions with a High DNA Fragmentation Index

Muhammad Umair[1], Heiko Henning[1,2], Tom A.E. Stout[1] and Anthony Claes[1]

1 Department of Clinical Sciences, Faculty of Veterinary Medicine, Utrecht University, Utrecht, The Netherlands

2 Friedrich-Loeffler-Institut, Federal Research Institute for Animal Health, Neustadt, Germany

Published as:

Umair, M.; Henning, H.; Stout, T.A.E.; Claes, A. A Modified Flotation Density Gradient Centrifugation Technique Improves the Semen Quality of Stallions with a High DNA Fragmentation Index. *Animals* **2021**, *11*, 1973. https:// doi.org/10.3390/ani11071973

Abstract

Sperm DNA fragmentation compromises fertilization and early embryo development. Since spermatozoa lack the machinery to repair DNA damage, to improve the likelihood of establishing a healthy pregnancy, it is preferable to process ejaculates of stallions with a high sperm DNA fragmentation index (DFI) before artificial insemination or intracytoplasmic sperm injection. The aim of this study was to examine a modified flotation density gradient centrifugation (DGC) technique in which semen was diluted with a colloid solution (Opti-prep™) to increase its density prior to layering between colloid layers of lower and higher density. The optimal Opti-prep™ solution (20–60%) for use as the bottom/cushion layer was first determined, followed by a comparison between a modified sedimentation DGC and the modified flotation DGC technique, using different Opti-prep™ solutions (20%, 25% and 30%) as the top layer. Finally, the most efficient DGC technique was selected to process ejaculates from Friesian stallions (n = 3) with high sperm DFI (>20%). The optimal Opti-prep™ solution for the cushion layer was 40%. The modified sedimentation technique resulted in two different sperm populations, whereas the modified flotation technique yielded three populations. Among the variants tested, the modified flotation DGC using 20% Opti-prep™ as the top layer yielded the best results; the average sperm recovery was 57%; the DFI decreased significantly (from 12% to 4%) and the other sperm quality parameters, including progressive and total motility, percentages of spermatozoa with normal morphology and viable spermatozoa with an intact acrosome, all increased ($p < 0.05$). In Friesian stallions with high sperm DFI, the modified flotation DGC markedly decreased the DFI (from 31% to 5%) and significantly improved the other semen quality parameters, although sperm recovery was low (approximately 20%). In conclusion, stallion sperm DFI and other sperm quality parameters can be markedly improved using a modified flotation DGC technique employing a 40% Opti-prep™ cushion and a 20% top layer.

Chapter 2

Introduction

Sperm DNA fragmentation has a negative impact on reproductive success, because it compromises fertilization and embryo development, leading to a lower likelihood of pregnancy and a higher incidence of pregnancy loss [1]. The integrity of sperm DNA can be assessed using the sperm chromatin structure assay (SCSA), in which the percentage of sperm with increased levels of single-stranded DNA is represented by the DNA fragmentation index (DFI) [2]. In stallions, there is a negative association between the DFI and seasonal pregnancy rate, and the DFI is significantly higher in subfertile than fertile stallions [3,4]. Although sperm motility and morphology are often reduced in the ejaculates of stallions with high sperm DFI, the general semen quality parameters sometimes fail to reflect a high sperm DFI [5]. Furthermore, subfertile stallions with high sperm DFI and/or poor semen quality parameters are not universally excluded from commercial breeding programs, because stallions are usually selected predominantly on the basis of their athletic performance compared to other domestic species (bulls and pigs) and pedigree rather than fertility potential. Since sperm cells lack the machinery to repair DNA damage [6], and sperm DNA fragmentation is thought to be a non-compensable defect [7], in instances of high sperm DFI, it is considered important to reduce the number of spermatozoa with a relatively high degree of fragmented DNA by applying a sperm selection technique prior to assisted reproductive technologies (ART) such as artificial insemination (AI), conventional in vitro fertilization (IVF) or intracytoplasmic sperm injection (ICSI).

Density gradient centrifugation (DGC) is a sperm selection technique that separates spermatozoa into subpopulations based on their density. This is accompanied by a relative enrichment of viable and/or motile sperm with more uniform morphology in one of the subpopulations [8]. For equine assisted reproduction, single- or double-layer density gradient systems predominate among commercially available products (for a review, see reference [9]). In this context, Opti-prepTM (Iodixanol 60%), originally developed as an X-ray contrast medium, is one of the colloid solutions that has previously been used to separate spermatozoa from men [10,11], bulls [8] and stallions [12]. Opti-prepTM is nonionic, iso-osmotic and extensively tested for toxicity towards biological materials and can be used to generate isotonic solutions with densities up to 1.32 g/mL [13]. This property of Opti-prepTM makes it suitable as a bottom or “cushion” layer to prevent the over- compaction of the sperm pellet during centrifugation. Less-concentrated solutions of Opti- prepTM can serve as the top layer in double-layer DGC, which separates spermatozoa into populations

with different qualities [8,12]. Thus, discontinuous double-layer DGC using Opti-prepTM [12] to make both a cushion layer and a selective top layer has been proposed to be superior to ordinary centrifugation or density gradient centrifugation systems (single or double-layer) using Percoll [14], EquiPure [15] or Androcoll [16], because, in the latter, the selected sperm are collected as a pellet at the bottom of the tube. Pelleting onto the bottom of the tube is thought to be deleterious, because the sperm are tightly packed together with the debris and reactive oxygen species released from dying cells [9,10,17].

Previously, a double-layer DGC method involving layering diluted semen onto a top layer of low-density Opti-prepTM, which serves to select out less dense sperm, and underlain by a bottom layer of high-density Opti-prepTM, which serves as a cushion [12], has been used to process stallion semen. However, in this classical approach, sperm recovery is low (33%) even for ejaculates from stallions with semen parameters within the normal range. An alternative method of DGC (modified flotation DGC) has been described for bull semen, where the semen is first diluted (1:1) with a gradient solution (Opti-prepTM) to increase its density and then layered beneath two layers of Opti-prepTM with decreasing density [8]. Whether and to what extent this different DGC setup may improve sperm recovery and the selection of sperm with intact DNA is not clear.

The aim of the current study was to systematically develop a DGC technique based on Opti-prepTM that consistently separates out sperm cells with damaged DNA, both from stallions with normal semen quality parameters and stallions with high DFI, but with a minimum of other adverse effects on the sperm quality and recovery. This was performed in stages. First, the optimal Opti-prepTM concentration to serve as a bottom/cushion layer was determined; this was followed by a comparison between a modified sedimentation and a modified flotation DGC using solutions of different densities. Finally, the modified DGC technique was used to process semen samples from a small number of Friesian stallions with very high sperm DFI (>20%) with the aim of enriching the selected population for progressively motile, morphologically normal spermatozoa with intact DNA.

Materials and Methods

Preparation of Different Density Gradient Solutions

Different density gradient solutions (20%, 25%, 30%, 40% and 50% Opti-prep^{TM} with calculated densities 1.110 g/mL, 1.137 g/mL, 1.163 g/mL, 1.215 g/mL and 1.268 g/mL, respectively) were prepared by diluting a 60% Opti-prepTM stock solution (60% Iodixanol;

Sigma-Aldrich Chemicals, Zwijndrecht, The Netherlands) with HBSS (Hanks Buffered Salt Solution; 5.33-mM KCl, 0.441-mM KH2PO4, 4.17-mM NaHCO3, 137.92-mM NaCl, 0.338-mM NaH2PO4 and 5.56-mM glucose, pH 7.4; Thermo Fisher Scientific, Ermelo, The Netherlands).

Semen Collection and Initial Processing

Semen was collected from stallions using a Hannover model artificial vagina. The volume of gel-free semen was measured, and the concentration of spermatozoa was deter- mined using a NucleoCounter SP-100 (Chemometec, Allerod, Denmark). Subsequently, the semen was prediluted (1:1) with prewarmed (37 ◦C) INRA-96 extender (INRA; IMV Technologies, L'Aigle, France) and transported to the laboratory in a Styrofoam box.

Determining the Optimal Opti-prepTM Solution to Use as the Bottom/Cushion Layer

Semen was collected from 6 stallions of different breeds (5 ± 1 years of age) and processed as described above. Semen diluted 1:1 in INRA-96 (2 mL) was then layered on top of a 20%, 30%, 40%, 50% or 60% Opti-prep™ solution (2 mL) in a 15-mL centrifugation tube with a conical bottom (Greiner Bio-one, GmbH, Frickenhausen, Germany). The tubes were then centrifuged at 1000× g for 20 min at room temperature [12]. The proportion of sperm that passed through the cushion layer (sperm loss) was calculated by measuring the volume and determining the sperm concentration of the pellet that developed beneath the Opti-prep™ solution after centrifugation, using a NucleoCounter SP-100 according to the manufacturer's instructions and with the following formula:

$$\text{Sperm loss \%} = (\text{total sperm in pellet} \div \text{total sperm loaded}) * 100$$

Modified Sedimentation and Modified Flotation DGC Techniques

Semen Collection and ProcessingFollowing the collection of an ejaculate from 7 stallions of different breeds (6.2 ± 4.2 years of age) and the initial processing, as described above, the diluted semen was divided into two portions. One portion was further diluted (1:1) with INRA-96 (DS = diluted semen) and used for the conventional double-layer density gradient technique (referred to as the modified sedimentation DGC technique), i.e., diluted semen was layered on top of two solutions of different densities (Figure 1a). A sub-portion of the diluted semen was kept at room temperature to serve as a diluted, non-centrifuged control (NC) sample. The other prediluted aliquot was further diluted (1:1) with Opti-prep™ 60% solution (DS-Opti-prep™) to increase the density of the semen and used for the modified

flotation DGC technique (Figure 1b). Semen samples recovered before (raw and diluted semen) and after centrifugation were snap-frozen for a subsequent DNA integrity analysis by the sperm chromatin structure assay (SCSA) and alkaline comet assay.

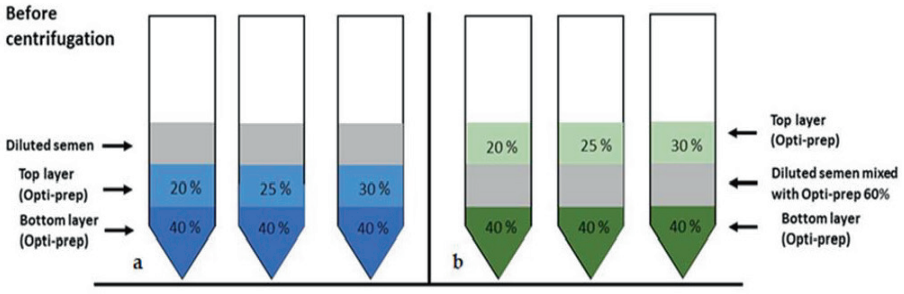

Figure 1. *Graphical illustration of the density gradient centrifugation (DGC) techniques before centrifugation at 1000× g for 20 min. (**a**) Modified sedimentation DGC technique before centrifugation. (**b**) Modified flotation DGC centrifugation technique before centrifugation.*

Density Gradient Centrifugation (Modified Sedimentation vs. Modified Flotation DGC)

Three density gradient tubes (15 mL) were prepared for each of the modified sedimentation (Figure 1a) and the modified flotation DGC techniques (Figure 1b) by pipetting 2-mL layers of density gradient solution or diluted semen (DS vs. DS-Opti-prep^{TM}). The order of the solutions from bottom to top was:

(1) Modified sedimentation DGC (2 mL/2 mL/2 mL)

(a) Opti-prep^{TM} 40%/Opti-prep^{TM} 20%/DS

(b) Opti-prep^{TM} 40%/Opti-prep^{TM} 25%/DS

(c) Opti-prep^{TM} 40%/Opti-prep^{TM} 30%/DS

(2) Modified flotation DGC (2 mL/2 mL/2 mL)

(a) Opti-prep^{TM} 40%/DS-Opti-prepTM/Opti-prep^{TM} 20%

(b) Opti-prep^{TM} 40%/DS-Opti-prepTM/Opti-prep^{TM} 25%

(c) Opti-prep^{TM} 40%/DS-Opti-prepTM/Opti-prep^{TM} 30%

In comparison to the report on bull semen [8], the 1:1:1 mixture of stallion semen, INRA96 and Opti-prep^{TM} 60% (DS-Opti-prep^{TM}) was less dense than pure 40% Opti- prep^{TM} and could not be placed on the bottom of the tube. Therefore, the DS-Opti-prep^{TM} layer was used as the intermediate layer. All tubes were centrifuged at 1000× g for 20 min at room temperature. After centrifugation (modified sedimentation and modified flotation DGC),

semen bands were recovered separately from the interfaces (from top to bottom) with a 1-mL pipette, and the sperm concentration was adjusted using INRA-96 or HBSS according to the semen parameters to be investigated and kept at room temperature until further analysis.

Semen Analysis

Sperm concentration, motility, viability, acrosome integrity, morphology and DNA integrity were determined prior to centrifugation and in all sperm bands after the modified sedimentation or modified flotation DGC techniques.

Sperm Recovery (SR %)

Sperm recovery was calculated by determining the sperm number in the initial sperm solution and in each band after modified sedimentation or modified flotation DGC by using the volume and concentration measured using a NucleoCounter SP-100 (Chemometec, Allerod, Denmark).

Sperm Motility

The following sperm motility and kinematic parameters were evaluated using a Computer-Assisted Sperm Analysis (CASA) system (Sperm Vision®; Minitüb, Tiefenbach, Germany): total motility (TM %), progressive motility (PM %), average path velocity (VAP μm/s), curved line velocity (VCL μm/s), straight line velocity (VSL μm/s), amplitude of lateral head displacement (ALH μm), straightness (STR % = VSL/VAP ∗ 100), linearity (LIN % = VSL/VCL ∗ 100), beat cross-frequency (BCF Hz) and wobble (WOB% = VAP/VCL ∗ 100). In short, semen samples (before and after centrifugation) were diluted to a concentration of 25–30 million/mL with INRA-96 and incubated at 37 ◦C for 5 min in a metal heating block; three microliters were then loaded into a 20-μm-deep Leja chamber slide (Leja Products BV, Nieuw-Vennep, The Netherlands). Sperm motility was examined in 12 sequential fields in the central part of the chamber, selected by an automated stage (30 frames/field at 60 Hz) using an Olympus BX41 microscope with a camera (resolution: 648 × 484 pixels, PulnixTM-6760CL; JAI A/S, Glostrup, Denmark) and an adaptor (U-PMTVC, Olympus, Hamburg, Germany) at 200× magnification and recorded using SpermVision® software (Version 3.5.6.; Minitüb, Germany). Settings for the classification of motile and progressively motile spermatozoa were as described by Brogan et al. [18].

Viability and Acrosome Integrity (VAI %)

Sperm viability was evaluated using a combination of fluorescent stains, namely Hoechst 33342 (50 µg/mL; Sigma-Aldrich Chemicals) and propidium iodide (PI, 1 mg/mL; Thermo Fisher Scientific). Acrosome intactness was assessed using peanut agglutinin conjugated to Alexa Flour™ 488 (PNA-AF488: 1 mg/mL; Thermo Fisher Scientific). Briefly, 484 µL of HBSS and 10 µL of sperm suspension (5×105 spermatozoa) was pipetted into a flow cytometry tube to which was added 2 µL of each fluorescent stain, i.e., Hoechst 33342 (H33342), PI and PNA-AF488. The cell suspension was gently vortexed, incubated for 15 min at room temperature and examined (10,000 cells per sample) using a FACS Canto II flow cytometer equipped with 405 nm (30 mW), 488 nm (20 mW) and 633 nm (17 mW) lasers. Blue (H33342), green (PNA-AF488) and red (PI) fluorescence were collected by 450/50 BP, 530/30 BP and 585/42 BP filters, respectively. After defining the single-cell population on the basis of forward and side scatter, the sperm population was further gated to obtain the percentages of viable (H33342-positive and PI-negative) and acrosome-intact (PNA-AF488-negative) spermatozoa in FCS Express software (version 3; De Novo Software, Los Angeles, CA, USA). Spectral overlap was compensated after acquisition of the data.

Normal Morphology (NM %)

Semen samples prior to (raw) and after centrifugation (all bands) were fixed in buffered formol saline [19]. Differential interference contrast (DIC) microscopy was used to evaluate the morphology of the sperm cells. A total of 200 sperm cells per sample were evaluated for sperm defects. Each sperm cell was examined at 1000× magnification (oil immersion) and scored individually for all defects of acrosome (knobbed); head (detached, crater, vacuole and pyriform); neck (proximal droplet); mid-piece (distal droplet, bent, mitochondrial aplasia and double) and tail (coiled/bent and double) to classify it as morphologically normal or abnormal [20,21].

Sperm DNA Integrity

Sperm Chromatin Structure Assay (SCSA)

Semen samples collected prior to (raw) and after centrifugation (all bands) were snap-frozen and stored in liquid nitrogen. Sperm DNA integrity was evaluated using the sperm chromatin structure assay (SCSA) as described by Evenson and Jost [22]. Acridine orange stain was used after acid denaturation to identify the proportion of spermatozoa possessing unstable chromatin. Fluorescence signals (green and red) were collected using the 530/30 BP and the

670-nm-long pass filter, respectively, on the FACS Canto II flow cytometer. FCS express software was used to evaluate the recorded files. Ten thousand spermatozoa were recorded for each sample. Analysis quality assurance was attained by running a semen sample with the known DNA fragmentation index (DFI) before starting a flow cytometry session and after every twenty samples in a session. Total DFI% was determined by including cells with moderate and high DFI [23].

Alkaline Comet Assay

The comet assay protocol was used as described by Simon et al. [24], with minor modifications. Briefly, 200 µL of normal melting point agarose gel (0.5%; Tebu-Bio, Heerhugowaard, The Netherlands) was pipetted onto prewarmed glass slides (45 ◦C) and covered with a 24 mm by 50 mm cover slip. Agarose was solidified by maintaining the slides at room temperature for 20 min, and the cover slip was then gently removed. Ten microliters of sperm suspension (snap-frozen samples thawed and diluted to 6 × 106/mL in PBS) was mixed with 75 µL of low melting point agarose (0.5%; Thermo Fisher Scientific) and pipetted on top of the normal melting point agarose. A cover slip was quickly placed, and the slides were left at room temperature for 20 min. After removing the cover slip, the slides were immersed in 45-mL lysis solution (2.5-M NaCl, 100-mM Na2EDTA and 10-mM Tris–HCl, kept at 4 ◦C and mixed with 500 µL of Triton X-100) and kept for 1 h at 4 ◦C in a coplin jar. The slides were removed, and 2.5 mL of Dithiothreitol (10mM) was added, and the coplin jar was inverted to ensure mixing. The slides were immersed again and kept for 30 min at 4 ◦C. After removing the slides, 2.5 mL of Lithium di-iodosalicylate (4 mM) were added into the coplin jar, and, after mixing, the slides were immersed again and maintained for 90 min at room temperature. The slides were removed and drained by standing them vertically on tissue paper and then immersed in fresh alkaline electrophoresis buffer (15 mL of 10-M NaOH and 2.5 mL of 200-mM EDTA in 1000-mL deionized distilled water) for 20 min. Electrophoresis was performed for 10 min by applying a 25-V current adjusted to 300 ± 4 mA. After electrophoresis, the slides were removed, drained as previously and flooded with three changes of neutralization buffer (0.4-M Tris) for 5 min each. The slides were drained again and stained with 50 µL of freshly prepared 1:9 diluted Ethidium bro- mide staining solution (stock solution 200mg/mL; Thermo Fisher Scientific) and covered with a cover slip. The slides were visualized with a TCS SPE-II system (Leica Microsystems GmbH, Wetzlar, Germany) attached to an inverted semiautomated DMI4000 microscope (Leica) with a 20× magnification objective (oil); images were saved for the subsequent analysis. Fifty comets

per slide (Figure 2) were analyzed using the Open comet tool [25]. The following comet parameters were recorded for analysis: (1) tail DNA% (tail DNA content as a percentage of the total comet DNA content), (2) tail moment (tail length multi- plied by tail DNA%), (3) olive moment (product of tail DNA% and the distance between the intensity-weighted centroids of the head and tail) and (4) tail length. Spermatozoa treated with DNase II (1mg/mL) served as a positive control and were included in each electrophoresis run.

Modified Flotation DGC Processing of Ejaculates from Friesian Stallions with High Sperm DFI

Semen was collected on alternate days from 3 mature Friesian stallions (10 ± 6 years) with high sperm DFI (range: 22–41%). In total, three ejaculates per stallion were processed using the modified flotation DGC with Opti-prepTM 20% as the top layer (Opti-prep^{TM} 40%/DS-Opti-prepTM/Opti-prepTM 20%), and sperm recovery, motility, morphology and DNA integrity (SCSA and comet assay) were determined as described earlier for Band 2 (interface between Opti-prepTM 20% and DS-Opti-prepTM). In addition, viability and acrosome integrity were assessed along with mitochondrial and total cellular ROS pro- duction using MitoSOX Red (MSR; Thermo Fisher Scientific) and dihydroethidium (DHE; Thermo Fisher Scientific) as described by Hall et al. [26], with some minor modifications. Briefly, 200 µL of sperm suspension in HBSS (2 million spermatozoa) were incubated at 37 ◦C for 15 min with Hoechst 33258 (H33258: final concentration, 1 µg/µL), PNA-Alexa Flour 647 (final concentration, 1 µg/µL) and 2 µM (final concentration) of MSR or DHE. Sperm cells treated with 25-µM arachidonic acid served as a positive control for high MSR or high DHE levels, because this treatment induces ROS generation via the mitochondrial pathway [27]; the arachidonic acid treatment was included in each flow cytometry session/replicate. Blue (H33258), far-red (PNA-AF647) and red (MSR or DHE) fluorescence were collected using the 450/50 BP, 660/20 BP and 585/42 BP filters, respectively. After defining the single-cell population, live acrosome-intact spermatozoa were gated for low mitochondrial or low total cell reactive oxygen species (ROS). The results are reported as the percentage of viable acrosome-intact sperm cells with low ROS.

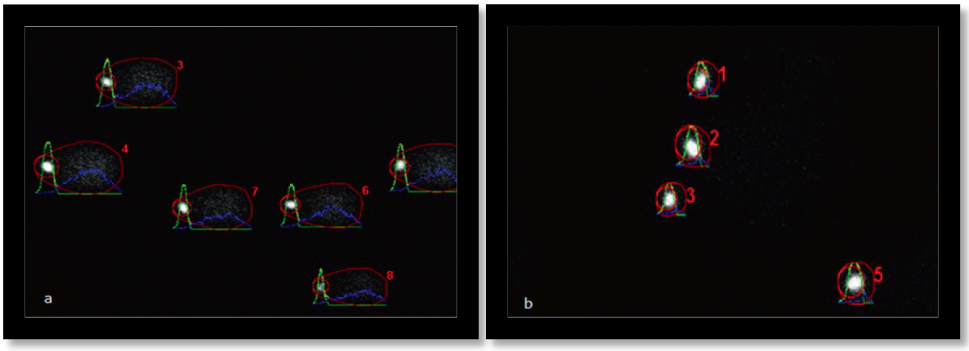

Figure 2. *Images of the alkaline comet assay analyzed using Open comet software.* ***(a)*** *Raw semen sample containing DNA-damaged spermatozoa.* ***(b)*** *Band2 from a modified flotation DGC (top layer Opti-prepTM 20% diluted semen mixed with Opti-prepTM 60% and bottom layer Opti-prepTM 40%) with spermatozoa without DNA damage. Red outline and number (regular comet suitable for evaluation), green profile (comet head), yellow profile (comet tail) and blue profile (comet equal to head plus tail) (full details at https://cometbio.org/documentation.html#interface, accessed on 30 June 2021).*

Statistical Analysis

The Wilcoxon matched pairs signed rank test was used to detect the differences in (a) sperm numbers passing through or collecting at the interfaces of the different Opti- prepTM solutions, (b) semen quality parameters before and after modified sedimentation or modified flotation DGC and (c) semen quality parameters between the three best methods of DGC. A linear mixed model was used to examine the effect of the modified flotation DGC on sperm DFI in ejaculates from Friesian stallions (n = 3) with high sperm DFI (n = 9 ejaculates). Statistical analysis was performed using JMP® software (version 15.2; SAS Institute, Cary, NC, USA), and a p-value ≤ 0.05 was considered statistically significant. Data are reported as the mean ± SD (standard deviation).

Results

Determination of the Optimal Opti-prep™ Solution to Use as Cushion/Bottom Layer

Sperm passage through the Opti-prep™ layer decreased significantly with an increase in the density of the Opti-prep™ solution (Figure 3). Sperm passage was significantly higher for the 20% and 30% Opti-prep™ solutions than for the 40%, 50% and 60% solutions and was significantly higher for the Opti-prep™ 20% than the 30% solution. However, no significant difference in sperm passage was evident between the 40%, 50% and 60% Opti- prep™

solutions. Therefore, an Opti-prep^{TM} 40% solution was used in the subsequent experiments as the cushion/bottom layer.

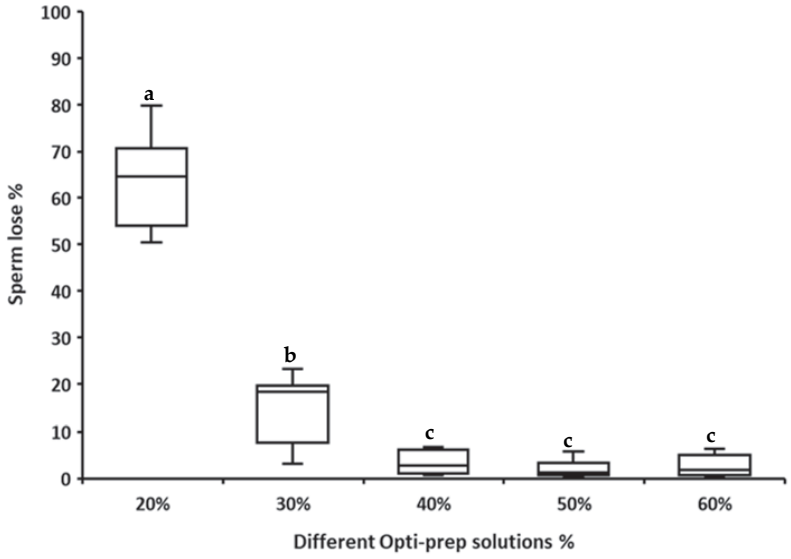

Figure 3. *Percentage of sperm lost through the cushion layer after centrifugation at 1000× g for 20 min using cushion layers consisting of different percentages of Opti-prepTM (20–60%). The lines ("whiskers") on the top and bottom of each box show the range of sperm lost, and the horizontal line on each box represents the median (n = 6 stallions). Different letters indicate boxes that differ significantly (p ≤ 0.05).*

Modified Sedimentation and Modified Flotation DGC Techniques

Modified Sedimentation DGC

The modified sedimentation density gradient centrifugation technique yielded two bands (sperm layers): one band at the interface between the diluted semen and Opti- prepTM top layer (Band1) and a second band at the interface between the Opti-prepTM top and bottom layers (Band2) (Figure 4a). The sperm recovery and quality parameters for all of the bands are presented in Table 1. The sperm cell recovery was highest in Band2 for Opti-prepTM 20% and 25% and in Band1 for Opti-prepTM 30% (Table 1), and these were therefore considered the most interesting for comparing the effects on sperm cell quality. The percentage of spermatozoa with an intact plasma membrane and acrosome was increased in Band1 for Opti-prepTM 25% and 30%. The percentage of sperm with normal morphology was increased in Band2 compared to non-centrifuged extended semen (NC) for all the top

layer Opti-prepTM concentrations tested and did not differ between the NC and Band1 for Opti-prepTM 30%. However, the total motility was increased above the NC only in Opti-prepTM 30% Band1, while the percentage of progressively motile spermatozoa did not increase above the NC in any of the post-DGC bands. The DFI was significantly lower in Band1 for Opti-prep^{TM} 30% than in raw semen but did not differ between raw semen and either Band1 or Band2 for Opti-prep^{TM} 20% and 25%. With regards to the bands of interest (Band2 Opti-prep^{TM} 20% and 25% and Band1 Opti-prep^{TM} 30%), the sperm DFI significantly decreased and percentages of viable acrosome-intact and (total) motile sperm increased in Band1 for Opti-prep^{TM} 30% using the modified sedimentation DGC. This approach was therefore considered the best for modified sedimentation DGC and used for the subsequent comparison with the modified flotation DGC.

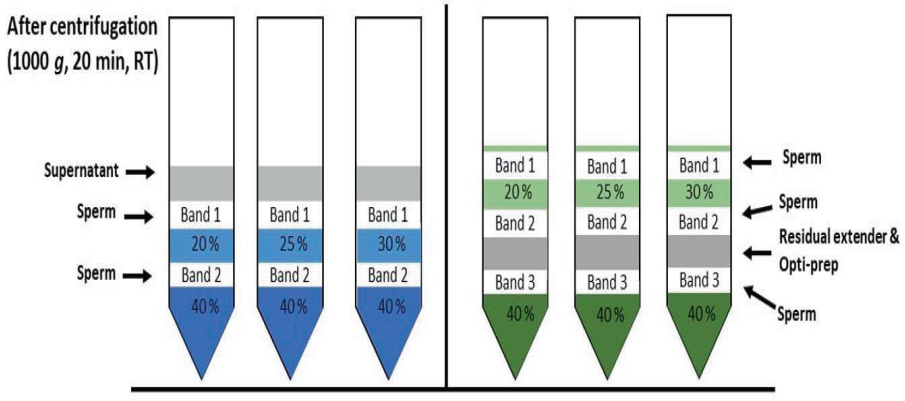

Figure 4. *Graphical illustration of the density gradient centrifugation (DGC) techniques after centrifugation at 1000× g for 20 min. (a) Modified sedimentation DGC technique after centrifugation. (b) Modified flotation DGC technique after centrifugation.*

Modified Flotation DGC

The modified flotation DGC yielded three bands (selected sperm populations): Band1 (on the Opti-prep^{TM} top layer), Band 2 (at the interface between the Opti-prep^{TM} top layer and the DS-Opti-prep^{TM}) and Band3 (interface between DS-Opti-prep^{TM} and the Opti-prep^{TM} bottom layer) (Figure 4b). The sperm recovery was the highest in Band2 for Opti-prep^{TM} 20% and 25% and Band1 for Opti-prep^{TM} 30% (Table 2). On the basis of a higher sperm yield, we focused on these three bands for their sperm quality parameters. The percentage of viable and acrosome-intact spermatozoa was significantly improved above the NC in Band2 for Opti-prep^{TM} 20% and 25%. The total and progressive motility were significantly

Table 1. Effect of modified sedimentation density gradient centrifugation (DGC) on stallion sperm populations. Semen parameters include sperm recovery (SR), viability and acrosome intactness (VAI), total motility (TM), progressive motility (PM), average path velocity (VAP), curvilinear velocity (VCL), straight line velocity (VSL), amplitude of lateral head displacement (ALH), beat cross-frequency (BCF), wobble (WOB), straightness (STR), linearity (LIN), DNA fragmentation index (DFI) and normal morphology (NM) before and after centrifugation by the modified sedimentation DGC (diluted semen layered onto the Opti-prep™ layers). Within a row, values with different superscript letters differ significantly ($p \leq 0.05$, $n = 7$ stallions).

Semen Parameters	Non-Centrifuged Semen	Opti-prep™ 20% Top Layer		Opti-prep™ 25% Top Layer		Opti-prep™ 30% Top Layer	
		Band1	Band2	Band1	Band2	Band1	Band2
SR %		9 ± 4^{a}	66 ± 14^{b}	32 ± 16^{c}	$46 \pm 13^{c,d}$	$63 \pm 11^{b,d}$	16 ± 6^{a}
VAI %	81 ± 6^{a}	$87 \pm 8^{a,c}$	62 ± 19^{b}	89 ± 6^{c}	52 ± 19^{b}	90 ± 6^{c}	20 ± 17^{d}
TM %	69 ± 7^{a}	$43 \pm 10^{b,c}$	64 ± 12^{a}	$65 \pm 10^{a,c}$	55 ± 16^{c}	80 ± 8^{d}	31 ± 21^{b}
PM %	50 ± 16^{a}	$25 \pm 8^{b,c}$	26 ± 9^{b}	47 ± 4^{a}	18 ± 9^{c}	55 ± 11^{a}	9 ± 12^{d}
VAP µm/s	99 ± 10^{a}	$89 \pm 9^{a,c}$	$64 \pm 13^{b,d}$	$84 \pm 20^{c,d}$	$60 \pm 16^{b,d}$	$87 \pm 15^{c,d}$	65 ± 20^{d}
VCL µm/s	157 ± 19^{a}	157 ± 14^{a}	$105 \pm 23^{b,c}$	$150 \pm 39^{a,c}$	103 ± 27^{c}	140 ± 19^{c}	113 ± 32^{c}
VSL µm/s	78 ± 11^{a}	$67 \pm 8^{a,c}$	$52 \pm 12^{b,c,e}$	$65 \pm 14^{c,e}$	$49 \pm 15^{d,e}$	$70 \pm 12^{c,e}$	51 ± 18^{e}
ALH µm	3.3 ± 0.6^{a}	$3 \pm 0.4^{a,c}$	$2.4 \pm 0.5^{b,c}$	$3 \pm 0.8^{a,b,c}$	$2.3 \pm 0.4^{b,c}$	$2.9 \pm 0.5^{a,b,c}$	2.5 ± 0.8^{c}
BCF Hz	42 ± 4^{a}	41 ± 3^{a}	38 ± 5^{a}	40 ± 3^{a}	37 ± 5^{a}	41 ± 3^{a}	38 ± 6^{a}
WOB %	$63 \pm 5^{a,c}$	$56 \pm 7^{b,c}$	$61 \pm 9^{a,b,c}$	57 ± 7^{b}	$58 \pm 6^{a,b,c}$	62 ± 5^{c}	$57 \pm 10^{a,b,c}$
STR %	80 ± 7^{a}	80 ± 6^{a}	80 ± 8^{a}	80 ± 6^{a}	80 ± 7^{a}	80 ± 6^{a}	80 ± 11^{a}
LIN %	$50 \pm 8^{a,b}$	$43 \pm 8^{a,b}$	$50 \pm 12^{a,b}$	44 ± 8^{b}	$47 \pm 9^{a,b}$	$50 \pm 7^{a,b}$	$45 \pm 14^{a,b}$
DFI %	12 ± 6^{a}	10 ± 11^{a}	10 ± 3^{a}	$10 \pm 9^{a,b}$	14 ± 7^{a}	5 ± 3^{b}	33 ± 17^{c}
NM %	52 ± 12^{a}	16 ± 12^{b}	62 ± 18^{c}	24 ± 10^{b}	74 ± 10^{d}	47 ± 15^{a}	67 ± 14^{e}

increased in Band2 for all the Opti-prep™ top layers tested. The DFI was significantly lower than in snap-frozen raw semen in Band1 and Band2 for nearly all the Opti-prep™ top layers examined (except Band2 for Opti-prep™ 30%) and was significantly higher in Band3 for all the top layers. The percentage of sperm cells with normal morphology was significantly higher in Band2 with Opti-prep™ 20% and 25%. Overall, the DFI was reduced in Band2 for Opti-prep™ 20% and 25% (Table 2), and the percentages of viable acrosome-intact, total and progressively motile, and morphology normal sperm all increased in Band2 for Opti-prep™ 20% and 25% compared to the uncentrifuged samples. Therefore, Band2 from Opti-prep™ 20% and 25% were chosen for further comparisons with the best variant from the modified sedimentation DGC.

Comparison between the Modified Sedimentation and Modified Flotation DGC Techniques

A comparison was made between one modified sedimentation DGC (Band1 from Opti-prep™ 30%) and two modified flotation DGC (Band2 from Opti-prep™ 20% and 25%) protocols to determine which method most improved the semen quality parameters (Table 3). One of the modified flotation DGCs (Band2 from Opti-prep™ 20%) and the modified sedimentation DGC (Band1 with Opti-prep™ 30%) protocol resulted in similar sperm recoveries (57 ± 7% and 63 ± 11%, respectively) that were much higher than for the other modified flotation DGC protocol (Band2 from Opti-prep™ 25%: 37 ± 14%; Table 3). All three protocols resulted in significant increases in the percentages of the (total) motile sperm cells and spermatozoa with an intact plasma membrane and acrosome compared to the NC and a significant drop in the DFI compared to raw semen, with no differences between the protocols. By contrast, the percentages of progressively

motile spermatozoa and sperm cells with normal morphology were significantly increased above the NC by both modified flotation DGC (Band2 with Opti-prep™ 20% and 25%) but not the modified sedimentation DGC (Band1 with Opti-prep™ 30%) protocol. Overall, although all three protocols significantly improved the DFI in the selected sperm population, the modified flotation DGC protocol using Opti-prep™ 20% as the top layer was preferred on the basis of better sperm recovery than the modified flotation DGC with an Opti-prep™ 25% top layer and higher percentages of progressively motile and morphologically normal sperm than the modified sedimentation DGC protocol with the 30% top layer. The modified flotation DGC with Opti-prep™ 20% was therefore selected to process the ejaculates from three Friesian stallions with high sperm DFI.

Table 2. Effect of a modified flotation density gradient centrifugation (DGC) protocol on stallion sperm populations. The semen parameters include sperm recovery (SR), viability and acrosome intactness (VAI), total motility (TM), progressive motility (PM), average path velocity (VAP), curvilinear velocity (VCL), straight line velocity (VSL), amplitude of lateral head displacement (ALH), beat cross-frequency (BCF), wobble (WOB), straightness (STR), linearity (LIN), DNA fragmentation index (DFI) and normal morphology (NM) before and after centrifugation by the modified flotation DGC (diluted semen mixed with Opti-prep™ 60% and layered between the top layer and a 40% Opti-prep™ bottom layer). Within a row, values with different superscript letters differ significantly ($p \leq 0.05$, $n = 7$ stallions).

Semen Parameters	Non-Centrifuged Semen	Opti-prep™ 20% Top Layer			Opti-prep™ 25% Top Layer			Opti-prep™ 30% Top Layer		
		Band1	Band2	Band3	Band1	Band2	Band3	Band1	Band2	Band3
SR %		8 ± 6 a,e	57 ± 7 b,d	10 ± 2 a,e	28 ± 14 a, c	37 ± 14 c,d	10 ± 2 a	47 ± 16 d	21 ± 10 e	9 ± 1 a
VAI %	81 ± 4 a	52 ± 31 b,d	89 ± 4 c	27 ± 7 b	67 ± 16 d	88 ± 5 c	25 ± 9 b	85 ± 4 a,c	85 ± 6 a,c	25 ± 10 b
TM %	69 ± 7 a	33 ± 14 b	82 ± 10 c,e	30 ± 13 b,d,f	52 ± 13 d	83 ± 10 e	30 ± 13 b,d,f	66 ± 10 f	77 ± 16 c,e	27 ± 14 d
PM %	50 ± 16 a	9 ± 6 b	62 ± 10 c,g	21 ± 13 b,d,f	19 ± 11 d	72 ± 9 e,g	22 ± 12 b,d,f	31 ± 9 f	70 ± 16 g	19 ± 13 b,d
VAP µm/s	99 ± 10 a	71 ± 21 b,d,e	90 ± 7 c,d	73 ± 11 b,d,e	79 ± 19 d,e	88 ± 17 a,d	78 ± 19 a,d,e	69 ± 11 e	91 ± 7 c,d	64 ± 15 e
VCL µm/s	157 ± 19 a	137 ± 41 a,b,c	142 ± 19 a	115 ± 31 b,c	142 ± 27 a	134 ± 33 a,b	117 ± 37 a,b,c	122 ± 20 b,c	139 ± 23 a	97 ± 33 c
VSL µm/s	78 ± 11 a	53 ± 14 b	72 ± 6 c	60 ± 5 b	57 ± 11 b,c	74 ± 13 a,c	65 ± 12 a,b,c	53 ± 9 b	76 ± 6 a	55 ± 9 b
ALH µm	3.3 ± 0.6 a,d	3.1 ± 0.8 a,d	2.8 ± 0.6 a	2.5 ± 0.9 a,d	3.2 ± 0.7 d,e	2.5 ± 0.7 e	2.2 ± 0.8 b,e	2.7 ± 0.5 c	2.6 ± 0.7 c	2 ± 0.8 c
BCF Hz	42 ± 4 a,b,c,d	37 ± 3 a,d	42 ± 2 b,d	39 ± 3 a,d	39 ± 2 a	43 ± 2 c,d	42 ± 3 d	38 ± 2 a	42 ± 3 b	41 ± 2 b
WOB %	63 ± 5 a,c,d	51 ± 6 b,c	63 ± 7 a,d	64 ± 8 a,b,c,d	54 ± 5 b,c,d	66 ± 6 a,d	67 ± 6 a,d	56 ± 5 c	66 ± 8 d	67 ± 8 a,d
STR %	80 ± 7 a,e	80 ± 9 a,b,c,e	80 ± 8 a,c,d,e	80 ± 8 a,c,d,e	70 ± 5 b	80 ± 7 c	90 ± 7 e	80 ± 7 a	80 ± 8 e	90 ± 6 d,e
LIN %	50 ± 8 a,b,d	40 ± 8 a,c,d	50 ± 1 b	60 ± 1 a,b,c	40 ± 3 c,d	60 ± 9 b	60 ± 9 b	40 ± 7 d	60 ± 1 b	60 ± 1 b
DFI %	12 ± 6 a,e	3 ± 2 b,d	4 ± 2 b	41 ± 13 c	3 ± 2 b,d	5 ± 4 b,e	42 ± 17 c	3 ± 1 d	7 ± 3 e	40 ± 18 c
NM %	52 ± 12 a	10 ± 5 b	66 ± 16 c,d	65 ± 9 a,c,d	13 ± 7 b	73 ± 7 d,f	63 ± 10 c	33 ± 15 e	76 ± 9 f	58 ± 14 a,c,d

Modified Flotation DGC Processing of Ejaculates from Friesian Stallions with High Sperm DFI

The average sperm recovery in Band2 after modified flotation DGC with an Opti-prep™ 20% top layer was only 20 ± 3% (Table 4). The percentages of viable acrosome-intact sperm cells with low mitochondrial and low total cellular ROS were significantly higher after (83 ± 8% and 77 ± 8%, respectively) than the prior-to-modification flotation DGC (62 ± 8% and 60 ± 6%, respectively). In addition, the modified flotation DGC resulted in significant increases compared to pre-centrifugation samples in total motility (TM; 66 ± 10% post- vs. 47 ± 7% pre-DGC, respectively), progressive motility (PM; 50 ± 14% post- vs. 23 ± 10% pre-DGC) and percentage of spermatozoa with normal morphology (NM; 49 ± 8% post- vs. 37 ± 10%). Most importantly, the sperm DFI as measured by SCSA was much lower after (5 ± 2%) than prior to (31 ± 11%) the modified flotation DGC. Similarly, the comet assay parameter, %tail DNA, was significantly reduced after the modified flotation DGC (38 ± 3%) compared to in raw semen (57 ± 3%). Finally, there were no significant differences in the percentage of sperm with low mitochondrial or total ROS levels within the viable, acrosome-intact sperm population.

Table 4. Effect of a modified flotation density gradient centrifugation (DGC) protocol on the sperm recovery (SR), viable acrosome-intact spermatozoa with low mitochondrial reactive oxygen species (VAI L-M-ROS), viable acrosome-intact spermatozoa with low total cellular reactive oxygen species (VAI L-T-ROS), total motility (TM), progressive motility (PM), DNA fragmentation index (DFI), comet assay tail length, tail DNA, tail moment, olive moment and normal morphology (NM) for 3 Friesian stallions (3 ejaculates per stallion, $n = 9$) with a high initial DFI. Within a row, an asterisk indicates values that differ before and after the modified flotation DGC ($p \leq 0.05$).

Semen Parameter	Stallion 1		Stallion 2		Stallion 3		Overall Average	
	Before	After	Before	After	Before	After	Before	After
SR%		18 ± 10		25 ± 6		20 ± 3		
VAI L-M-ROS%	56 ± 8	75 ± 10	63 ± 9	87 ± 5	66 ± 1	86 ± 3	62 ± 8	83 ± 8 *
VAI L-T-ROS %	54 ± 5	74 ± 6	59 ± 2	78 ± 3	66 ± 4	80 ± 13	60 ± 6	77 ± 8 *
TM%	42 ± 3	56 ± 8	45 ± 9	61 ± 1	54 ± 3	75 ± 3	47 ± 7	66 ± 10 *
PM%	12 ± 4	38 ± 6	24 ± 5	43 ± 8	34 ± 2	64 ± 5	23 ± 10	50 ± 14 *
DFI%	41 ± 15	7 ± 3	22 ± 2	4 ± 2	30 ± 2	4 ± 1	31 ± 11	5 ± 2 *
Tail length µm	93 ± 5	43 ± 16	33 ± 31	15 ± 19	74 ± 10	70 ± 6	67 ± 13	42 ± 26 *
Tail DNA%	65 ± 3	32 ± 11	26 ± 10	13 ± 4	80 ± 4	69 ± 9	57 ± 25	38 ± 26 *
Tail moment µm	63 ± 5	17 ± 7	4 ± 3	4 ± 3	59 ± 11	51 ± 3	42 ± 29	24 ± 21
Olive moment µm	39 ± 4	9 ± 4	2 ± 2	3 ± 2	37 ± 8	32 ± 2	26 ± 18	15 ± 13
NM%	25 ± 6	39 ± 3	37 ± 2	52 ± 2	46 ± 2	55 ± 6	37 ± 10	49 ± 8 *

Discussion

The aim of the current study was to optimize a DGC technique for removing DNA fragmented spermatozoa from the semen of stallions with high DFI levels, without any adverse effects on the other aspects of sperm quality or excessive loss of "normal" sperm. The modified flotation DGC protocol that involved mixing extended equine semen with Opti-prep™ (Iodixanol 60%) to increase its density prior to layering between the gradient solutions of lower and higher density does not appear to have been reported previously for stallion semen. This modified flotation DGC protocol proved superior to the modified sedimentation DGC in that, while both significantly reduced the DFI of the selected sperm cell population, only the modified flotation DGC reliably increased the percentages of (progressively) motile spermatozoa and spermatozoa with normal morphology. Moreover, the modified flotation DGC appears to be useful for processing ejaculates of (Friesian) stallions with high sperm DFI (>20%), because it reduced the mean sperm DFI from 31% to 5% while simultaneously improving the other semen quality parameters, including the percentages of viable, acrosome-intact, motile, progressively motile and morphologically normal spermatozoa.

Opti-prep™ 40% was selected as the most suitable density to serve as a cushion layer, because only a small percentage (4%) of sperm cells passed through this solution. This suggests that the majority of stallion spermatozoa had a density of less than 1.215 g/mL. The selected cushion layer contrasts to a previous study in which Opti-prep™ 30% was used as a bottom layer [12]. Although the same centrifugation force and time were used in both studies (1000× g, 20 min), we compared different density gradient solution percentages (Opti-prep™ 20–60%) to establish the optimal bottom layer. Opti-prep™ 30% appeared to be less suitable as a bottom layer in our study, because approximately 20% of the sperm cells passed through the cushion during centrifugation.

The modified flotation DGC yielded three different sperm populations, compared to the two different sperm populations resulting after the modified sedimentation DGC protocol. Clearly, this is related to the number of colloid density interfaces created and yielding three populations via the modified flotation DGC replicated the results of a study on bull semen [8]. Although the colloid densities used in this study and the exact layering procedure differed between the current study and the bull semen study [8], this was a requirement of the difference in density between stallion and bull spermatozoa. Nevertheless, this suggests that the modified flotation DGC allows a more accurate separation of spermatozoa into

different populations with distinct densities. This was apparent both for stallions of various breeds with grossly normal semen parameters and the subfertile Friesian stallions. The modified flotation DGC selected higher quality spermatozoa without any obvious adverse effects on the other parameters of sperm quality. The yield of high- quality spermatozoa was higher than reported for double-layer DGC in previous studies using Opti-prep™ [12], Percoll [14] or EquiPure [28]. However, the improvement in DFI in the recovered spermatozoa in our study was comparable to previous studies [12,28].

The three sperm populations separated by the modified flotation DGC technique were separated based on the spermatozoa's density. It was obvious that a majority of morphologically defective spermatozoa were less dense and moved upwards to the top of the Opti-prep™ layer with the lowest density (20% or 25%), indicating that they had densities of less than 1.110 g/mL or 1.137 g/mL. The majority of the progressively motile and morphologically normal spermatozoa with intact DNA also moved upwards but stayed at the interface between the low-density Opti-prep™ and the layer of diluted semen mixed with Opti-prep™. The density of the mixed layer was theoretically close to a 30% Opti-prep™ layer. Therefore, the density of the cells must range between 1.110 g/mL and 1.163 g/mL. Nonviable (membrane-damaged) spermatozoa and spermatozoa with a high DFI were generally dense and, therefore, stayed at the interface of semen mixed with Opti-prep™ and the cushion layer after centrifugation [8].

Among the three most promising DGC variants selected for direct comparison, the modified flotation DGC with an upper layer of Opti-prep™ 20% appeared to be the best, because it combined improvement in the range of semen quality parameters with a relatively high sperm recovery. Using Opti-prep™ 25% as the top layer in a modified flotation DGC protocol similarly improved many of the semen quality parameters and seemed to select a population with better progressive motility than Opti-prep™ 20%; however, the sperm recovery was almost half that recorded for Opti-prep™ 20%. This would be a disadvantage if the spermatozoa were being collected for insemination, because it would lead to a smaller dose, or fewer insemination doses, and might therefore negatively influence the number of mares that could be inseminated and become pregnant. On the other hand, the modified flotation DGC with Opti-prep™ 25% could be beneficial when selecting small numbers of high-quality spermatozoa for assisted reproductive technologies, such as intracytoplasmic sperm injection. Although the sperm recovery and DFI appeared to be similar between the modified sedimentation DGC with Opti-prep™ 30% and the modified flotation DGC with

Opti-prep™ 20%, the percentages of progressively motile and morphologically normal sperm were lower after the modified sedimentation DGC. This would result in a lower number of high-quality spermatozoa available for insemination.

This study indicated that the modified flotation DGC could have clinical value for processing ejaculates of stallions with high sperm DFI levels (>20–30%). Given that sperm DFI levels > 25% have been reported to compromise fertility [29] and the defect is non- compensable, it is imperative to decrease the percentage of spermatozoa with damaged DNA prior to insemination by applying a sperm selection technique. The modified flotation DGC was effective in markedly reducing the percentage of sperm with fragmentated DNA in ejaculates from Friesian stallions, from levels considered very likely to compromise fertility (30%) to levels compatible with normal-to-good fertility (5%). While the SCSA quantifies the ratio of single-stranded to double-stranded DNA in a single cell, the alkaline comet assay detects the extent of single- and double-stranded breaks, incomplete excision repair sites, crosslinks and alkaline labile sites in the DNA (reviewed by Kumaravel et al. [30]). In analogy to the SCSA, the alkaline comet assay showed that the modified flotation DGC enriched for cells with fewer average DNA damage/labile sites (37% tail DNA) than in the original sample (non-selected sperm: 57% tail DNA). Nevertheless, it remains to be determined to what extent selecting spermatozoa using this modified flotation DGC improves the fertility of these stallions after artificial insemination. While the modified flotation DGC also improved the other semen quality parameters (i.e., viability, acrosome integrity, total motility, progressive motility and normal morphology), the sperm recovery by DGC of semen with a high DFI was low (approximately 20%). This low sperm recovery could, however, be considered a predictable consequence of the high percentage of DNA-damaged and morphologically abnormal spermatozoa present in the ejaculates of stallions with a high sperm DFI. Processing the whole ejaculates for the three Friesian stallions included in this study would have resulted in total mean yields of 222×106, 118 ×106 and 382×106 morphologically normal, motile sperm per ejaculate. This low sperm recovery may therefore mean that low dose deep-intrauterine insemination close to ovulation needs to be performed to compensate for low insemination doses after applying this modified flotation DGC (a standard dose for insemination with fresh semen is 300 × 106 morphologically normal, motile sperm [31]). Certainly, further studies are required to upscale this modified flotation DGC to process whole ejaculates for AI, since, in the current study, only a portion of the ejaculate was processed.

Finally, the semen samples from the Friesian stallions were also evaluated for mitochondrial and total cellular reactive oxygen species (ROS) prior to and after centrifugation. It has been suggested that the physical shearing forces associated with sperm centrifugation can trigger ROS generation [32]. However, we did not detect a significant increase in viable spermatozoa with elevated ROS levels after centrifugation, indicating that this modified flotation DGC has no indirect detrimental effect on the oxidative status of stallion spermatozoa. The stepwise development of the modified flotation DGC methods presented in this manuscript can likewise be transferred to semen from other species and facilitate improvements in the density gradient-based selection of sperm subpopulations.

Conclusions

In conclusion, a modified flotation density gradient centrifugation protocol in which semen was mixed 1:1 with Opti-prep^{TM} 60% and layered between an Opti-prep^{TM} 20% top layer and Opti-prep^{TM} 40% bottom layer was an effective method for decreasing the percentage of sperm cells with fragmentated DNA and increasing the percentage that were viable, acrosome-intact, motile and morphologically normal. While the number of recovered spermatozoa from stallions with initially poor semen quality may be limiting for conventional insemination, it should be adequate for deep intrauterine insemination and ample for ICSI.

Author Contributions: Conceptualization, M.U., H.H., T.A.E.S. and A.C.; data curation, M.U.; investigation, M.U.; methodology, M.U., H.H., T.A.E.S. and A.C.; software, M.U., H.H. and A.C.; supervision, H.H., T.A.E.S. and A.C.; visualization, M.U., H.H., T.A.E.S. and A.C.; writing—original draft, M.U. and writing—review and editing, M.U., H.H., T.A.E.S. and A.C. All authors have read and agreed to the published version of the manuscript.

Funding: This work was supported by the Punjab Educational Endowment Fund (PEEF), Punjab, Pakistan (PEEF/SSMS/18/222).

Institutional Review Board Statement: No ethical approval was required, because semen samples were obtained from the stallions presented for routine semen evaluation.

Informed Consent Statement: Stallion owners were enquired to sign informed consent forms to use the semen of their stallions for research.

Data Availability Statement: The data presented in this study are available in A Modified Flotation Density Gradient Centrifugation Technique Improves the Semen Quality of Stallions with a High DNA Fragmentation Index, Umair et al., 2021.

Acknowledgments: The authors thank Arend Rijneveld for helping with the CASA analysis.

Conflicts of Interest: The authors have no conflict of interest to declare.

References

1.Lewis, S.; Aitken, R.J. DNA damage to spermatozoa has impacts on fertilization and pregnancy. Cell Tissue Res. 2005, 322, 33–41.

2.Evenson, D.P. The sperm chromatin structure assay (SCSA®) and other sperm DNA fragmentation tests for evaluation of sperm nuclear DNA integrity as related to fertility. Anim. Reprod. Sci. 2016, 169, 56–75.

3.Kenney, R.M.; Evenson, D.P.; Garcia, M.C.; Love, C.C. Relationships between sperm chromatin structure, motility, and morphology of ejaculated sperm, and seasonal pregnancy rate. Biol. Reprod. 1995, 52, 647–653.

4.Love, C.C.; Kenney, R.M. The relationship of increased susceptibility of sperm DNA to denaturation and fertility in the stallion. Theriogenology 1998, 50, 955–972.

5.Le, M.T.; Nguyen, T.A.T.; Nguyen, H.T.T.; Nguyen, T.T.T.; Nguyen, V.T.; Le, D.D.; Nguyen, V.Q.H.; Cao, N.T. Does sperm DNA fragmentation correlate with semen parameters? Reprod. Med. Biol. 2019, 18, 390–396.

6.Aguilar, C.; Meseguer, M.; García-Herrero, S.; Gil-Salom, M.; O'Connor, J.E.; Garrido, N. Relevance of testicular sperm DNA oxidation for the outcome of ovum donation cycles. Fertil. Steril. 2010, 94, 979–988.

7.Evenson, D.P.; Wixon, R. Clinical aspects of sperm DNA fragmentation detection and male infertility. Theriogenology 2006, 65, 979–991.

8.Beer-Ljubic´, B.; Aladrovic´, J.; Marenjak, T.S.; Majic´-Balic´, I.; Laškaj, R.; Milinkovic´-Tur, S. Biochemical properties of bull spermatozoa separated in iodixanol density solution. Res. Vet. Sci. 2012, 92, 292–294.

9.Morrell, J.M. Update on semen technologies for animal breeding. Reprod. Domest. Anim. 2006, 41, 63–67.

10. Smith, T.T.; Byers, M.; Kaftani, D.; Whitford, W. The use of iodixanol as a density gradient material for separating human sperm from semen. Arch. Androl. 1997, 38, 223–

230.

11. Harrison, K. Iodixanol as a density gradient medium for the isolation of motile spermatozoa. J. Assist. Reprod. Genet. 1997, 14, 385–387.
12. Stuhtmann, G.; Oldenhof, H.; Peters, P.; Klewitz, J.; Martinsson, G.; Sieme, H. Iodixanol density gradient centrifugation for selecting stallion sperm for cold storage and cryopreservation. Anim. Reprod. Sci. 2012, 133, 184–190.
13. Ford, T.; Graham, J.; Rickwood, D. Iodixanol: A nonionic iso-osmotic centrifugation medium for the formation of self-generated gradients. Anal. Biochem. 1994, 220, 360–366.
14. Sieme, H.; Martinsson, G.; Rauterberg, H.; Walter, K.; Aurich, C.; Petzoldt, R.; Klug, E. Application of techniques for sperm selection in fresh and frozen–thawed stallion semen. Reprod. Domest. Anim. 2003, 38, 134–140.
15. Macpherson, M. Use of a silane-coated silica particle solution to enhance the quality of ejaculated semen in stallions. Theriogenology 2002, 58, 317–320.
16. Morrell, J.M.; Johannisson, A.; Strutz, H.; Dalin, A.; Rodriguez-Martinez, H. Colloidal centrifugation of stallion semen: Changes in sperm motility, velocity, and chromatin integrity during storage. J. Equine Vet. Sci. 2009, 29, 24–32.
17. Pickett, B.W.; Sullivan, J.J.; Byers, W.W.; Pace, M.M.; Remmenga, E.E. Effect of centrifugation and seminal plasma on motility and fertility of stallion and bull spermatozoa. Fertil. Steril. 1975, 26, 167–174.
18. Brogan, P.T.; Beitsma, M.; Henning, H.; Gadella, B.M.; Stout, T. Liquid storage of equine semen: Assessing the effect of D-penicillamine on longevity of ejaculated and epididymal stallion sperm. Anim. Reprod. Sci. 2015, 159, 155–162.
19. Hancock, J.L. The morphology of boar spermatozoa. J. R. Microsc. Soc. 1956, 76, 84–97.
20. Graham, J.K. Analysis of stallion semen and its relation to fertility. Vet. Clin. N. Am. Equine Pract. 1996, 12, 119–130.
21. Varner, D.D. Developments in stallion semen evaluation. Theriogenology 2008, 70, 448–462.
22. Evenson, D.; Jost, L. Sperm chromatin structure assay is useful for fertility assessment. Methods Cell Sci. 2000, 22, 169–189.
23. Larson, K.L.; Brannian, J.D.; Hansen, K.A.; Jost, L.K.; Evenson, D.P. Relationship between assisted reproductive techniques (ART) outcomes and DNA fragmentation (DFI)

as measured by the sperm chromatin structure assay (SCSA®). Fertil. Steril. 2002, 78, S206.

24. Simon, L.; Carrell, D.T. Sperm DNA damage measured by comet assay. In Anonymous Spermatogenesis; Springer: Berlin/Heidelberg, Germany, 2013; pp. 137–146.
25. Gyori, B.M.; Venkatachalam, G.; Thiagarajan, P.S.; Hsu, D.; Clement, M. OpenComet: An automated tool for comet assay image analysis. Redox Biol. 2014, 2, 457–465.
26. Hall, S.E.; Aitken, R.J.; Nixon, B.; Smith, N.D.; Gibb, Z. Electrophilic aldehyde products of lipid peroxidation selectively adduct to heat shock protein 90 and arylsulfatase A in stallion spermatozoa. Biol. Reprod. 2017, 96, 107–121.
27. Aitken, R.J.; Smith, T.B.; Lord, T.; Kuczera, L.; Koppers, A.J.; Naumovski, N.; Connaughton, H.; Baker, M.A.; De Iuliis, G.N. On methods for the detection of reactive oxygen species generation by human spermatozoa: Analysis of the cellular responses to catechol oestrogen, lipid aldehyde, menadione and arachidonic acid. Andrology 2013, 1, 192–205.
28. Edmond, A.J.; Brinsko, S.P.; Love, C.C.; Blanchard, T.L.; Teague, S.R.; Varner, D.D. Effect of centrifugal fractionation protocols on quality and recovery rate of equine sperm. Theriogenology 2012, 77, 959–966.
29. Love, C.C. The sperm chromatin structure assay: A review of clinical applications. Anim. Reprod. Sci. 2005, 89, 39–45.
30. Kumaravel, T.S.; Vilhar, B.; Faux, S.P.; Jha, A.N. Comet assay measurements: A perspective. Cell Biol. Toxicol. 2009, 25, 53–64.
31. Colenbrander, B.; Gadella, B.M.; Stout, T. The predictive value of semen analysis in the evaluation of stallion fertility. Reprod. Domest. Anim. 2003, 38, 305–311.
32. Aitken, R.J.; Clarkson, J.S. Significance of reactive oxygen species and antioxidants in defining the efficacy of sperm preparation techniques. J. Androl. 1988, 9, 367–376.

Chapter 3

In vitro aging of stallion spermatozoa during prolonged storage at 5˚C

Muhammad Umair[1], Anthony Claes[1], Marijn Buijtendorp[2], Juan Cuervo-Arango[3], Tom A.E. Stout[1], Heiko Henning[4]

1 Department of Clinical Sciences, Faculty of Veterinary Medicine, Utrecht University, Utrecht, The Netherlands

2 Dierenartsenpraktijk Horst e.o., Americaanseweg 33, 5961GN Horst, The Netherlands

3 Equine Fertility Group, Faculty of Veterinary Medicine, Universidad CEU Cardenal Herrera, CEU Universities, Alfara del Patriarca, Valencia, Spain

4 Friedrich-Loeffler-Institut, Federal Research Institute for Animal Health, Neustadt, Germany

Published as:

Umair M, Claes A, Buijtendorp M, Cuervo-Arango J, Stout TAE, Henning H. In vitro aging of stallion spermatozoa during prolonged storage at 5°C. Cytometry. 2023;103(6):479-91. https:/ /doi.org/10.1002/ cyto.a.24712

Abstract

Artificial insemination with chilled stallion semen is hampered by a limited period of maximum fertility maintenance (24-48 h). This study used multiparametric flow cytometry to simultaneously measure reactive oxygen species (ROS) production, mitochondrial function or $[Ca^{2+}]i$ and plasma membrane fluidity in viable, acrosome-intact spermatozoa, with the aim of providing insight into changes in sperm function during storage at 5 ˚C. High proportions of viable and acrosome-intact spermatozoa (71 ± 8%) remained after 96 h of storage demonstrating that the basic integrity of the cells was well preserved *(n* = 17 stallions). In addition, more than 90% of viable, acrosome-intact spermatozoa had active mitochondria and low intra-cellular or mitochondrial ROS levels. By contrast, the percentage of viable, acrosome-intact sperm with low plasma membrane fluidity and low $[Ca^{2+}]$; decreased over time (1 h: 63 ± 16%, 96 h: 29 ± 18%; $p < 0.05$). The $[Ca^{2+}]i$ in viable sperm rose 3.1-fold *(*$p < 0.05$) over the 4 days, and fewer spermatozoa responded to bicarbonate stimulation (1 h: 46 ± 17%, 96 h: 19 ± 12%) with an increase in plasma membrane fluidity following prolonged storage. Overall, prolonged storage of stallion semen at 5 ˚C resulted in disturbed calcium homeostasis and increased plasma membrane fluidity. The decline in fertility of stallion semen during cooled-storage may therefore relate to aspects of in vitro aging (changes in plasma membrane fluidity and intracellular calcium) which impairs capacitation-associated cell functions.

Chapter 3

Introduction

Artificial insemination (Al) with chilled semen is still the most wide-spread assisted reproductive technology in horse breeding. Semen extenders and protocols for preparing and storing semen have been refined in recent years, but recommended storage times for shipped semen are still typically no longer than 24-48 h. Relatively short transport durations are common practice in the field despite some reports indicating that semen can be stored for longer with acceptable maintenance of quality (motility and viability) [1-3]. Some studies suggest that excess reactive oxygen species (ROS) production in stored semen samples might compromise the fertilizing capacity of stallion spermatozoa stored for longer periods [4, 5] (reviewed in [6]). ROS production has been proposed to lead to structural damage (lipids, proteins, and DNA) and may also impair the spermatozoon's ability to optimally regulate its capacitation response, because ROS play a pivotal role in sperm capacitation [7, 8]. Capacitation is a physiological maturation process that spermatozoa must undergo to acquire the ability to fertilize an oocyte [9]. However, cellular alterations which have been observed in the context of capacitation have also been reported to occur due to semen processing and as a result of cryopreservation in a range of species [10-14]. These so-called "capacitation-like changes" may include an increase in plasma membrane fluidity and a rise in the free intra-cellular Ca^{2+} concentration. In a more neutral sense, such capacitation-like deviations in cell homeostasis may more accurately be referred to as aging-related phenomena. In any case, the disturbed cell homeostasis is thought to reduce the sperm population capable of undergoing physiological capacitation in vivo or in vitro, because an increase in plasma mem- brane fluidity may trigger acrosomal exocytosis (the acrosome reaction; an irreversible event) [9, 15]. A rise in the intra-cellular Ca^{2+} concentration may also compromise the establishment of a sperm reservoir in the mare's oviduct, because only spermatozoa with a low intra-cellular Ca^{2+} concentration are able to bind to oviduct epithelial cells in vitro [16]. In short, premature capacitation or comparable aging-related changes in sperm status would be expected to compromise subsequent sperm function and, therefore, reduce fertilizing capacity in vivo [17]. Despite all the hypothetical assumptions, it is still unclear whether and to what extent ROS, ROS-induced cell damage and/or capacitation-like or aging-related changes occur during prolonged chilled storage of stallion semen, that is, up to 96 h at 5 ˚C.

The aim of the current study was to investigate whether the loss of fertilizing capacity during prolonged storage of stallion semen in liquid form can be ascribed primarily to an increased abundance of ROS and ROS-induced damage in viable, acrosome-intact stallion sperm or a

loss of normal cell homeostasis, including regulation of intra-cellular Ca^{2+} concentration and membrane fluidity, which mimic early capacitation steps and compromise subsequent induction of physiological capacitation.

MATERIALS AND METHODS

Experimental design

Stallion semen samples (n = 17 stallions) were processed for routine chilled semen storage and stored at 5 ˚C for up to 96 h. Semen quality was evaluated on the day of semen collection after semen processing.

MATERIALS AND METHODS

Experimental design

Stallion semen samples (n = 17 stallions) were processed for routine chilled semen storage and stored at 5 ˚C for up to 96 h. Semen quality was evaluated on the day of semen collection after semen processing that is, approximately 1 h after collection, and also after 8 h of chilling towards 5 ˚C, and subsequently on a daily basis during storage at 5 ˚C (24, 48, 72, and 96 h). Please note that the samples had not been chilled below room temperature at the time the first evaluation took place. All samples (n = 17) were evaluated for motility parameters by computer-assisted semen analysis (CASA), while flow cytometry was used to assess DNA integrity (sperm chromatin structure assay), elevated intra- cellular Ca^{2+} concentration and plasma membrane fluidity, in viable, acrosome-intact spermatozoa. In addition, one subset of the samples (n = 8 stallions) was used to assess the ability of viable, acrosome-intact stallion spermatozoa to respond to bicarbonate with an increase in plasma membrane fluidity. In another subset (n = 9 stallions), the mitochondrial membrane potential, mitochondrial ROS content, total cellular ROS content, or the accumulation of 4-hydroxynonenal in viable, acrosome-intact spermatozoa were monitored.

Chemicals

All chemicals were purchased from Sigma Aldrich (Zwijndrecht, The Netherlands), unless otherwise stated, and were of analytical quality.

Semen collection and processing

Semen was collected from 17 healthy warmblood stallions (5.6 ± 4.2 years) using a Hanover model artificial vagina, after the stallion had mounted a phantom in the presence of an estrous

mare. After removal of the gel fraction by filtration through gauze, semen was diluted (1:1) with prewarmed INRA-96® extender (IMV Technologies, l'Aigle, France) and transported to the laboratory in a Styrofoam box. Cushion centrifugation (1000 *g,* 20 min, room temperature) was per- formed in 50 ml conical centrifugation tubes using 1 ml of Opti-prep™ 40% as a cushion [18]. After centrifugation, the supernatant and the bulk of the cushion fluid were removed by aspiration and the concentration of the remaining sperm pellet was determined using a Nucleo-counter Sp-100 (Chemometec, Denmark). The sperm pellet was then resuspended to 50 x 10^6/ml using INRA-96®, and five 10 ml syringes (without a rubber plunger) were each filled completely with 10 ml diluted semen, excluding air. One syringe was prepared for each storage examination time point (8, 24, 48, 72, and 96 h). Syringes were sealed with parafilm (Bemis, Neenah, USA) and dual-stop luer-lock 2 caps (Vygon, France). A non-cooled and non-stored sample from each if ejaculate was evaluated immediately after the initial processing.

Semen storage

The sealed, semen-filled syringes were placed upright in 500 ml beakers (5 syringes per beaker) filled with water (400 ml) at room temperature. Beakers were placed in a refrigerator (5° C) and, after 5 h, the syringes were taken out of the beakers and placed horizontally to pre- vent sperm pellet formation in the tip of the syringes. Semen samples were stored without agitation until analysis at the respective storage time points (8, 24, 48, 72, and 96 h) at 5 ˚C.

Semen evaluation

Computer-assisted sperm analysis (CASA)

A SpermVision® CASA system (version 3.5.6, Minitub, Tiefenbach, Germany) equipped with a camera adapter (U-PMTVC, Olympus, Hamburg, Germany) and a 648 x 484-pixel camera (Pulnix TM-6760CL, JAi A/S, Glostrup, Denmark) was used for motility analysis (n = 17 stallions). The microscope had an automated, heated micro- scope stage set to 38 ˚C. All pipette tips used for sample loading, and glassware used for motility recording, were pre-heated to 38°C. Stored semen was diluted at room temperature with chilled (5 ˚C) INRA-96® extender to 25 x 10^6 spermatozoa/ml. Five hundred microliters of the sperm suspension was placed in a 1.5 ml Eppendorf cup incubated with the lid open for 15 min at 38 ˚C in a metal heating block in air. After incubation, samples were briefly mixed by inversion of the Eppendorf cups and 3 µI of a sample was pipetted into a chamber of a 4-chamber Leja-slide with 20 µm chamber depth (Leja Prod- ucts BV, Nieuw-Vennep, The Netherlands). Twelve

consecutive fields were analyzed at 60 Hz frame rate (0.5 s recording time per field) in the central axis of the Leja chamber. The following semen motility parameters were evaluated; total motility (TM %), progressive motility (PM %), and sperm kinematic parameters: average path velocity (VAP µm/s), curved line velocity (VCL µm/s), the average straight-line velocity (VSL µm/s), amplitude of lateral head-displacement (ALH µm), straightness (STR = VSL/VAP), linearity (LIN = VSL/VCL), beat cross frequency (BCF Hz), and wobble coefficient (WOB = VAP/VCL). Algorithms for the classification of spermatozoa as motile and progressively motile were based on Brogan et al. [19]. Spermatozoa were classified as motile if they met one of the following three definitions: (1) average head orientation > 7° and BCF > 25 Hz, (2) DSL > 3.5 µm, VSL > 8 µm/s, and DCL > 15 µm, (3) VAP > 15 µm. Motile spermatozoa were further classified as progressive if they met one of the following criteria: (1) DSL > 15 µm, (2) BCF > 40 Hz and radius > 5 µm, (3) VSL > 20 µm/s, DCL 20 µm, (4) STR > 0.3 and LIN > 0.2, (5) radius > 10 µm, (6) BCF > 30 and ALH > 0.85.

Sperm morphology

Aniline blue-eosin staining was used to assess the morphology of raw semen preparations (n = 17 stallions). In brief, a drop of raw semen was placed on a prewarmed glass slide, followed by a drop of Aniline blue-eosin stain. After mixing the drops, another slide was used as a spreader to make a smear. The slide was immediately dried on a slide warmer (37 ˚C) and subsequently analyzed for sperm morphology using an Olympus BX40 microscope (Olympus Optical Co., Tokyo, Japan) at 1000x magnification via an oil immersion lens. A minimum of two hundred spermatozoa were evaluated for the presence of morphological defects [20]. Ejaculates with a minimum of 60% morphologically normal spermatozoa in the viable (unstained) sperm fraction were considered usable for the experiments.

Flow cytometric analyses

The viable, acrosome-intact sperm population of the semen samples was analyzed for plasma membrane fluidity and intra-cellular Ca^{2+} concentration, mitochondrial reactive oxygen species (ROS), total cellular ROS or mitochondrial transmembrane potential (MMP) after short-term incubation (15 minutes) in a non-capacitating Tyrode's medium ($Tyr_{Control}$; 111 mM NaCl, 3.1 mM KCl, 0.4 mM $MgSO_4$, 5 mM glucose, 0.3 mM KH_2PO_4, 20 mM HEPES, 21.7 mM Na-lactate, 1 mM Na-pyruvate and 100 µg/mL gentamycin, 300 ± 5 mOsm/kg, pH 7.40±0.05 at room temperature). A capacitating variant of Tyrode's medium (Tyr_{Bic}; differences to non-capacitating medium: 96 mM NaCl, 15 mM $NaHCO_3$) was used for

assessing bicarbonate-induced early capacitation events, i.e., a shift towards higher plasma membrane fluidity in viable spermatozoa. Prior to use, all media were passed through a Millex GP filter (0.22 μm pores, MerkMillipore BV, Amsterdam, The Netherlands). The capacitating medium was equilibrated overnight in a CO_2 incubator (37 ˚C, 5% CO_2-in-air and 100% humidity) prior to use.

The flow cytometer (FACS Canto II; BD Biosciences, Breda, The Netherlands) was equipped with 3 lasers (violet: 405 nm, 30mW; blue: 488 nm, 20mW; red: 633 nm, 17mW) and filters for blue (450/50 BP), green (530/30 BP), red (585/42 BP) and far-red fluorescence (660/20 BP). For each sample, signals from 10,000 single spermatozoa, as defined by forward and side scatter characteristics (c.f., Figure 1), were recorded at low flow rate. Data analysis was performed using FCS express software (version 3: De Novo Software, Angeles, CA, USA). Spectral overlap was compensated after acquisition.

Assessment of plasma membrane fluidity and intra-cellular Ca^{2+} concentration, and stimulation of cells with bicarbonate

In brief, 492 μL of a sperm suspension (n = 17) made up of 10 μL of diluted semen and 482 μL of either non-capacitating or capacitating Tyrode's medium was prepared. Sperm viability, acrosome integrity, plasma membrane fluidity and intra-cellular Ca^{2+} concentration was assessed using Hoechst 33258 (2 μL; stock solution: 0.1 mg/mL, Sigma-Aldrich Chemicals), PNA-Alexa Fluor™ 647 (2 μL; 0.25 mg/mL), Merocyanine 540 (M540; 2 μL; 750 μM) and Fluo-4 (2 μL; 0.05 mM) respectively. Samples in capacitating medium were incubated in an incubator at 37 ˚C in an atmosphere of 5% CO_2-in-air for 15 minutes, whereas samples in non-capacitating medium were incubated for 15 minutes in metal heating blocks maintained at 37 ˚C. Fluorescent signals were assessed using the following laser and filters: Hoechst 33258 (laser: 405 nm; filter 450/50 nm BP), Fluo-4 (488 nm; 530/30 nm BP), Merocyanine 540 (488 nm; 585/42 nm BP), and PNA-AlexaFluor™647 (633 nm; 660/20 nm BP). The basic gating strategy to study the sperm population of interest is illustrated in Figure 1. The single sperm population was identified by forward and side-scatter characteristics (Figure 1 A). Small particles (debris), large events, and agglutinated cells were excluded from the analysis based on the same plot (Figure 1 A). Their staining characteristics for Hoechst 33258 and PNA-Alexa Fluor™ 647 are illustrated in Supplemental Figure 1. The extent of DNA-free (= non-sperm) events in the single sperm gate was assessed in a subset of the ejaculates (Supplemental Figure 2). Only a minor fraction of DNA-free events (1 h: 2.4 ± 1.4%) was detected in the single sperm gate; this proportion remained constant over storage time (96 h:

2.7 ± 2.0%; Supplemental Figure 2 D). Therefore, the bias of non-DNA containing particles on the overall results was considered negligible (c.f. [21]).

Next, the subset of viable (H33258-negative), acrosome-intact (PNA-negative) spermatozoa was defined (Figure 1 B) and further sub-classified as cells with either low (M540 negative) or high plasma membrane fluidity (M540 positive) and with either low free intra-cellular Ca^{2+} concentration (low Fluo-4 fluorescence intensity) or high free intra-cellular Ca^{2+} concentration (high Fluo-4 fluorescence intensity, Figure 1 C) (9). Samples measured directly after dilution (1h after collection) in the non-capacitating medium served as a reference for setting thresholds for basal plasma membrane fluidity and intra-cellular calcium concentrations (Figure 1 C). The change in the percentage of these subpopulations

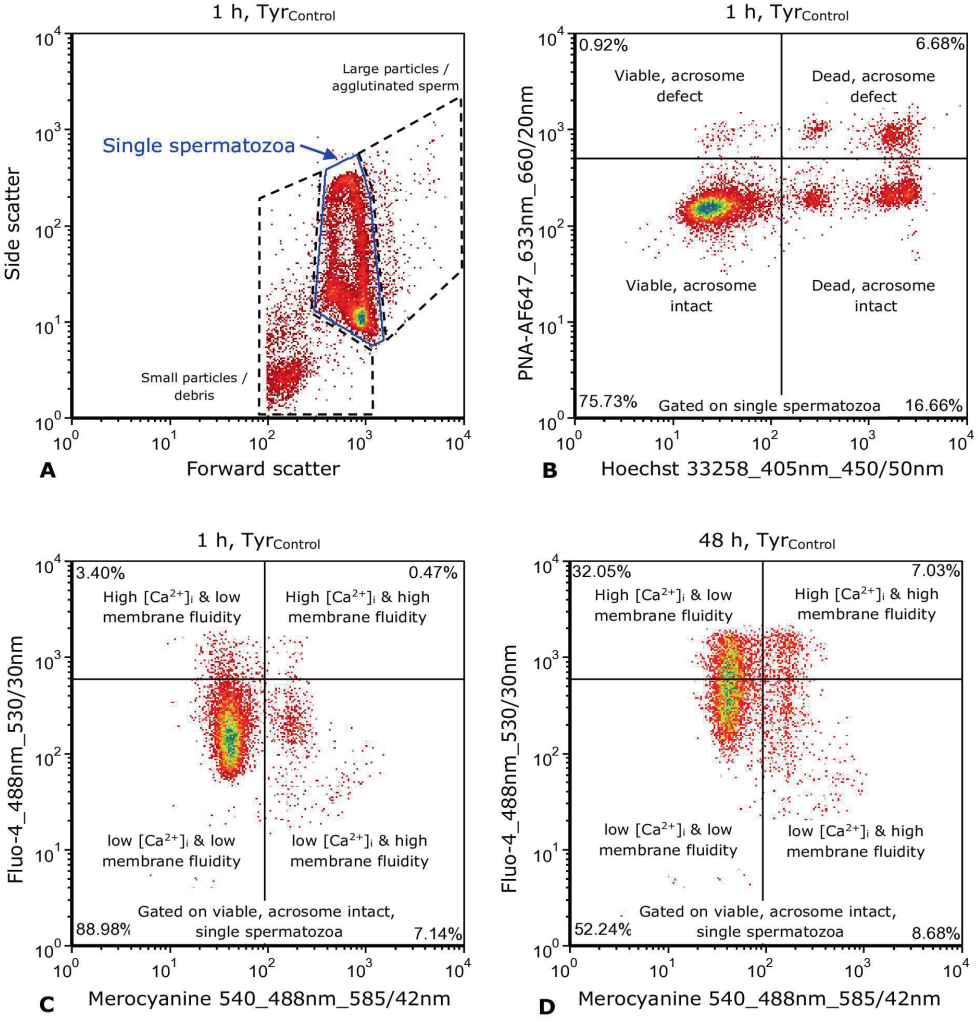

Figure 1

Representative plots illustrating the gating strategy for analyzing plasma membrane fluidity and intra-cellular Ca2+ concentration in viable, acrosome-intact single spermatozoa

The single sperm population was identified by its characteristic appearance in the forward and side scatter plot (area of signals plotted) and distinguished from small particles and debris as well as large particles and agglutinated spermatozoa (A). Subsequently, viability (Hoechst 33258) and acrosome integrity (PNA-AlexaFluor™647) were assessed (B). The subset of viable, acrosome intact spermatozoa was further evaluated for membrane fluidity (Merocyanine 540) and the free intra-cellular Ca^{2+} concentration (Fluo4; C) of the cells. Thresholds were set based on samples after 1 h storage (C) and kept constant for evaluating measurements from later storage times (e.g. 48 h, D).

over storage time was investigated (Figure 1 D). Staining characteristics with respect to Fluo-4 and merocyanine 540 for dead cells or viable, acrosome defective sperm are illustrated in Supplemental Figure 3.

In addition to changes in the percentage of sperm subpopulations, the Fluo-4 fluorescence intensity in viable, acrosome intact spermatozoa was assessed (Supplemental Figure 4). The geometric mean of the Fluo-4 fluorescence intensity in a given sample immediately after dilution (1 h) was considered as the reference point. Subsequently, all median values from a sample were normalized by dividing the value at a given time point (1 h-96 h) by the value at 1 h.

Finally, the sperm population that was able to respond to bicarbonate within a 15-minute incubation at 37 ˚C was estimated. To this end, the percentage of viable, acrosome-intact spermatozoa with high plasma membrane fluidity in Tyrode's medium without bicarbonate ($Tyr_{Control}$) was compared to that in Tyrode's medium with 15 mM bicarbonate (Tyr_{Bic}) (n= 8, Supplemental Figure 5). The difference (delta) in viable, acrosome intact spermatozoa with high membrane fluidity between the two media (% cells in Tyr_{Bic} - % cells in $Tyr_{Control}$) was considered as an indicator of the responsive sperm population.

Mitochondrial (M-ROS) or total cellular (T-ROS) reactive oxygen species

The abundance of mitochondrial (M-ROS; n= 9) or total cellular reactive oxygen species (T-ROS; n= 9) was assessed as described by Hall et al. [22] using MitoSOX™ Red (MSR; Thermo Fisher Scientific, Scoresby, VIC) or dihydroethidium (DHE; Thermo Fisher Scientific) with some minor modifications. Briefly, 4 µL of semen was diluted in 192 µL of non-capacitating Tyrode's medium and incubated at 37 ˚C for 15 minutes with Hoechst 33258 (2 µL; Stock solution: 0.1 mg/mL), PNA-Alexa Fluor™ 647 (2 µL; 0.25 mg/mL) and a final concentration of 2 µM of either MSR (4 µL; 100 µM stock) or DHE (0.8 µL; 500 µM stock) making a total volume of 200 µL. The two probes were incubated separately as indicated

above. A positive control for high MSR or DHE staining intensity was produced by treating spermatozoa with 25 µM arachidonic acid, which induces ROS generation by the mitochondrial pathway [23]; this control was included on each day of analysis. Fluorescent signals were assessed using the following laser and filters: Hoechst 33258 (laser: 405 nm; filter 450/50 nm BP), MSR or DHE (488 nm; 585/42 nm BP), and PNA-AlexaFluor™647 (633 nm; 660/20 nm BP). After gating the spermatozoa on the basis of viability and acrosome-intactness (as described in Figure 1 B), a further discrimination was performed in relation to high or low fluorescence intensity of the ROS indicators (Supplemental Figure 6). Data from 1 stallion (T-ROS) were discarded from the analysis due to difficulties gating the FCS-files. Results are reported as percentage of viable, acrosome-intact spermatozoa with low M-ROS or T-ROS.

Mitochondrial membrane potential (MMP)

Mitochondrial membrane potential (n = 9) was evaluated by staining with JC-1 (Thermo Fisher Scientific), a lipophilic cationic dye that remains a monomer emitting green fluorescence in sperm with low MMP, but forms aggregates emitting red fluorescence in sperm with high MMP. Briefly, 10 µL of semen diluted in 472 µL of $Tyr_{Control}$ medium was incubated and sperm viability, acrosome integrity and MMP were assessed by staining with Hoechst 33258 (2 µL; 0.1 mg/mL), PNA-Alexa Fluor™ 647 (2 µL; 0.25 mg/mL) and JC-1 (10 µL; 250 µM) respectively. Fluorescent signals were assessed using the following laser and filters: Hoechst 33258 (laser: 405 nm; filter 450/50 nm BP), JC-1 monomers (488 nm; 530/30 nm BP), JC-1 aggregates (488 nm/ 585/42 nm BP), and PNA-AlexaFluor™647 (633 nm; 660/20 nm BP). After incubation, the viable, acrosome-intact sperm population was gated as described above and further divided into spermatozoa with high MMP (more intense red fluorescence) and spermatozoa with low MMP (green fluorescence; Supplemental Figure 7).

Sperm chromatin structure assay (SCSA)

Sperm DNA integrity (n = 17) was evaluated using the sperm chromatin structure assay (SCSA) following the procedures described by Evenson and Jost [24]. After acid denaturation, acridine orange staining was used to distinguish double-stranded (green) versus single-stranded (red) DNA and thereby the proportion of sperm cells possessing an elevated amount of unstable chromatin was detected. Samples were processed on ice as stated in the original assay description. Fluorescent signals (green and red) of stained sperm were collected on a FACS Canto II flow cytometer (BD Biosciences) using the 488 nm laser and

filters at 530/30 nm BP (green) and 585/42 nm BP (orange-red). Fluorescence intensities were plotted on linear scales. The DNA fragmentation index was calculated as in [25]:

$$DFI = \frac{red\ fluorescence}{total\ (red+green)\ fluorescence}$$

The %DFI was determined by including cells with moderate or high DFI [26]. Representative plots of the gating strategy are available e.g., in references 25 and 26. Quality assurance was obtained by running a semen sample with known DNA fragmentation index before starting every flow cytometry session and after every twenty samples of a session.

Lipid peroxidation (4-Hydroxynonenal)

An anti-4-Hydroxynonenal primary antibody (Rabbit anti-4-HNE serum, HNE11-S, Alpha Diagnostic International, San Antonio, TX, USA) was used to evaluate the presence of the lipid peroxidation by-product 4-HNE in semen samples (n = 9) after prolonged storage at 5 ˚C [27]. To this end, 500 µL of diluted semen was centrifuged at 612 *g* for 5 minutes, and the supernatant was removed. The sperm pellet was resuspended with 500 µL of $Tyr_{Control}$ medium. Next, 100 µL of this sperm suspension was incubated for 1 h at 37 ˚C with anti-4-HNE primary antibody (0.03 µg/µL) and then centrifuged at 612 *g* for 5 minutes. The sperm pellet was again resuspended with $Tyr_{Control}$ medium and incubated at 37 ˚C for 30 minutes with the secondary antibody (Goat anti-rabbit Alexa Fluor™ 488; 0.03 µg/µL, A-11034, Thermo Fisher Scientific), Hoechst 33258 (2 µL; 0.1 mg/mL) and PNA-Alexa Fluor™ 647 (2 µL; 0.25 mg/mL). After incubation, samples were centrifuged once again at 612 *g* for 5 minutes. Then, the sperm pellet was resuspended in 200 µL $Tyr_{Control}$ medium and analyzed on the flow cytometer. Fluorescent signals were assessed using the following laser and filters: Hoechst 33258 (laser: 405 nm; filter 450/50 nm BP), Goat anti-rabbit Alexa Fluor™ 488 (488 nm; 530/30 nm BP), and PNA-AlexaFluor™647 (633 nm; 660/20 nm BP). The viable, acrosome-intact sperm population was further divided into subsets of cells with low or high anti-4-HNE labeling. Negative control samples were run by omitting the primary antibody and staining the samples with only the secondary antibody. Non-viable (Hoechst 33258 positive) spermatozoa served as an internal positive control, because the majority of non-viable spermatozoa showed intense labeling (Supplemental Figure 8). Fluorescence intensity for anti-4HNE staining (geometric mean) was evaluated to quantify changes in labeling intensity (i.e., in 4-HNE adduct formation) over storage time. Due to a high standard deviation in labeling intensities, normalized values have been provided as well (Supplemental Table 2). Fluorescence intensities of fresh diluted spermatozoa (1 h after dilution) were

considered as reference point.

Statistical analysis

Statical analysis was carried out using GraphPad Prism 8 (GraphPad Software, San Diego, CA, USA). Data were analyzed for normality using the Shapiro-Wilk test. Effect of storage time on semen quality parameters was assessed using general linear model: repeated measures ANOVA. F and P values from an ANOVA table with Greenhouse Geisser correction are presented in the respective sections. Pair-wise comparison was used to check the differences between storage time points for each parameter by estimated marginal means, with the Tukey's test as post hoc test. Pearson's correlation method was used to find the correlation between the parameters. P-values from the correlation analysis were corrected by the Benjamini-Hochberg method to control the false detection rate. Differences were considered statically significant when $p < 0.05$. Data is presented as mean ± SD (standard deviation). Graphical illustration of data was achieved using Microsoft Excel 365.

Results

Sperm Motility

The percentages of total and progressively motile sperm was influenced by storage time (total motile; F= 35.4, $p < 0.001$ and progressively motile; F= 19.5, $p < 0.001$) (Figure 2). Mean (± SD) starting values directly after semen dilution (1 h) were 69±10% and 50±13%, respectively. Both parameters were stable during the first 24 h of storage, but a gradual decline ($p < 0.05$) in the percentage of motile spermatozoa was evident from 48 h onwards (Figure 2 A, B), reaching values of 46±13% for total and 32±13% for progressively motile spermatozoa at storage time point 96 h. However, even at 96 h of storage 12 out of 17 samples still had a total motility of ≥35 %, a value generally considered sufficient for a reasonable chance of pregnancy after artificial insemination (28). Most of the kinematic parameters for the progressively motile spermatozoa showed little systematic change over time (Supplemental Table 1), with only the VCL increasing ($p < 0.05$) gradually from 143 ± 24 µm/s (1 h) to 161 ± 22 µm/s (96 h).

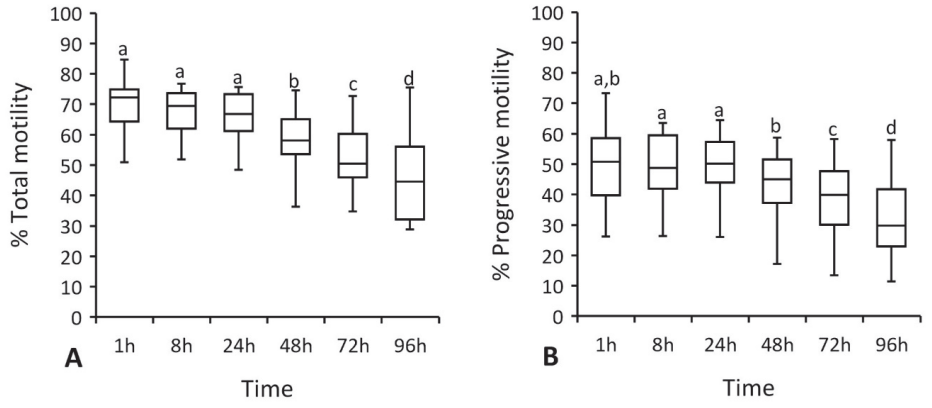

FIGURE 2

Motility of stallion spermatozoa assessed by computer assisted semen analysis during prolonged (up to 96h) storage at 5 °C. *A) Total motility, B) Progressive motility. The lines ("whiskers") on the top and bottom of each box show the minimum and maximum value, the box represents the IQR and the horizontal line within each box represents the median (n = 17 stallions). Different letters depict values that differ significantly, p <0.05.*

Flow cytometric analyses

Viability, acrosome intactness, plasma membrane fluidity and intra-cellular Ca^{2+} concentration

Semen samples were analyzed for percentages of spermatozoa that were viable, acrosome-intact and exhibiting aging-related changes in cell homeostasis, i.e., an increase in plasma membrane fluidity and free intra-cellular Ca^{2+} concentration, after incubating in $Tyr_{Control}$ medium at 37 ˚C for 15 minutes. The percentage of viable, acrosome-intact spermatozoa decreased significantly over storage time (F= 6.883, p <0.001; Figure 3 A). Initially a small, but significant decline was recorded after 8 h of storage (73± 11% compared to 77±9% at 1 h). However, no further decline was observed between 8 h and 96 h (71±8%).

Fresh diluted semen contained predominantly viable, acrosome-intact spermatozoa with low plasma membrane fluidity and a low intra-cellular Ca^{2+} concentration (1 h: 63±16%). Thereafter, this sperm population decreased in size (F= 45.417, p <0.001) daily (Figure 3 B), until by 96 h of storage it was less than half of the initial value (29±18%, p <0.05, n = 17).

In the early storage period, the decline in the proportion of viable, acrosome-intact sperm with low plasma membrane fluidity and a low intra-cellular Ca^{2+} concentration was driven mainly by an increase in sperm with an elevated free intra-cellular Ca^{2+} concentration, as

indicated by an increase in the Fluo-4 fluorescence intensity over time (F= 52.99, p <0.001; Figure 3 C). Fluo-4 fluorescence intensity increased from as early as 8 h of storage (Figure 3 C), and had doubled by 48 h (2.3 ± 0.8-fold). By 96 h, the Fluo-4 fluorescence intensity was 3.1 ± 1.0-fold higher than in fresh diluted semen.

In the later stages of storage, a time-dependent increase in the percentage of viable, acrosome-intact spermatozoa with increased plasma membrane fluidity was also observed (F15.414, p <0.001); Figure 3 D). From the time of semen dilution (1 h; 15±7%, n = 17), the

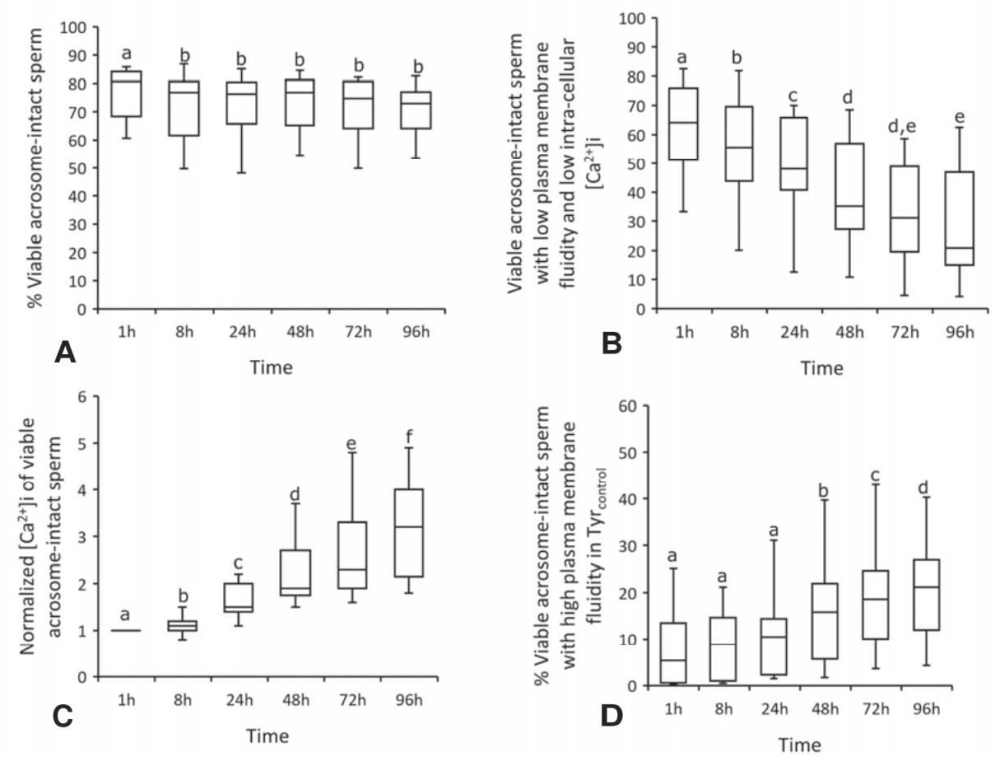

FIGURE 3

Changes in semen quality parameters during prolonged storage, assessed flow cytometrically. *A) Viable acrosome-intact stallion sperm, B) Viable acrosome-intact sperm with low membrane fluidity and low $[Ca^{2+}]_i$, C) Normalized $[Ca^{2+}]_i$ of viable acrosome-intact sperm, D) Viable acrosome-intact sperm with high membrane fluidity in $Tyr_{Control}$ (non-capacitating Tyrode's medium). The lines ("whiskers") on the top and bottom of each box show the minimum and maximum value, the box represents the IQR, and the horizontal lines within each box represents the median (n = 17 stallions). Values with the same letters do not differ significantly, p > 0.05.*

proportion of viable, acrosome-intact spermatozoa with increased plasma membrane fluidity

rose to reach 25±4% by 96 h, with a significant rise first evident after 48 h (Figure 3 D).

Ability of sperm to show an increase in plasma membrane fluidity in response to bicarbonate

The sperm population able to respond to bicarbonate within a 15-minute incubation at 37 ˚C was calculated as the difference between the percentage of viable, acrosome-intact spermatozoa with high plasma membrane fluidity in Tyrode's medium without versus with 15 mM bicarbonate (Figure 4 A, n = 8).

With increasing storage time, the population of viable, acrosome-intact spermatozoa with increased plasma membrane fluidity in the absence of bicarbonate (one of the signs of aging-related changes) increased gradually (Figure 4 A, $Tyr_{Control}$) while the population that showed an increase in plasma membrane fluidity after exposure to bicarbonate declined (Figure 4 A, Tyr_{Bic}). Consequently, the sperm population classified as having responded to bicarbonate tended to decline with time in storage from 46±17% (1 h) spermatozoa to 19±12% spermatozoa (96 h, $p = 0.0603$, n = 8), with the first evidence of a reduction observed after 48 h storage (25 ± 19% $p < 0.05$, Figure 4 B).

Mitochondrial (M-ROS) and total cellular reactive oxygen species (T-ROS)

There was also an effect of time on the population of viable, acrosome-intact spermatozoa with low mitochondrial reactive oxygen species (M-ROS) content ($F=4.662$, $p =0.0353$; n= 9 stallions; Figure 5 A). In this case, the viable, acrosome-intact sperm population with low M-ROS was stable between 1 h (75±6%) and 72 h (74±6%; $p >0.05$), while reaching lowest values after 96 h of storage (69±7%).

Similarly, the percentage of viable, acrosome-intact spermatozoa with a low total cellular reactive oxygen species (T-ROS) content declined significantly during prolonged storage ($F=5.273$, $p = 0.011$; n = 8; Figure 5 B). Compared to the value recorded immediately after dilution (1 h: 75±6%), a decline in the viable, acrosome-intact sperm population with a low T-ROS was only observed after 96 h storage (60±13%, $p < 0.05$).

Mitochondrial membrane potential (MMP)

The proportion of viable, acrosome-intact spermatozoa with high MMP declined over time ($F= 8.199$, $p = 0.010$; n = 9; Figure 5 C), first dropping below the initial level (1 h: 73±7%) after 72 h (65±6%, $p <0.05$) and reaching a minimum at 96 h (60±11%, $p <0.05$).

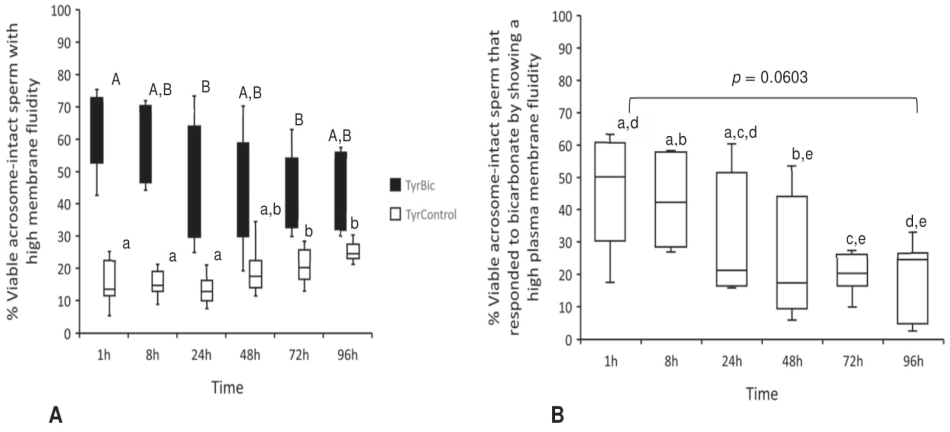

FIGURE 4

Changes in semen quality parameters during prolonged storage, assessed by flow cytometry. *A) Viable acrosome-intact stallion spermatozoa with high membrane fluidity* Tyr_{Bic} *(capacitating Tyrode's medium) and* $Tyr_{Control}$ *(non-capacitating Tyrode's medium), B) Viable acrosome-intact stallion spermatozoa that responded to exposure to 15 mM bicarbonate with an increase in membrane fluidity. The lines ("whiskers") on the top and bottom of each box show the minimum and maximum value, the box represents the IQR, and the horizontal line on each box represents the median (n = 8 stallions). Values with the same letter do not differ significantly, p > 0.05.*

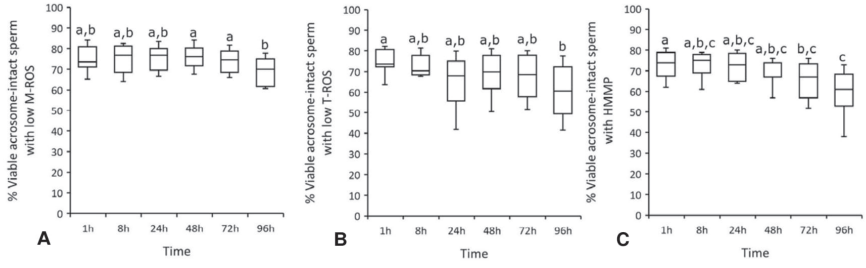

FIGURE 5

Mitochondrial (M-ROS) and total cellular reactive oxygen species (T-ROS) and mitochondrial membrane potential (MMP) assessed by flow cytometry. *A) Viable acrosome-intact stallion sperm with low mitochondrial ROS (M-ROS), B) Viable acrosome-intact sperm with low Total cellular ROS (T-ROS), C) Viable acrosome-intact spermatozoa with high mitochondrial membrane potential (HMMP) . The lines ("whiskers") on the top and bottom of each box show the minimum and maximum value, the box represents the IQR, and the horizontal line on each box represents the median (A,C; n = 9 and B; n= 8 stallions respectively). Values with the same letter do not differ significantly, p > 0.05.*

Lipid peroxidation (4- Hydroxy nonenal)

Lipid peroxidation was measured indirectly by quantifying the percentage of viable, acrosome-intact spermatozoa with intense (high) anti- 4- Hydroxy nonenal (HNE) antibody labeling (Figure 6). Over the 96-h storage period, the percentage of viable, acrosome-intact

sperm with high anti-4HNE labeling remained low and did not change (Supplemental Table 2). Likewise, no significant absolute or relative change in anti-4-HNE labeling intensity was observed ($p > 0.05$; Supplemental Table 2). Numerical increases in the mean values were due to 2 out of 9 stallions, in which elevated labeling intensities were detected after 72 h and 96 h storage. High labeling intensity was regularly observed in non-viable spermatozoa.

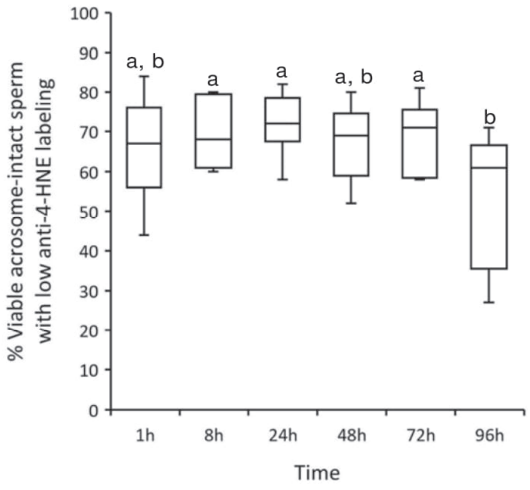

FIGURE 6

Lipid peroxidation in stallion spermatozoa as estimated by staining for the peroxidation by-product, 4-HNE, using an anti-4-HNE antibody. *The lines ("whiskers") on the top and bottom of each box show the minimum and maximum value, the box represents the IQR, and the horizontal line on each box represents the median (n = 7 stallions). Values with the same letter do not differ significantly, p > 0.05.*

Sperm chromatin structure assay (SCSA)

The DNA fragmentation index (DFI) increased gradually over time (F= 6.641, $p = 0.0008$; n =17 stallions; Figure 7), from 9±5% (1 h) to 12±8% (96 h; $p < 0.05$).

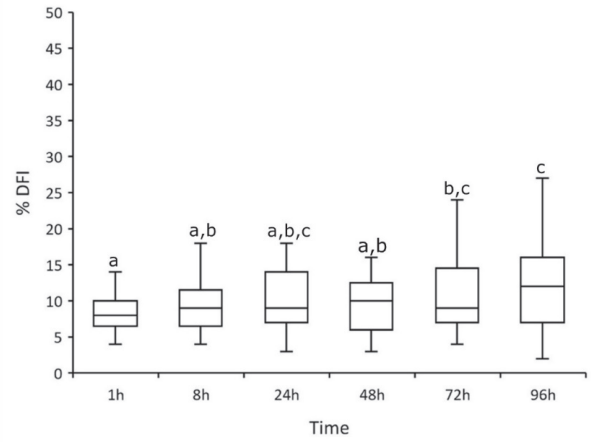

FIGURE 7

DNA fragmentation index (DFI) in stored stallion spermatozoa assessed using the Sperm Chromatin Structure Assay (SCSA).

The lines ("whiskers") on the top and bottom of each box show the minimum and maximum value, the box represents the IQR, and the horizontal line on each box represents the median (n = 17 stallions). Values with the same letter do not differ significantly, p > 0.05.

Correlations between selected semen quality parameters

Correlations between selected flow cytometrically determined semen quality parameters, CASA motility and DFI are shown in Supplemental Table 3 and Supplemental Figure 9. There was a strong correlation between the percentage of viable, acrosome-intact spermatozoa with low membrane fluidity and low intra-cellular Ca^{2+} concentration and the percentages of progressively motile (r = 0.72, p <0.001) and total motile spermatozoa (r = 0.69, p <0.001; Supplemental Table 3, Supplemental Figure 9 A and B). In particular, the mean calcium content in viable, acrosome-intact spermatozoa was inversely correlated with the percentage of progressively motile (r = - 0.74, p <0.001) and total motile spermatozoa (r = - 0.84, p <0.001) (Supplemental Table 3, Supplemental Figure 9 C and D).

The correlations between the percentage of viable, acrosome-intact spermatozoa with low M-ROS or T-ROS and total or progressive motility were moderate and mostly lower than the correlation between the percentage of viable, acrosome-intact spermatozoa and DFI (Supplemental Table 3). In the context of ROS and DNA damage, a moderate to high negative correlation between the percentage of viable, acrosome-intact spermatozoa with low T-ROS (r = - 0.53) or M-ROS (r = - 0.64) with %DFI was apparent (both p <0.001; Supplemental Table 3). A similar correlation was observed for the percentage of viable, acrosome-intact spermatozoa and %DFI (r = - 0.53; p <0.001; Supplemental Table 3).

Discussion

Total and progressive motility are still widely used, basic semen quality parameters in equine AI. Diluted, chilled semen suffers an inevitable reduction in the motile sperm fraction over time [2, 29]. However, under our experimental conditions using INRA96® extender, the first small decline in the percentage of motile spermatozoa was only observed between 24h and 48h of storage. This suggests a robust initial maintenance of this basic sperm function following cooling from room temperature to 5 ˚C. A previous study demonstrated a similar decline in motility parameters during 48 h to 96 h of storage; nevertheless, a very high pregnancy rate (90%) was achieved after inseminating mares with semen stored for 48 h [30]. In clinical equine practice, chilled semen is seldom stored for more than 48 h. Generally accepted threshold values for considering a semen dose as acceptable for AI have not been defined, although several suggestions have been made [31]. When AI is to be performed with chilled semen stored for 24-30 h after collection (minimum 600 x 10^6 progressively motile sperm at the time of dose preparation), it is considered desirable that progressive motility is not less than 35% at the time of AI [32]. Our data confirm that progressive motility percentages above 35% can be achieved in stallion semen stored at 5 ˚C for up to 72 h (12 out of 17 samples). However, before recommending routine use of extended chilled storage periods, data from insemination trials need to confirm that fertility is not hampered by prolonged storage of stallion semen.

Interestingly, the percentage of viable, acrosome-intact spermatozoa was considerably higher during the later stages of storage (48 h to 96 h) than the percentage of spermatozoa that retained motility. This suggests that despite intact plasma and outer acrosomal membranes, storage at 5 ˚C is accompanied by changes at the subcellular level that impair flagellar activity after rewarming to 37 ˚C, as has been proposed previously [30]. One possible key element underlying the loss of motility during semen storage may be the free intra-cellular Ca^{2+} concentration. Free intra-cellular Ca^{2+} levels are usually tightly regulated (within the nanomolar range) in somatic cells and spermatozoa [33]. While small rises and oscillations in the free intra-cellular Ca^{2+} concentration result in modified motility patterns (reviewed in [34]), prolonged presence of higher free intra-cellular Ca^{2+} concentration can lead to a Ca^{2+} overload in mitochondria, induction of apoptosis, increased ROS production and, consequently, a loss of mitochondrial function (reviewed in [35-38]). However, a complete breakdown of mitochondrial function was only apparent in a small subset of stored sperm (i.e., < 10%). Moreover, an increased ROS (superoxide anion) production was not observed.

Nonetheless, the progressive rise in the free intra-cellular Ca^{2+} concentration in viable cells during cooled storage is apparently a pathological aspect of in vitro aging, because it is highly correlated with the decline in motile or progressively motile spermatozoa. Whether there is a direct impact of the free intra-cellular Ca^{2+} concentration on motility, and what other factors may be involved requires further investigation, since we did not assess intra-cellular calcium concentration and motility simultaneously in the same spermatozoa. In future experiments, microscopic imaging of the location of Fluo-4 signals or the use of image cytometry would be helpful in localizing the cellular compartments in which the Ca^{2+} concentration is elevated.

Prolonged storage of stallion semen not only had an impact on calcium homeostasis, but also on plasma membrane organization. Plasma membrane organization, i.e., lipid packing and asymmetry, in somatic cells is maintained by ATP-dependent amino phospholipid translocases (APTs) and multi-drug resistance (MDR) transporters [39]. Notably, their activity is (partly) controlled by free intracellular calcium levels. Whether an increase in free intra-cellular Ca^{2+} concentration beyond a threshold level in a subset of viable stallion spermatozoa during storage and rewarming is involved in a downregulation of APTs and an upregulation of scramblase activity, and consequently an increased membrane fluidity remains to be demonstrated.

The shift from a state of low membrane fluidity to a state of high membrane fluidity is one of the earliest signs of bicarbonate-induced capacitation in spermatozoa [40]. Therefore, we included in our assessment of sperm functionality a test for whether viable sperm are able to respond to a capacitating stimulus; a more dynamic feature than a simple description of endpoint measurements. The observation that with increasing storage time fewer spermatozoa were able to respond to bicarbonate suggests that the number of fertilization-competent cells gradually decreases during prolonged cooled storage. Similar observations were previously made for boar spermatozoa [41].

Determining the viable, acrosome-intact sperm population by flow cytometry is a straightforward way to assess sperm integrity. We refined our definition for an ‘intact’ spermatozoon as one having a low intra-cellular Ca^{2+} concentration and low membrane fluidity. Thus, taking advantage of the capabilities of multi-laser instruments which are now available for veterinary andrology laboratories. Our new definition of an ‘intact’ spermatozoon covered the majority of viable sperm directly after semen collection and dilution. During chilled storage, there was a gradual fall in the newly defined ‘intact’ sperm population over time. This was in stark contrast to the old definition of ‘intact’ sperm, which

clearly demonstrates the advantage of multi-parametric sperm assessment to elucidate functional changes in stallion sperm during chilled storage. Nonetheless, one should be aware that a possible limitation of the assay may be the interpretation of the Fluo-4 data. Loading of the cells took place at 38 ˚C, which may have resulted in compartmentalization of the dye. Increases in Fluo-4 intensity may therefore only be indicative of an increased permeability of the membrane systems in preserved stallion spermatozoa to this dye. On the other hand, gentle preparation of the stored semen samples ensured that artifacts in calcium assessments due to centrifugation stress were avoided [27]. Therefore, we believe that the newly defined 'intact' sperm population is a sensitive measure of cellular integrity and function in preserved stallion semen samples.

Chilled storage of stallion semen has been proposed to be associated with increased intracellular production of reactive oxygen and nitrogen species leading to oxidative damage to the spermatozoa (for review see [42]). At the same time, extra-cellular oxidative stress in stored spermatozoa may occur by production or release of ROS from contaminating cells (e.g., leucocytes) or dead spermatozoa [43]. We could not confirm these concepts for chilled stallion spermatozoa. This suggests that intra-cellular oxidative stress, based on superoxide anions, was not a major issue during cooled storage and that the turning point at which the preservation system becomes unstable is, for most stallion semen samples, somewhere beyond 96 h of storage. In line with this assumption, the increase in DFI was too modest to confirm ROS-induced damage as a major fertility-limiting factor. A critical factor in our experiments might have been that the assessment was based on a short post-storage incubation of only 15 minutes, and it only covered one reactive oxygen species. MitoSOX^{TM} Red and DHE are probes which are mainly used to detect the presence of superoxide anions [44], although they may also label other oxidants [45]. Other ROS or RNS than the one tested in this study, e.g., H_2O_2 or $ONOO^-$, may play a role in the pathological aging-related changes in stallion semen stored for long periods. Our data also do not preclude the possibility that total ROS levels would increase during longer storage durations if, for example, a longer incubation period at body temperature was applied. Such temperature stress or thermo-resistance tests may reveal, provoke or intensify discrepancies in cellular stability between samples from different treatments [46-47].

Arguably, the key observation of this study was that calcium homeostasis began to break down during cooled (liquid) storage of stallion semen. Semen preservation strategies could therefore aim to limit the amount of freely diffusible extra-cellular Ca^{2+} in the semen

extender. In this respect, initial attempts have been made to include calcium-chelators in extenders for stallion semen [48], a practice that is quite common in pig AI [49]. However, equine semen extenders are currently based predominantly on skimmed milk and/or egg yolk, which both have a high calcium content [50]. Relatively few attempts have been made to design a chemically-defined stallion semen extender [51]. Nevertheless, recently an attempt was made to store stallion semen for longer periods (up to 7 days) at ambient temperature with promising results. This could revolutionize the strategies to store stallion semen for longer periods. However, in field fertility rates after prolonged ambient temperature storage is still underway, to ascertain the clinical effectiveness [52].

Conclusions

This study demonstrates that aging of stallion semen during liquid storage at 5 ˚C is, after rewarming to body temperature, associated with changes in sperm calcium homeostasis and membrane organization. However, excess ROS production and DNA damage were not evident. Overall, this suggests that current semen extenders may have adequate antioxidant capacity and that strategies for optimizing liquid preservation of stallion semen should concentrate on restricting the availability of ionized free calcium to the spermatozoa.

Authors contribution

Umair M Methodology, Formal analysis, Investigation, data curation, writing - original draft, Visualization

Claes A Resources, Writing - Review & Editing, Supervision

Buijtendorp M Formal analysis, Investigation, writing - original draft, Visualization

Cuervo-Arango J Resources, Supervision

Stout TAE Resources, Writing - Review & Editing, Supervision, Project administration, Funding acquisition

Henning H Conceptualization, Methodology, Formal Analysis, Investigation, data curation Writing - Review & Editing, Visualization

Data availability

Data presented in this study is available in ‘Stallion spermatozoa undergo capacitation-like changes during prolonged storage at 5 ˚C’.

Funding

The Punjab Educational Endowment Fund (PEEF) Punjab, Pakistan supported M. Umair (PEEF/SSMS/18/222).

Institutional Review Board Statement

Semen samples were obtained from stallions presented for routine semen evaluation. Therefore, no ethical approval was required.

Informed Consent Statement

Stallion owners were asked to sign informed consent forms allowing use of the semen from their stallions for research.

Acknowledgments

The authors thank Jon De Rijk, Wilbert Beukens and Esther Akkermans for helping in semen collection, and Arend Rijneveld for helping with the CASA analysis. Flow cytometry assessments were performed at The Flow Cytometry And Cell Sorting Facility of The Faculty of Veterinary Medicine, Utrecht University.

Conflict of interest

Authors declare no conflict of interest

Supplementals

Supplemental figures and tables in this chapter are available at *Cytometry Part A* (https://onlinelibrary.wiley.com/doi/10.1002/cyto.a.24712) online.

References

1. Lindahl J, Dalin A, Stuhtmann G, Morrell JM. Stallion spermatozoa selected by single layer centrifugation are capable of fertilization after storage for up to 96 h at 6 ˚C prior to artificial insemination. Acta Vet Scand 2012;54:1-5.

2. Papin J, Stuhtmann G, Martinsson G, Sieme H, Lundeheim N, Ntallaris T, Morrell JM. Stored Stallion Sperm Quality Depends on Sperm Preparation Method in INRA82 or INRA96. Journal of Equine Veterinary Science 2021;98:103367.

3. Bozkurt T, Türk G, Gür S. The time dependent motility and longevity of stallion spermatozoa diluted in different spermatozoal concentrations and extenders during cool-storage. Revue Méd.Vét 2007;158:67-72.

4. Ball B. The effect of oxidative stress on equine sperm function, seme n storage and stallion fertility. Journal of Equine Veterinary Science 2000;20:95-96.

5. Pintus E, Ros-Santaella JL. Impact of Oxidative Stress on Male Reproduction in Domestic and Wild Animals. Antioxidants 2021;10:1154.

6. Gibb Z, Aitken RJ. The impact of sperm metabolism during in vitro storage: the stallion as a model. BioMed Research International 2016;2016.

7. Baumber J, Sabeur K, Vo A, Ball BA. Reactive oxygen species promote tyrosine phosphorylation and capacitation in equine spermatozoa. Theriogenology 2003;60:1239-1247.

8. Aitken RJ. Reactive oxygen species as mediators of sperm capacitation and pathological damage. Mol Reprod Dev 2017;84:1039-1052.

9. Rathi R, Colenbrander B, Bevers MM, Gadella BM. Evaluation of in vitro capacitation of stallion spermatozoa. Biol Reprod 2001;65:462-470.

10. Ortega-Ferrusola C, Anel-Lopez L, Martin-Munoz P, Ortiz-Rodriguez JM, Gil MC, Alvarez M, De Paz P, Ezquerra LJ, Masot AJ, Redondo E. Computational flow cytometry reveals that cryopreservation induces spermptosis but subpopulations of spermatozoa may experience capacitation-like changes. Reproduction 2017;153:293-304.

11. Bergqvist A, Johannisson A, Bäckgren L, Dalin A, Rodriguez-Martinez H, Morrell JM. Single Layer Centrifugation of Stallion Spermatozoa through Androcoll™-E does not Adversely Affect their Capacitation-Like Status, as Measured by CTC Staining. Reprod Domest Anim 2011;46:e74-e78.

12. Leahy T, Gadella BM. Capacitation and capacitation-like sperm surface changes induced by handling boar semen. Reprod in Domest Anim 2011;46:7-13.

13. Talukdar DJ, Ahmed K, Sinha S, Deori S, Das GC, Talukdar P. Cryopreservation induces capacitation-like changes of the swamp buffalo spermatozoa. Buffalo Bulletin 2017;36:221-230.

14. Cormier N, Bailey JL. A differential mechanism is involved during heparin-and cryopreservation-induced capacitation of bovine spermatozoa. Biol Reprod 2003;69:177-185.

15. Thomas AD, Meyers SA, Ball BA. Capacitation-like changes in equine spermatozoa following cryopreservation. Theriogenology 2006;65:1531-1550.

16. Dobrinski I, Suarez SS, Ball BA. Intracellular calcium concentration in equine spermatozoa attached to oviductal epithelial cells in vitro. Biol Reprod 1996;54:783-788.

17. Meyers SA, Liu IK, Overstreet JW, Vadas S, Drobnis EZ. Zona pellucida binding and zona-induced acrosome reactions in horse spermatozoa: comparisons between fertile and subfertile stallions. Theriogenology 1996;46:1277-1288.

18. Umair M, Henning H, Stout TA, Claes A. A Modified Flotation Density Gradient

Centrifugation Technique Improves the Semen Quality of Stallions with a High DNA Fragmentation Index. Animals 2021;11:1973.

19. Brogan PT, Beitsma M, Henning H, Gadella BM, Stout T. Liquid storage of equine semen: assessing the effect of D-penicillamine on longevity of ejaculated and epididymal stallion sperm. Anim Reprod Sci 2015;159:155-162.

20. Bretschneider LH. Een normentafel ten gebruike bij de morphologische beoordeling van stierensperma. Tijdschr Diergeneeskd 1948;73:421-433.

22. Hall SE, Aitken RJ, Nixon B, Smith ND, Gibb Z. Electrophilic aldehyde products of lipid peroxidation selectively adduct to heat shock protein 90 and arylsulfatase A in stallion spermatozoa. Biol Reprod 2017;96:107-121.

23. Aitken RJ, Smith TB, Lord T, Kuczera L, Koppers AJ, Naumovski N, Connaughton H, Baker MA, De Iuliis GN. On methods for the detection of reactive oxygen species generation by human spermatozoa: analysis of the cellular responses to catechol oestrogen, lipid aldehyde, menadione and arachidonic acid. Andrology 2013;1:192-205.

24. Evenson D, Jost L. Sperm chromatin structure assay is useful for fertility assessment. Methods in Cell Science 2000;22:169-189.

25. Evenson DP. The Sperm Chromatin Structure Assay (SCSA®) and other sperm DNA fragmentation tests for evaluation of sperm nuclear DNA integrity as related to fertility. Anim Reprod Sci 2016;169:56-75.

26. Larson KL, Brannian JD, Hansen KA, Jost LK, Evenson DP. Relationship between assisted reproductive techniques (ART) outcomes and DNA fragmentation (DFI) as measured by the sperm chromatin structure assay (SCSA®). Fertil Steril 2002;78:S206.

27. Ghosh S, Serafini R, Love CC, Teague SR, Hernández-Avilés C, LaCaze KA, Varner DD. Effects of media and promoters on different lipid peroxidation assays in stallion sperm. Anim Reprod Sci 2019;211:106199.

28. Heiskanen M, Huhtinen M, Pirhonen A, Mäenpää PH. Insemination results with slow-cooled stallion semen stored for 70 or 80 hours. Theriogenology 1994;42:1043-1051.

29. Del Prete C, Stout T, Montagnaro S, Pagnini U, Uccello M, Florio P, Ciani F, Tafuri S, Palumbo V, Pasolini MP. Combined addition of superoxide dismutase, catalase and glutathione peroxidase improves quality of cooled stored stallion semen. Anim Reprod Sci 2019;210:106195.

30. Tharasanit T, Manee-In S, Khamenkhetwit P, Sirivaidyapong S, Lohachit C. The effect of cold storage on the quality of stallion semen and pregnancy rate after artificial insemination. The Thai Journal of Veterinary Medicine 2007;37:39-48.

31. Brinsko SP. Insemination doses: How low can we go? Theriogenology 2006;66:543-550.

32. Sieme H. Chapter 6 - Semen Evaluation. In: Samper JC. editor. Equine Breeding Management and Artificial Insemination (Second Edition). Saint Louis: W.B. Saunders; 2009. p 57-74.

33. Wennemuth G, Babcock DF, Hille B. Calcium clearance mechanisms of mouse sperm. J Gen Physiol 2003;122:115-128.

34. Mata-Martínez E, Sánchez-Cárdenas C, Chávez JC, Guerrero A, Treviño CL, Corkidi G, Montoya F, Hernandez-Herrera P, Buffone MG, Balestrini PA. Role of calcium oscillations in sperm physiology. BioSystems 2021;209:104524.

35. Orrenius S, Gogvadze V, Zhivotovsky B. Calcium and mitochondria in the regulation of cell death. Biochem Biophys Res Commun 2015;460:72-81.

36. Zhang L, Wang Z, Lu T, Meng L, Luo Y, Fu X, Hou Y. Mitochondrial Ca2 Overload Leads to Mitochondrial Oxidative Stress and Delayed Meiotic Resumption in Mouse Oocytes. Frontiers in Cell and Developmental Biology 2020;8:1053.

37. Strubbe-Rivera JO, Schrad JR, Pavlov EV, Conway JF, Parent KN, Bazil JN. The mitochondrial permeability transition phenomenon elucidated by cryo-EM reveals the genuine impact of calcium overload on mitochondrial structure and function. Scientific Reports 2021;11:1-15.

38. Singh S, Mabalirajan U. Mitochondrial calcium in command of juggling myriads of cellular functions. Mitochondrion 2021;57:108-118.

39. Sahu SK, Gummadi SN, Manoj N, Aradhyam GK. Phospholipid scramblases: an overview. Arch Biochem Biophys 2007;462:103-114.

40. Harrison R, Ashworth P, Miller N. Bicarbonate/CO2, an effector of capacitation, induces a rapid and reversible change in the lipid architecture of boar sperm plasma membranes. Molecular Reproduction and Development: Incorporating Gamete Research 1996;45:378-391.

41. Henning H, Ngo TT, Waberski D. Centrifugation stress reduces the responsiveness of spermatozoa to a capacitation stimulus in in vitro-aged semen. Andrology 2015;3:834-842.

42. Pena FJ, García BM, Samper JC, Aparicio IM, Tapia JA, Ferrusola CO. Dissecting the molecular damage to stallion spermatozoa: the way to improve current cryopreservation protocols? Theriogenology 2011;76:1177-1186.

43. Martinez-Alborcia MJ, Valverde A, Parrilla I, Vazquez JM, Martinez EA, Roca J. Detrimental effects of non-functional spermatozoa on the freezability of functional spermatozoa from boar ejaculate. PLoS One 2012;7:e36550.

44. Hardy M, Zielonka J, Karoui H, Sikora A, Michalski R, Podsiadły R, Lopez M, Vasquez-Vivar J, Kalyanaraman B, Ouari O. Detection and characterization of reactive oxygen and nitrogen species in biological systems by monitoring species-specific products. Antioxidants & Redox Signaling 2018;28:1416-1432.

45. Zielonka J, Kalyanaraman B. Hydroethidine-and MitoSOX-derived red fluorescence is not a reliable indicator of intracellular superoxide formation: another inconvenient truth. Free Radical Biology and Medicine 2010;48:983-1001.

46. Schulze M, Henning H, Rüdiger K, Wallner U, Waberski D. Temperature management during semen processing: Impact on boar sperm quality under laboratory and field conditions. Theriogenology 2013;80:990-998.

47. Bollwein H, Fuchs I, Koess C. Interrelationship between plasma membrane integrity, mitochondrial membrane potential and DNA fragmentation in cryopreserved bovine spermatozoa. Reproduction in Domestic Animals 2008;43:189-195.

48. Wu S, Canisso IF, Yang W, Ul Haq I, Liu Q, Han Y, Zeng S. Intracellular calcium chelating agent (BAPTA-AM) aids stallion semen cooling and freezing–thawing. Reproduction in Domestic Animals 2018;53:1235-1242.

49. Johnson LA, Weitze KF, Fiser P, Maxwell W. Storage of boar semen. Anim Reprod Sci 2000;62:143-172.

50. Pommer AC, Linfor JJ, Meyers SA. Capacitation and acrosomal exocytosis are enhanced by incubation of stallion spermatozoa in a commercial semen extender. Theriogenology 2002;57:1493-1501.

51. Gibb Z, Lambourne SR, Quadrelli J, Smith ND, Aitken RJ. L-carnitine and pyruvate are prosurvival factors during the storage of stallion spermatozoa at room temperature. Biol Reprod 2015;93:104, 1-9.

52. Gibb Z, Clulow JR, Aitken RJ, Swegen A. First publication to describe a protocol for the

liquid storage of stallion spermatozoa for 7 days. Journal of Equine Veterinary Science 2018;66:37-40.

Chapter 4

Vitrifying expanded equine embryos collapsed by blastocoel aspiration is less damaging than slow-freezing

M Umair[1], M Beitsma[1], M de Ruijter-Villani[1], C Deelen[1], C Herrera[2], TAE Stout[1], A Claes[1]

1 Department of Clinical Sciences, Faculty of Veterinary Medicine, Utrecht University, Utrecht, The Netherlands

2 Clinic of Reproductive Medicine, Vetsuisse Faculty, University of Zurich, Lindau, Switzerland

Published as:

M. Umair, M. Beitsma, M. de Ruijter-Villani, C. Deelen, C. Herrera, T.A.E. Stout, A. Claes, Vitrifying expanded equine embryos collapsed by blastocoel aspiration is less damaging than slow-freezing, Theriogenology, Volume 202, 2023, Pages 28-35, ISSN 0093-691X, https://doi.org/10.1016/j.theriogenology.2023.02.028.

Abstract

The cryotolerance of equine blastocysts larger than 300 µm can be improved by aspirating blastocoele fluid prior to vitrification; however, it is not known whether blastocoele aspiration also enables successful slow-freezing. The aim of this study was therefore to determine whether slow-freezing of expanded equine embryos following blastocoele collapse was more or less damaging than vitrification. Grade 1 blastocysts recovered on day 7 or 8 after ovulation were measured (>300-550 µm, n=14 and >550 µm, n=19) and blastocoele fluid was aspirated prior to slow-freezing in 10% glycerol (n=14), or vitrification (n=13) in 16.5% ethylene glycol/16.5% DMSO/0.5M sucrose. Immediately after thawing or warming, embryos were cultured for 24 h at 38°C and then graded and measured to assess re-expansion. Control embryos (n=6) were cultured for 24 h following aspiration of blastocoel fluid, without cryopreservation or exposure to cryoprotectants. Subsequently, embryos were stained to assess live/dead cell proportion (DAPI/TOPRO-3), cytoskeleton quality (Phalloidin) and capsule integrity (WGA). For 300-550 µm embryos, quality grade and re-expansion were impaired after slow-freezing but not affected by vitrification. Slow-freezing embryos >550 µm induced additional cell damage as indicated by a significant increase in dead cell proportion and disruption of the cytoskeleton; neither of these changes were observed in vitrified embryos. Capsule loss was not a significant consequence of either freezing method. In conclusion, slow-freezing of expanded equine blastocysts collapsed by blastocoel aspiration compromises post-thaw embryo quality more than vitrification.

Chapter 4

Introduction

Cryopreservation of equine embryos has several potential benefits, including more efficient use of recipient mares, collection of embryos outside the physiological breeding season, international trade and cryo-banking of embryos, for example, from young mares that are in training and yet to prove themselves [1–3] . Despite these advantages, embryo cryopreservation is not routinely performed in equine practice, mainly due to a lack of super-ovulatory agents and the limited ability of embryos larger than 300 μm to survive cryopreservation. The poor cryotolerance of large embryos is attributed to their physical characteristics [4–7]; the lower surface-to-volume ratio affects the diffusion of cryoprotectants in and out of the cells, and therefore, reduces the rate at which the cryoprotectant reaches equilibrium in and outside the cells [8]; more blastocoele fluid (BF) predisposes larger embryos to ice crystal formation during the freezing process which can, in turn, result in damage to organelles and loss of cellular integrity [7,9]. In addition, the blastocyst capsule increases in thickness during embryo development [10] and is thought to impede the diffusion of cryoprotectants into the embryo [11]. However, it is now known that puncture or puncture accompanied by aspiration of blastocoele fluid prior to vitrification markedly improves the cryotolerance of large embryos [12–15]; on the other hand, to our knowledge the impact of slow-freezing of collapsed large embryos on post-thaw embryo quality has not been reported.

Although the ability to generate a viable pregnancy remains the most important embryo quality parameter for equine practitioners, information on other aspects of embryo quality following slow-freezing or vitrification is limited, even though it is of potential value for refining cryopreservation protocols. In this respect, it is difficult to assess embryo quality immediately post-thaw or warming since the embryos are often still collapsed/shrunken. In addition, transfer of slow-frozen or vitrified embryos results either in success or failure to establish a pregnancy, but gives no additional information concerning embryo quality. By contrast, when embryos are evaluated after 24 hours (h) of culture, more detailed information can be recorded about cellular viability, organelle function and whether the capsule remains intact. Furthermore, embryo re-expansion after 24 h of culture (post-thawing or warming) has been proposed as an indicator of embryonic viability [16]. The aim of this study was to compare the impact of slow-freezing with that of vitrification on embryo quality grade, re-

expansion, and cellular and capsular integrity of flushed equine expanded blastocysts following puncture and collapse.

Materials and methods

Reproductive management of donor mares

The reproductive tract of donor mares (n=14; age 14±3 years (mean ± S.D.)) was examined on alternate days by transrectal ultrasonography. Once a growing, dominant follicle (>35 mm) was observed in the presence of uterine edema, ovulation was induced using buserelin acetate (0.33µg/kg Suprefact®, IM: CHEPLAPHARM, Greifswald, Germany). The day after induction of ovulation, mares were examined and inseminated with at least 500 million progressively motile sperm from a single fertile stallion; ovulation was confirmed the following day.

Embryo recovery and aspiration of blastocoele fluid

Embryos (n=33) were recovered at either day 7 or 8 after ovulation by uterine lavage with lactated Ringer´s solution (ADCCB2165S, Baxter Healthcare SA, Switzerland) supplemented with 0.5% fetal bovine serum (758093, Greiner Bio-One BV, Alphen aan den Rijn, The Netherlands), as described by Stout [16]. Recovered embryos were identified using a stereomicroscope (SZ-ST, Olympus®, Japan) and washed 4 times in H-SOF (HEPES buffered synthetic oviductal fluid [17]; AVANTEA, Cremona, Italy). Embryos were examined in more detail using an Olympus® IX71 microscope and their size (diameter in µm), quality (grade 1, excellent to 4, degenerated or dead) [18] and developmental stage were recorded. Only grade 1 expanded blastocysts >300 µm were included in this study, while embryos <300 µm (n=8) were used for other experiments. Embryos (1-3 per mare) were randomly divided into two groups depending on their size (>300-550 µm and >550 µm), and were then assigned into three different treatment groups: control (n=3, in each size group), slow-freezing (n=5, >300-550 µm and n=9, >550 µm), vitrification (n=6, >300-550 µm and n=7, >550 µm).

Next, all of the embryos including the controls, were punctured and more than 85% of the blastocoele fluid was aspirated, in a modification of the technique described by Herrera [12]. In brief, embryos were placed in H-SOF (control and slow-freezing group) or PBS without Ca and Mg (D8537, Sigma-Aldrich, Zwijndrecht, The Netherlands: Vitrification group) supplemented with 0.4% BSA (wt/vol, A6003, Sigma-Aldrich) and 0.1% PVP360

(Polyvinylpyrrolidone, wt/vol, 9003-39-8, Sigma-Aldrich), under mineral oil (ART-4008-5P, Coopersurgical, Målov Denmark) at room temperature (RT; 19-21˚C). The embryos were punctured and the blastocyst fluid was aspirated using an Olympus® IX71 microscope equipped with a micromanipulation system (Eppendorf TransferMan NK2, Hamburg, Germany), and either an injection needle (5µm inner diameter; MIC-50-30, Coopersurgical) or a biopsy needle (15µm inner diameter; MPB-BS-30, Coopersurgical) for embryos between 300 and 550 µm or larger than 550 µm, respectively.

Treatment groups

Control

After blastocoele collapse, control embryos (n=6) were cultured individually in micro drops (50 µL) under mineral oil in a petri dish (Nunc™ IVF Petri Dishes, 150255, Thermo Scientific™) for 24 h in a Dulbecco's Modified Eagle Medium (DMEM)-based culture medium; DMEM (D6421, Sigma-Aldrich) supplemented with 10% fetal calf serum (FCS, v:v, F4135 Sigma-Aldrich) and Gly-Gln monohydrate (0.5814 mg/mL, G5149 Sigma-Aldrich) at 38˚C in an incubator (Flatbed G185, Coopersurgical, Målov Denmark) containing an atmosphere of 6.5% CO_2 and 5% O_2 in air. Prior to use, the embryo culture medium was equilibrated for 24 h in the incubator (6.5% CO_2 and 5% O_2 in air).

Slow-freezing and thawing

Embryos were slow-frozen using the protocol described by Lazzari et al. [19], with minor modifications. In short, the collapsed embryo was incubated in 5% glycerol (v:v in H-SOF, 49767; Sigma-Aldrich) for 5 minutes followed by 20 minutes in 10% glycerol (v:v in H-SOF, 49767; Sigma-Aldrich) at RT (19-21˚C) in a four well dish (Nunc™ IVF multi-dish, 179830 Thermo Scientific™). Next, the embryo was loaded (fluid column, air bubble, droplet containing the embryo, air bubble and fluid column) into a 0.25 mL straw (F01, Agtech, USA). After the open end of the 0.25 mL straw had been heat-sealed, it was partially inserted into an outer, labelled 0.5 mL straw (for identification) and kept in aluminum foil to protect it from light until frozen. All procedures described above were carried out within the 20 minutes of the 10% glycerol incubation. Subsequently, the straw containing the embryo was loaded into the ethanol bath of a programmable freezing machine (2-stage cascade-cooling circulator; JULABO GmbH, Seelbach, Germany) at -6.5˚C for 5 minutes, and ice nucleation (seeding) was induced by briefly touching the straw with a metal forceps pre-cooled in liquid

nitrogen (LN_2). After observing the crystallization visually, the freezing process was continued according to the slow-freezing program (holding for 5 minutes at -6.5 ˚C, followed by cooling at -0.5˚C/minute down to -35˚C) after which the straw was plunged into, and stored in, LN_2 until thawing.

Thawing of slow-frozen embryos was performed by removing the straw containing the embryo from the LN_2, holding it in the air for 8 seconds and then plunging it into a water bath at RT for 20-30 seconds. Subsequently, the contents of the straw were expelled into a 3 cm petri dish. The embryo was then washed by passage through a series of H-SOF solutions containing decreasing concentrations of glycerol (8%, 6%, 4%, 2%, v:v in H-SOF) for 5 minutes each in a four well dish. After washing out the glycerol and brief examination, embryos were cultured for 24 h, as described for control embryos.

Vitrification and warming

The vitrification of embryos was performed as described by Herrera [12], with minor modifications. All steps were performed at RT. In brief, the collapsed embryo was held in 500 µL embryo holding medium (HM; PBS (D8537) supplemented with 20% fetal calf serum (FCS, v:v, F4135, Sigma-Aldrich) and 5 µg/mL gentamicin (15750-037, Gibco™) for 1 minute, and then transferred into 500 µL of vitrification solution 1 (VS1; HM containing 7.5% (v:v) ethylene glycol (EG, 324558, Sigma-Aldrich) and 7.5% (v:v) dimethyl sulphoxide (DMSO, D4540, Sigma-Aldrich)) for 3 minutes. Next, the embryo was incubated in 500 µL of vitrification solution 2 (VS2; HM containing 16.5% (v:v) EG, 16.5% (v:v) DMSO, and 0.5 M sucrose; S0389, Sigma-Aldrich). Finally, the embryo was loaded onto a hemi-straw and the excess media was removed to leave just a thin film of VS2 around the embryo. The hemi-straw containing the embryo was then plunged into LN_2, 45 seconds after the embryo was first placed in VS2. The hemi-straw was then part inserted into a labeled 0.5 mL straw under LN_2 and stored in LN_2 until warming and further processing.

The warming protocol for vitrified embryos was adopted from Herrera [12], with minor modifications, and involved sequential passage at 37 ˚C through three solutions: 1) Warming solution (WS) 1: Holding medium (HM) supplemented with 0.33 M sucrose, 2) WS2: HM supplemented with 0.2 M sucrose, 3) WS3: HM without sucrose. Briefly, after removing the straw from the LN_2, the outer (labeled) straw was removed, and the hemi-straw immediately submerged in WS1 and the embryo incubated for 5 minutes at 37 ˚C; 1 minute in well 1 (1000 µL, WS1) and 4 minutes in well 2 (500 µL, WS1) of a four well plate. Next, the embryo was

transferred to WS2 (500 µL, well 3) with a minimum volume of WS1 and incubated for 5 minutes at 37 ˚C. Finally, the embryo was transferred to WS3 (500 µL, well 4) and incubated for 5 minutes. After completion of the warming process and brief examination, embryos were cultured for 24 h, as described for the other groups.

Post-culture embryo evaluation

Immediately after the 24 h culture, embryos were transferred to a micromanipulation dish containing pre-warmed (37 ˚C) H-SOF under mineral oil. Embryos were graded (1 to 4, as described earlier; representative embryos are shown in Fig. 1) and measured (diameter in µm) to calculate embryo re-expansion [embryo re-expansion (%) = (embryo diameter after collapsing, slow-freezing/vitrification and 24 h of culture/embryo original diameter) x 100], and the relationship between embryo grade and embryo re-expansion was assessed.

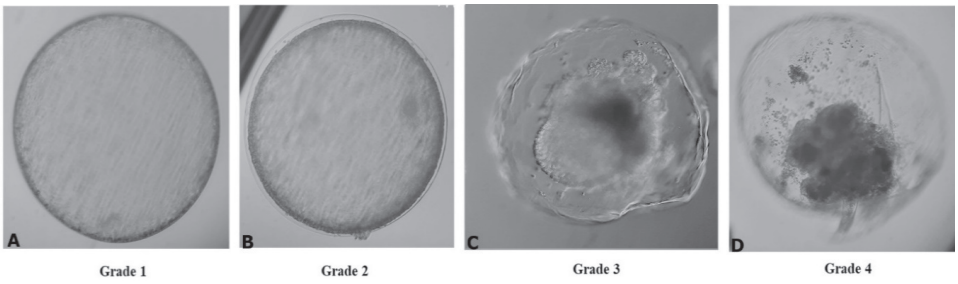

Figure 1. Embryo grading after thawing/warming and 24 h of culture of expanded equine embryos collapsed by blastocoele puncture prior to cryopreservation. *A) Excellent; no visual imperfections, B) Good; minor imperfections, limited separation between trophoblast and capsule, C) Poor; moderate imperfection, D) Dead or degenerated; severe defects, for details [17].*

If herniation of part of the embryo through the capsule occurred, a mean of two measurements was taken (perpendicular to each other with one going through both the capsule-contained and herniated area) to give an estimate of the expansion. Embryos that expanded to at least their pre-cryopreservation size were considered to have 're-expanded'. Subsequently, each embryo was washed three times (5 minutes each) in PBS containing 0.1% (wt/vol) PVP (P0930-50G, Sigma-Aldrich), incubated for 30 minutes at 37 ˚C in PBS containing DAPI (4',6-diamidino-2-phenylindoledihydrochloride, 1:500), and washed again three times (5 minutes each) in PBS-PVP. Next, each embryo was fixed in 4% paraformaldehyde PBS-PVP for 1 h at RT (19-21˚C) and washed three times (5 minutes each) in PBS containing 0.1% Triton X100 (PBST), and permeabilized by incubation for 30 minutes at RT in PBST. Embryos were stained for 1 h at RT in PBS-PVP containing: 1:100 Alexa Fluor™ 568

Phalloidin (A12380, Invitrogen) to stain the cytoskeleton; 1:500 TO-PRO™-3 iodide 642 (T3605, Invitrogen) to counter-stain the nuclei and 1:500 wheat germ agglutinin (WGA-FITC; L4895, Sigma- Aldrich) to stain the capsule and assess its integrity. After washing three times (5 minutes each) in PBS-PVP, embryos were washed once in a 10 µL drop of an antifade agent (VECTASHIELD; Vector Laboratories, Burlingame, CA, USA) and mounted on a glass slide (Super-frost Plus; Menzel, Braunschweig, Germany) within a spacer (0.12 mm eight-well Secure-Seal Spacer, Molecular Probes) containing 8 µL of antifade agent. After covering with a coverslip (22x30mm, $1^{1/2}$ thickness, ERIE Scientific, Portsmouth, USA), each embryo was flattened by gently pressing the coverslip, and the edges were sealed with nail polish. Slides were stored at 4 ˚C until microscopic analysis. The embryos were protected from light during all incubation steps.

Confocal microscopy was performed using a Nikon A1R/STORM system equipped with four lasers (405 nm for DAPI; 488 nm for WGA; 561 nm for Phalloidin; and 640 nm for TO-PRO ™ -3 iodide) to assess dead cell proportion, cytoskeleton quality and capsule integrity. The dichroic filter was a quad line laser filter (405/488/561/640) and the emission filters were 482/32, 515/30, 595/50 and 700/75 for DAPI, FITC, Alexa Fluor 568 ™ and TO-PRO-3 ™, respectively. Z-stacks (2 µm thickness with top and bottom acquisition defined manually) were acquired using a 20X/0.75 NA (numerical aperture) air immersion lens (1000 µm working distance). Pinhole size was 26.82 µm and images (512x512 pixels) were collected in bidirectional mode with a pixel size of 0.97 µm. 3D rendering and image analysis was performed using NIS elements software (NIKON, Japan, vs 5.21.03). Nuclei were preprocessed by median filtering (count 3) and segmentation thresholds were set to 2047 and 2518 intensity for the DAPI and TO-PRO-3 channels, respectively. The proportion of dead cells was estimated by expressing the DAPI positive cell area as a proportion of the TO-PRO-3® (total cells after fixation) positive area (supplementary data file 1). Dead cell proportion was classified as follows: no cell death (0% dead cells), mild cell death (1-10% dead cells), moderate cell death (11-20% dead cells), extensive cell death (>20% dead cells) (Fig. 2; maximum intensity projections of representative embryos). Evaluation of the cytoskeleton of embryos was performed as described by Tharasanit et al. [6]; precise and sharp delineation of actin staining around the cell borders was classified as a grade 1 cytoskeleton, (Fig. 3: A and A 1); less distinct outlining of the cells, combined with occasional small clumps of actin within the cytoplasm, was classified as a grade 2 cytoskeleton (Fig. 3: B and B 1); large areas lacking actin staining, with the visible actin largely agglomerated into intracytoplasmic

clumps, resulted in classification as a grade 3 cytoskeleton, (Fig. 3: C and C 1). The blastocyst capsule was classified as either intact (no visible abnormality or puncture hole (Fig. 4 A) or damaged (large rent in the capsule and/or significant herniation of the embryo through the hole (Fig. 4 B).

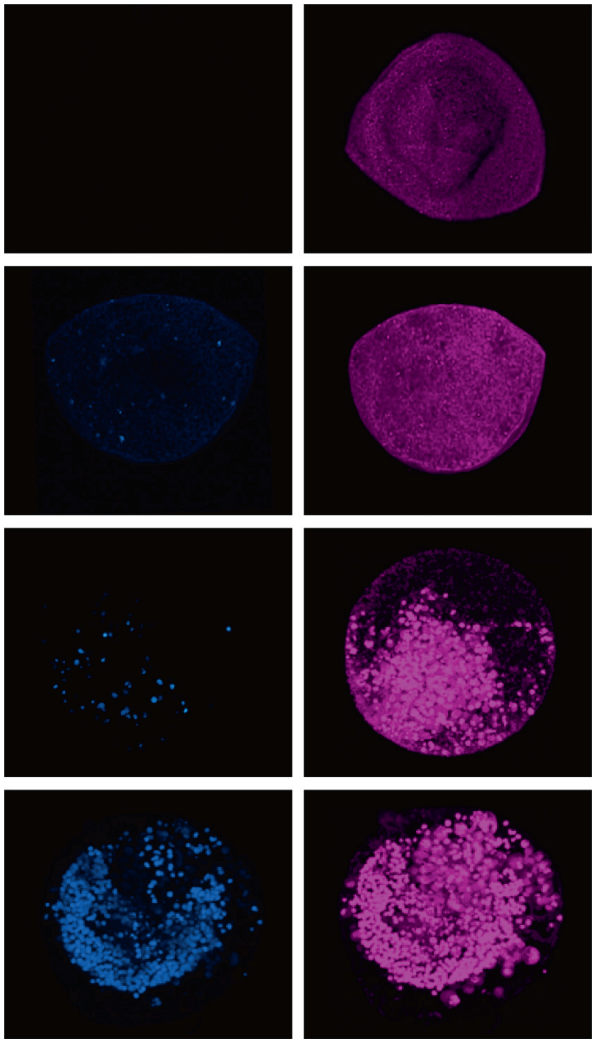

Figure 2. Dead cell proportion after thawing/warming and 24 h of culture of expanded equine embryos collapsed by blastocoele puncture prior to cryopreservation. *Embryos were stained with DAPI before fixation (viability stain; nuclei of membrane damaged cells) and with TO-PRO-3® after fixation (all nuclei). Each image is a maximum intensity projection of an embryo; A) No cell death (0% dead cells); A1) all cells; B) Mild cell death (1-10% dead cells); B1) all cells; C) Moderate cell death (11-20% dead cells); C1) all cells, D) Extensive cell death (>20% dead cells); D1) all cells. Scale bar = 100 µm*

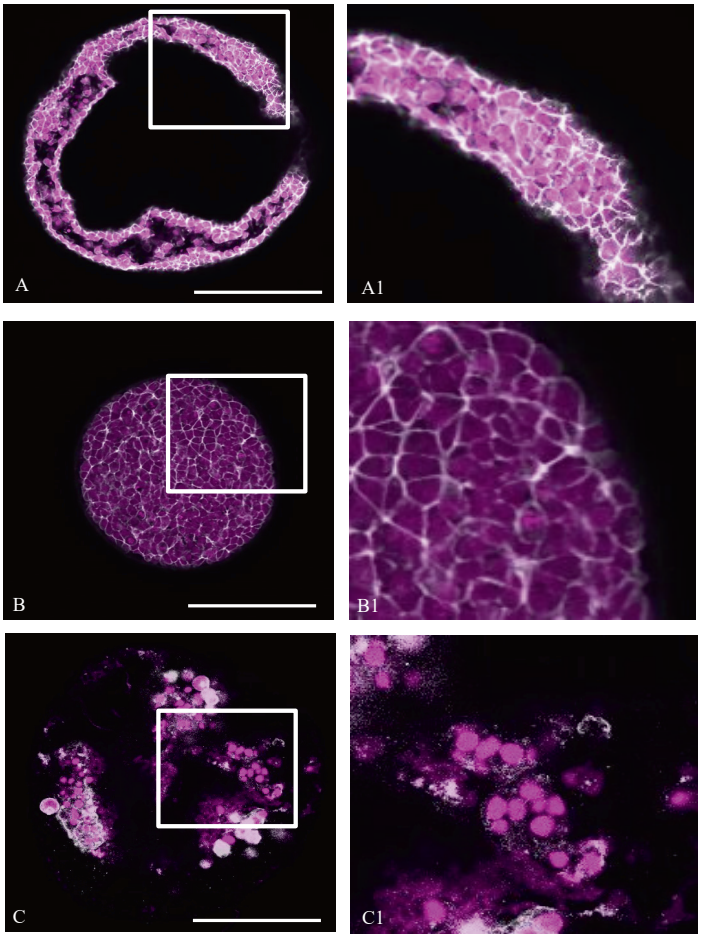

Figure 3. Cytoskeleton quality after thawing/warming and 24 h culture of expanded equine embryos collapsed by blastocoele puncture prior to cryopreservation. *Fixed embryos were stained with Phalloidin-Alexa Fluor® 568 (cytoskeleton stain, grey) and TOPRO-3 (Nuclei, magenta). Each image is from a z-stack of an embryo. A) Grade I cytoskeleton (precise, sharp restriction of actin staining to the cell borders: A1; magnified area represented by white square in A). B) Grade II cytoskeleton (less distinct outlining of the cells, combined with occasional small clumps of actin in the cytoplasm: B1; magnified area represented by white square in B). C) Grade III cytoskeleton (large areas lacking actin staining, with the visible actin largely agglomerated in intracytoplasmic clumps: C1; magnified area represented by white square in C). Scale bar = 100 µm*

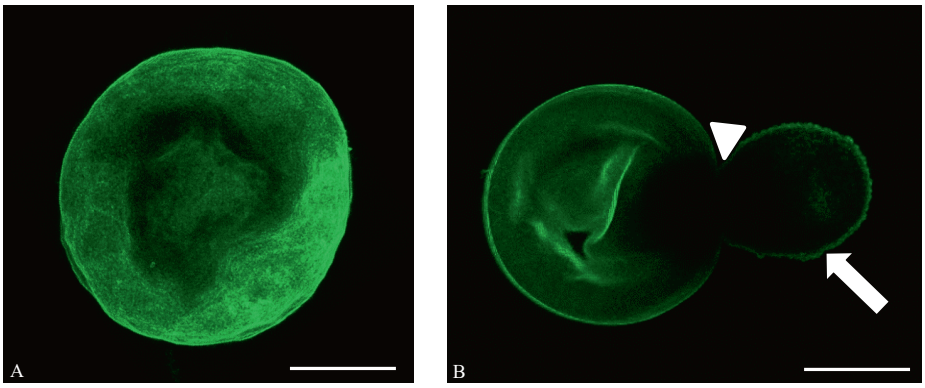

Figure 4. Integrity of blastocyst capsule after thawing/warming and 24 h culture of expanded equine embryos collapsed by blastocoele puncture prior to cryopreservation. *Fixed embryos were stained with WGA-FITC. Each image is a 3D reconstruction of an embryo A) No visible defect in the capsule, B) Large rent in the capsule (arrowhead) and herniation of the embryo from the capsule (arrow); Scale bar = 100 µm*

Statistical analysis

Differences in embryo re-expansion between control, vitrified and slow frozen embryos were examined using a one-way ANOVA, with a Tukey post hoc test. Kruskal-Wallis tests with Dunn's post hoc testing was used to detect differences in embryo grade, dead cell proportion and cytoskeleton grade between control, slow-frozen and vitrified embryos, while differences in capsule integrity were determined using Fisher's exact test. Student's t test with Welch's correction was used to examine the differences in post-thaw or post-warming embryo expansion between good quality embryos (grade 1 and 2) and poor quality (grade 3 and 4) embryos. Statistical analysis was performed using GraphPad prims software version 8 (GraphPad Software, San Diego, CA, USA). A p-value less than 0.05 was considered to indicate a statistical difference.

Results

All frozen and vitrified embryos were still collapsed and shrunken within the capsule immediately after thawing or warming (Supplementary Fig. 1). Categorical data, i.e. the embryo quality grade, dead cell proportion and cytoskeleton quality are shown as proportions (Fig. 5) and median, while continuous data for embryo expansion is shown as mean ± SEM.

Embryo grade and re-expansion after culture

After 24 h culture, all of the 300-550 μm control embryos were classified as grade 1 (3/3, median=1). Slow-freezing of embryos led to a significant reduction in embryo quality grade (100% [5/5] grade 3, median=3) whereas vitrification did not significantly affect embryo quality (67% [4/6] grade 1 and 33% [2/6] grade 3, median=1: Fig. 5 A). For embryos >550 μm, embryo quality grade was significantly lower after slow-freezing (11% [1/9] grade 2, 78% [7/9] grade 3 and 11% [1/9] grade 4, median=3: Fig. 6) than vitrification (14% [1/7] grade 1 and 86% [6/7] grade 2, median=2: Fig. 6). However, neither differed significantly from control embryos (100% [3/3] grade 2, median=2: Fig 5 A).

Embryo re-expansion (percentage change in embryo diameter after collapse of the blastocoele, cryopreservation and culture for 24 h) was significantly higher for grade 1 and 2 embryos (137±7%) than grade 3 and 4 embryos (66±9%). Moreover, slow-freezing had a negative impact on embryo re-expansion, which was significantly lower (73±15%) than for vitrified (148±11%) and control (179±4%) embryos between 300 and 550 μm (Fig. 5 B); embryo re-expansion did not differ between control and vitrified embryos. The effect of the freezing method on embryo re-expansion was even more pronounced in larger (>550 μm) embryos; embryo re-expansion was significantly lower in slow-frozen embryos (52±8%) than in control (129±7%) and vitrified embryos (115±3%) but did not differ between the latter 2 groups (Fig. 5 B).

Dead cell proportion

The freezing method did not influence the proportion of dead cells in embryos between 300 and 550 μm; dead cell proportion was not significantly different between control (67% [2/3] no cell death and 33% [1/3] mild cell death, median=1), vitrified (33% [2/6] no cell death, 50% [3/6] mild cell death, 0% moderate cell death and 17% [1/6] extensive cell death, median=2) and slow-frozen (60% [3/5] no cell death and 40% [2/5] extensive cell death, median=1) embryos (Fig. 5 C). By contrast, the freezing method did have a significant impact on cell death in embryos >550 μm, with the proportion of dead cells significantly higher in slow-frozen embryos (0% no cell death, 22% [2/9] mild cell death, 0% moderate cell death and 78% [7/9] extensive cell death, median=4) than in control (100% [3/3] no cell death, median=1) and vitrified (57% [4/7] no cell death, 43% [3/7] mild cell death, median=1) embryos (Fig. 5 C).

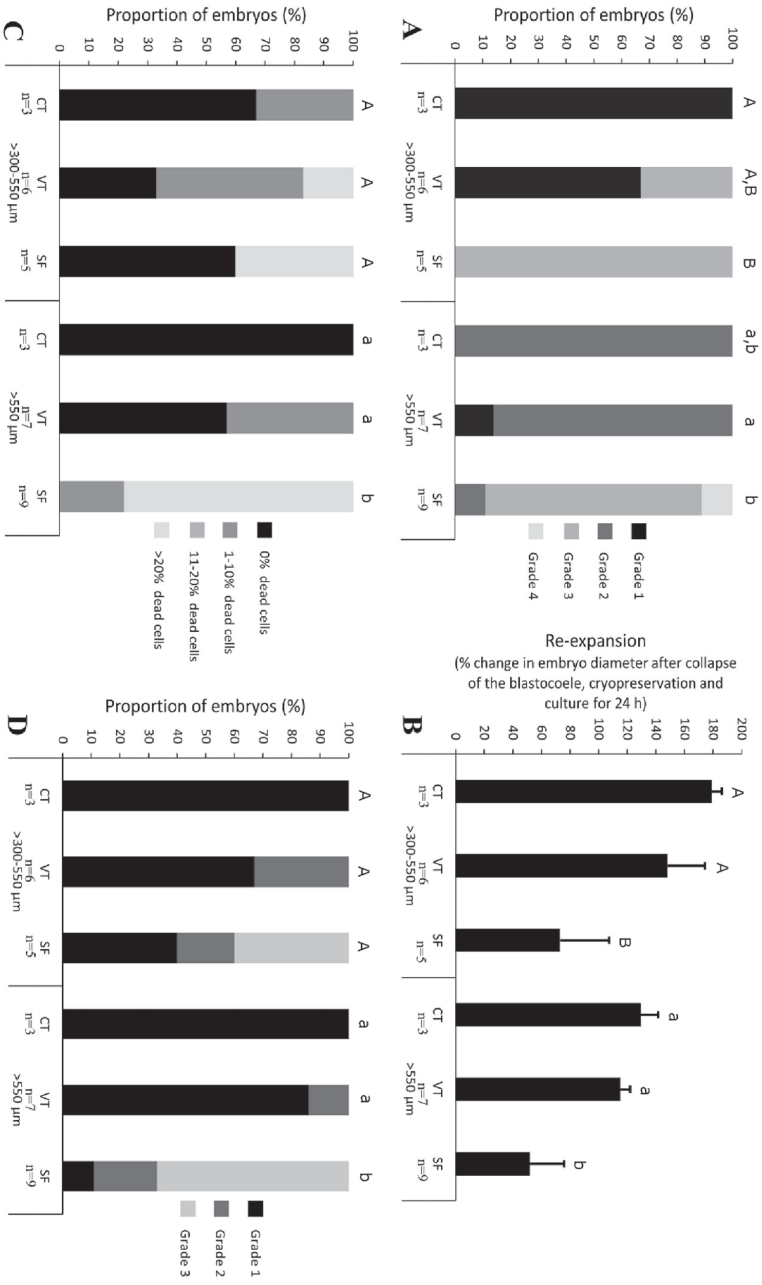

Figure 5. Embryo quality parameters for control (CT), vitrified (VT) and slow-frozen (SF) expanded equine embryos (>300-550 µm and >550 µm) after thawing/warming and 24 h culture. A) Embryo grade: (graded from 1 (excellent, Black) to 4 (dead, light grey), B) Embryo re-expansion (% change in embryo diameter after collapse of the blastocoele, cryopreservation and culture for 24 h), *C) Dead cell proportion: divided into 4 categories; no cell death (0% dead cells), mild cell death*

(1-10% dead cells), moderate cell death (10-20% dead cells), extensive cell death (>20% dead cells), D) Cytoskeleton quality: graded from 1 (excellent, black) to 3 (poor, light grey). n= number of embryos in each treatment group. Bars in Fig. 5 A, C and D (upper case for embryos >300-550 µm and lower case for embryos >550 µm) with the same superscript do not differ significantly between treatment groups, based on Kruskal-Wallis tests; data are plotted as proportions. Different superscript above the bars in Fig. 5 B (upper case for embryos >300-550 µm and lower case for embryos >550 µm) indicate statistically significant differences in embryo re-expansion; data is depicted as mean ± SEM.

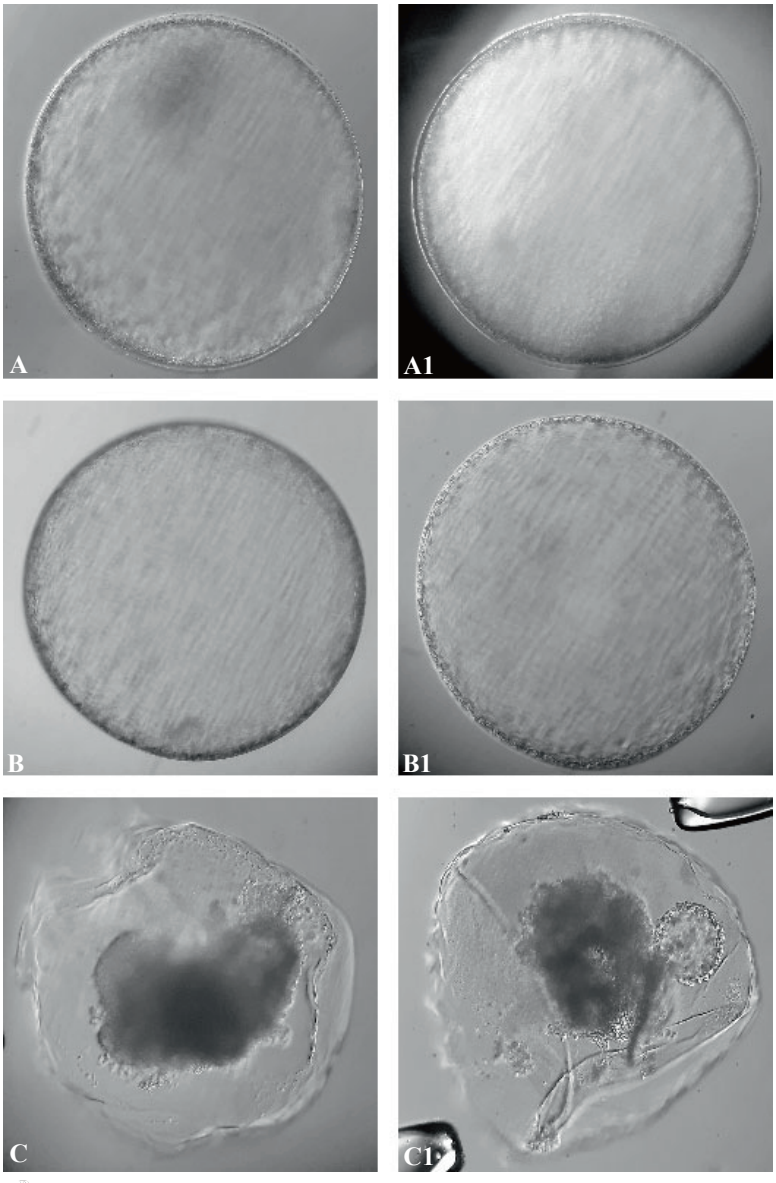

Figure 6. Appearance of large control, vitrified and slow-frozen equine embryos after 24 h culture subjected to blastocoele collapse prior to cryopreservation. *Control embryos (A and A1), Vitrified embryos (B and B2), and slow-frozen embryos (C and C1).*

Cytoskeleton quality

Although cytoskeleton quality appeared subjectively to be compromised in slow-frozen embryos, there were no statistically verifiable differences in cytoskeleton quality between control (100% [3/3] grade 1, median=1), slow-frozen (40% [2/5] grade 1, 20% [1/5] grade 2 and 40% [2/5] grade 3, median=3), and vitrified (67% [4/6] grade 1 and 33% [2/6] grade 2, median=1) embryos between 300 and 550 µm (Fig. 5 D). Slow-frozen embryos larger than 550 µm did, however, suffer more cytoskeleton disruption (11% [1/9] grade 1, 22% [2/9] grade 2 and 67% [6/9] grade 3, median=3) than control (100% [3/3] grade 1, median=1) or vitrified (86% [6/7] grade1 and 14% [1/7] grade 2, median=1) embryos (Fig. 5 D).

Embryonic capsule integrity

The integrity of the capsule after thawing or warming was not significantly influenced by the freezing method in either embryo size group (>300-550 µm and >550 µm). Although a large percentage of slow-frozen embryos between 300 and 550 µm had a damaged capsule, there were no significant differences between slow-frozen (20% [1/5] intact and 80% [4/5] damaged capsule), control (100% [3/3] intact capsule) and vitrified embryos (67% [4/6] intact and 33% [2/6] damaged capsule), presumably in part because of the small number of embryos analyzed. Similarly, no significant differences were detected in capsule integrity between control (100% [3/3] intact capsule), slow-frozen (78% [7/9] intact and 22% [2/9] damaged capsule) or vitrified embryos (100% [7/7] intact capsule) larger than 550µm.

Discussion

To the authors' knowledge, this is the first study to examine the impact of slow-freezing on post-thaw quality of expanded horse blastocysts cryopreserved following blastocoele puncture and aspiration. This is surprising since previous studies suggested that, for non-punctured horse embryos, slow-freezing induced less cell damage than vitrification [7]. Surprisingly, in the current study, slow-freezing turned out to be more detrimental than vitrification to embryo grade and re-expansion in embryos >300-550 µm and, in embryos larger than 550 µm also resulted in more extensive cell death and cytoskeleton disruption. Irrespective of embryo size, vitrification was less harmful than slow-freezing in terms of post-warming embryo grade, embryo re-expansion, live-dead cell proportion and cytoskeleton quality, none of which differed significantly to control embryos. We conclude

that vitrification appears to be a superior method for cryopreserving *in vivo* developed horse embryos >300 μm in diameter after blastocoele aspiration.

Slow-freezing of collapsed embryos induced more damage than vitrification, while cryo-damage also increased with embryo size as reported previously [6,7]. One of the advantages of vitrification is that it prevents the formation of ice crystals by inducing an instantaneous transition from a liquid to a glass-like state. To achieve this transition, ultra-rapid cooling (20,000 to 30,000 ˚C/min by plunging embryos directly in LN_2 in an open system; Hemi-straw) with a minimum volume of cryoprotectant solution (<1 μL) is critical. By contrast, the much slower cooling rate (-0.2 to -0.5 ˚C/min) of the slow-freezing process predisposes embryonic cells to intra-cellular ice crystal formation, particularly if the cryoprotectant has not fully equilibrated between the cells and the medium. Puncturing the embryo and removing blastocoel fluid would be expected to reduce the surface area-to-volume ratio and improve cryoprotectant access, thereby reducing the risk of cryo-damage of large embryos preserved by vitrification. This hypothesis is supported by the poor cryo-tolerance of expanded blastocysts vitrified without blastocoel aspiration [7], and the improved survival when more of the blastocyst fluid is removed from larger blastocysts prior to vitrification [13, 14]. Surprisingly blastocoel fluid aspiration did not markedly ameliorate cryo-damage after slow-freezing, despite breaching of the capsule and reduction of embryo volume. Possibly, the small hole made in the capsule and/or the equilibration times used are insufficient to allow adequate influx of cryoprotectant, and efflux of intracellular water.

The other possible reason for the higher levels of damage during slow freezing, could be a sub-optimal freezing rate during the chosen slow-freezing protocol. Previously, it was reported that the cryo-survival of equine embryos after reducing the volume of blastocoel fluid by dehydration (≈50% reduction in the volume) could be improved by reducing the cooling rate (-0.3 ˚C/min (-6 ˚C to -30 ˚C) and -0.1 ˚C/min (-30 ˚C to -33 ˚C) instead of -0.5 ˚C/min). The decreased cooling rate increased the total cooling period and allowed larger embryos to dehydrate more completely as the freezing process progressed, and the cryoprotectants would also have more time to reach equilibrium in and outside of the cells [8]. In the current study, the freezing rate was kept at 0.5 ˚C/min because this works well with small embryos (<250 μm) [4,6,7] and a significant volume (≥85%) of the blastocoel fluid was aspirated before cooling.

It is challenging and difficult to assess embryo quality immediately after thawing or warming, because the embryos are frequently still collapsed/shrunken and separated from the surrounding capsule. However, culturing embryos for 24 h after thawing or warming allows them to re-expand, after which embryo quality parameters, such as embryo grade, re-expansion, cellular viability, cytoskeleton quality and capsule integrity, can be assessed. Moreover, embryo re-expansion during culture is likely to reflect embryo viability and could, therefore, have value in predicting pregnancy outcome after transfer. In our study, embryo re-expansion appeared to be linked to post-thaw/warming embryo quality, with limited re-expansion of poor quality (grade 3 and 4) embryos. Re-expansion of embryos post thawing/warming is positively correlated with the pregnancy outcome for human embryos; the likelihood of obtaining a pregnancy is higher for re-expanded human blastocysts than blastocysts that do not re-expand [20–22].

The likelihood of pregnancy after the transfer of collapsed vitrified embryos has been reported to exceed 70 % [13, 14]. On the other hand, there is no data on pregnancy rates following transfer of collapsed slow-frozen horse embryos. Although none of the slow-frozen or vitrified embryos were transferred into recipient mares, we presume that the likelihood of obtaining a viable pregnancy after transfer of a slow-frozen, collapsed expanded blastocyst would be low. In particular, with the exception of one large embryo, slow-frozen embryos were predominately classified as grade 3 after 24 h culture. For non-cryopreserved horse embryos, the likelihood of pregnancy is known to be lower after transfer of grade 3 (44%) than grade 1 or 2 (87%) embryos, and recipient mares that receive a grade 3 embryo are more likely to experience subsequent embryonic or fetal loss [23]. Furthermore, slow-frozen embryos larger than 550 μm had a higher percentage of dead cells (>20%). Equine embryos with more than 20% dead cells were previously reported to be non-viable (degenerated) [25]. In conjunction with the high percentage of dead cells, the cytoskeleton of the majority of the slow-frozen large embryos was severely disrupted (grade 3), whereas 86% of the vitrified large embryos had a grade 1 cytoskeleton. Whether these alterations in cytoskeleton integrity in equine embryos influence pregnancy outcome is unknown. However, it has been shown that porcine embryos with a grade 2 cytoskeleton are less likely to result in a pregnancy than embryos with a grade 1 cytoskeleton [26].

Conclusion

In conclusion, vitrification should be preferred over slow-freezing as the cryopreservation method of choice for large expanded equine blastocysts subjected to blastocyst puncture and aspiration.

Authors contribution

Conceptualization: M Umair, TAE Stout and A Claes, **Methodology:** M Umair, M Beitsma, M de Ruijter-Villani, C Deelen, C Herrera, **Data curation:** M Umair, **Software:** M Umair, M de Ruijter-Villani and A Claes, **Supervision:** TAE Stout and A Claes, **Resources:** TAE Stout, **Writing-Original draft preparation:** M Umair and A Claes, **Writing- Reviewing and Editing:** M Umair, M Beitsma, M de Ruijter-Villani, C Herrera, TAE Stout and A Claes.

Acknowledgments

Authors acknowledge the help of Bart Leemans and Soledad Martin Pelaez with embryo flushing, and Jon de Rijk, Wilbert Beukens, Esther Akkermans and Leonie Arnold with semen collection. The authors thank the Punjab Educational Endowment Fund (PEEF), Punjab, Pakistan (PEEF/SSMS/18/222) for supporting this study. Confocal imaging and image analyses were performed at the Center for Cell Imaging (CCI) at the Faculty of Veterinary Medicine, Utrecht University (Utrecht, The Netherlands). The authors also thank Richard Wubbolts and Esther van t Veld for their help and technical support in confocal imaging and image analyses.

Declaration of interest

Authors have no conflict of interest to declare.

Supplementals

Supplementary data file and figure is available at *Theriogenology* (https://doi.org/10.1016/j.theriogenology.2023.02.028) online.

References

1. Stout T. Cryopreservation of Equine Embryos: Current State-of-the-Art: Cryopreservation of Equine Embryos. Reprod Domest Anim 2012;47:84–9. https://doi.org/10.1111/j.1439-0531.2012.02030.x.

2. Squires EL. Breakthroughs in Equine Embryo Cryopreservation. Vet Clin North Am Equine Pract 2016;32:415–24. https://doi.org/10.1016/j.cveq.2016.07.009.
3. McCue PM. Embryo Cryopreservation. In: Dascanio J, McCue P, editors. Equine Reprod. Proced. 1st ed., Wiley; 2021, p. 241–3. https://doi.org/10.1002/9781119556015.ch66.
4. Slade NP, Takeda T, Squires EL, Elsden RP, Seidel GE. A new procedure for the cryopreservation of equine embryos. Theriogenology 1985;24:45–58. https://doi.org/10.1016/0093-691X(85)90211-0.
5. Squires EL, Seidel GE, Mckinnon AO. Transfer of cryopreserved equine embryos to progestin-treated ovariectomised mares. Equine Vet J 2010;21:89–91. https://doi.org/10.1111/j.2042-3306.1989.tb04689.x.
6. Tharasanit T, Colenbrander B, Stout TAE. Effect of cryopreservation on the cellular integrity of equine embryos. Reproduction 2005;129:789–98. https://doi.org/10.1530/rep.1.00622.
7. Hendriks WK, Roelen BAJ, Colenbrander B, Stout TAE. Cellular damage suffered by equine embryos after exposure to cryoprotectants or cryopreservation by slow-freezing or vitrification: Cellular damage suffered by equine embryos during cryopreservation. Equine Vet J 2015;47:701–7. https://doi.org/10.1111/evj.12341.
8. Barfield JP, McCue PM, Squires EL, Seidel GE. Effect of dehydration prior to cryopreservation of large equine embryos. Cryobiology 2009;59:36–41. https://doi.org/10.1016/j.cryobiol.2009.04.003.
9. Dobrinsky JR. Cellular approach to cryopreservation of embryos. Theriogenology 1996;45:17–26. https://doi.org/10.1016/0093-691X(95)00351-8.
10. Kingma SEG, Thibault ME, Betteridge KJ, Schlaf M, Gartley CJ, Chenier TS. Permeability of the equine embryonic capsule to ethylene glycol and glycerol in vitro. Theriogenology 2011;76:1540–51. https://doi.org/10.1016/j.theriogenology.2011.06.026.
11. Legrand E, Krawiecki JM, Tainturier D, Corniere P, Delajarraud H, Bruyas J-F. Does the embryonic capsule impede the freezing of equine embryos? Proc 5th Int Symp Equine Embryo Transf Havemeyer Found Monogr 2000;3:62–5.
12. Herrera C. Vitrification of Equine In Vivo-Derived Embryos After Blastocoel Aspiration. In: Wolkers WF, Oldenhof H, editors. Cryopreserv. Free.-Dry. Protoc., vol. 2180, New York, NY: Springer US; 2021, p. 517–22. https://doi.org/10.1007/978-1-0716-0783-1_25.

13. Choi YH, Velez IC, Riera FL, Roldán JE, Hartman DL, Bliss SB, et al. Successful cryopreservation of expanded equine blastocysts. Theriogenology 2011;76:143–52. https://doi.org/10.1016/j.theriogenology.2011.01.028.
14. Wilsher S, Rigali F, Couto G, Camargo S, Allen WR. Vitrification of equine expanded blastocysts following puncture with or without aspiration of the blastocoele fluid. Equine Vet J 2019;51:500–5. https://doi.org/10.1111/evj.13039.
15. Canesin HS, Ortiz I, Rocha Filho AN, Salgado RM, Brom-de-Luna JG, Hinrichs K. Effect of warming method on embryo quality in a simplified equine embryo vitrification system. Theriogenology 2020;151:151–8. https://doi.org/10.1016/j.theriogenology.2020.03.012.
16. Stout TAE. Equine embryo transfer: review of developing potential. Equine Vet J 2010;38:467–78. https://doi.org/10.2746/042516406778400529.
17. Tervit HR, Whittingham DG, Rowson LEA. SUCCESSFUL CULTURE IN VITRO OF SHEEP AND CATTLE OVA. Reproduction 1972;30:493–7. https://doi.org/10.1530/jrf.0.0300493.
18 .McCue PM. Embryo Evaluation. In: Dascanio JJ, McCue PM, editors. Equine Reprod. Proced., Hoboken, NJ, USA: John Wiley & Sons, Inc; 2014, p. 169–72. https://doi.org/10.1002/9781118904398.ch52.
19 .Lazzari G, Colleoni S, Crotti G, Turini P, Fiorini G, Barandalla M, et al. Laboratory Production of Equine Embryos. J Equine Vet Sci 2020;89:103097. https://doi.org/10.1016/j.jevs.2020.103097.
20 .Aparici. González M, Herrer. Grassa L, Cascale. Romero L, Lláce. Aparicio J, Te. Morro J, Bernabe. Pérez R. P–264 Clinical relevance of re-expansion after blastocyst thawing. Hum Reprod 2021;36:deab130.263. https://doi.org/10.1093/humrep/deab130.263.
21 .Shu Y, Watt J, Gebhardt J, Dasig J, Appling J, Behr B. The value of fast blastocoele re-expansion in the selection of a viable thawed blastocyst for transfer. Fertil Steril 2009;91:401–6. https://doi.org/10.1016/j.fertnstert.2007.11.083.
22 .Zhao J, Yan Y, Huang X, Sun L, Li Y. Blastocoele expansion: an important parameter for predicting clinical success pregnancy after frozen-warmed blastocysts transfer. Reprod Biol Endocrinol 2019;17:15. https://doi.org/10.1186/s12958-019-0454-2.
23. Foss R, Wirth N, Schiltz P, Jones J. Nonsurgical Embryo Transfer in a Private Practice (1998). Proc 45th Ann Conv AAEP 1999;45.
24. Moussa M, Bersinger I, Doligez P, Guignot F, Duchamp G, Vidament M, et al. In vitro comparisons of two cryopreservation techniques for equine embryos: Slow-cooling and

open pulled straw (OPS) vitrification. Theriogenology 2005;64:1619–32. https://doi.org/10.1016/j.theriogenology.2005.04.001.

25. Zijlstra C, Kidson A, Schoevers EJ, Daemen AJJM, Tharasanit T, Kuijk EW, et al. Blastocyst morphology, actin cytoskeleton quality and chromosome content are correlated with embryo quality in the pig. Theriogenology 2008;70:923–35. https://doi.org/10.1016/j.theriogenology.2008.05.055.

Chapter 5

In vitro-produced Equine Blastocysts Exhibit Greater Dispersal and Intermingling of Inner cell mass Cells than In vivo Embryos

Muhammad Umair[1], Veronica Flores da Cunha Scheeren[1], Mabel Beitsma[1], Silvia Colleoni[2], Cesare Galli[2], Giovanna Lazzari[2], Marta de Ruijter-Villani[1], Tom Stout[1] and Anthony Claes[1]

1 Department of Clinical Sciences, Faculty of Veterinary Medicine, Utrecht University, Utrecht, The Netherlands

2 Avantea, Via Porcellasco 7f, Cremona, Italy.

Published as:

Umair, M.; da Cunha Scheeren, V.F.; Beitsma, M.; Colleoni, S.; Galli, C.; Lazzari, G.; de Ruijter-Villani, M.; Stout, T.; Claes, A. In vitro-produced equine blastocysts exhibit greater dispersal and intermingling of inner cell mass cells than in vivo embryos. Int. J. Mol. Sci. 2023, 24, x. https://doi.org/10.3390/ijms24119619

Abstract

In vitro production (IVP) of equine embryos is increasingly popular in clinical practice, but suffers from higher incidences of early embryonic loss and monozygotic twin development than transfer of *in vivo* derived (IVD) embryos. Early embryo development is classically characterized by two cell fate decisions:1) first, trophectoderm (TE) cells differentiate from inner cell mass (ICM), 2) second, the ICM segregates into epiblast (EPI) and primitive endoderm (PE). This study examined the influence of embryo type (IVD versus IVP), developmental stage or speed, and culture environment (*in vitro* versus *in vivo*) on the expression of the cell lineage markers, CDX-2 (TE), SOX-2 (EPI) and GATA-6 (PE). The numbers and distribution of cells expressing the 3 lineage markers were evaluated in day 7 IVD early blastocysts (n=3) and blastocysts (n=3), and IVP embryos first identified as blastocysts after 7 (fast development, n=5) or 9 (slow development, n=9) days. Further day 7 IVP blastocysts were examined after additional culture for 2 days either *in vitro* (n=5) or *in vivo* (after transfer into recipient mares, n=3). In IVD early blastocysts, SOX-2 positive cells were encircled by GATA-6 positive cells in the ICM, with SOX-2 co-expression in some presumed PE cells. In IVD blastocysts, SOX-2 expression was exclusive to the compacted presumptive EPI, while GATA-6 and CDX-2 expression were consistent with PE and TE specification, respectively. In IVP blastocysts, SOX-2 and GATA-6 positive cells were intermingled and relatively dispersed, and co-expression of SOX-2 or GATA-6 was evident in some CDX-2 positive TE cells. IVP blastocysts had lower TE and total cell numbers than IVD blastocysts, and displayed larger mean inter-EPI cell distances; these features were more pronounced in slower-developing IVP blastocysts. Transferring IVP blastocysts into recipient mares led to compaction of SOX-2 positive cells into a presumptive EPI, whereas extended *in vitro* culture did not. In conclusion, IVP equine embryos have a poorly compacted ICM with intermingled EPI and PE cells, features accentuated in slowly developing embryos but remedied by transfer to a recipient mare.

Chapter 5

Introduction

Coincident with blastocyst formation, a mammalian embryo undergoes two cell lineage segregations; the first is characterized by differentiation of the outer cells into trophectoderm (TE), which form the outer cell layer of the blastocyst and are subsequently restricted to the placenta, whereas the remaining cells compact into the inner cell mass (ICM) [1,2]. During the second cell lineage segregation, the ICM differentiates into the epiblast (EPI) and primitive endoderm (PE). The pluripotent cells of the EPI give rise to the embryo proper, whereas the PE cells migrate to line the inside of the trophectoderm thereby completing formation of the yolk sac, the bilaminar primitive nutrient absorbing structure (primitive placenta) [1,2]. The process of cell lineage segregation in embryos involves differential expression of transcriptional regulators and, as a result, the different cell types e.g. TE, EPI and PE can be distinguished by differential expression of transcription factors; for example, TE cells express CDX-2 (caudal-type homeodomain protein) and GATA-3 (GATA-3 binding protein), whereas EPI cells specifically express SOX-2 ((SRY (Sex Determining Region Y) -box 2)) and NANOG (homeobox protein nanog) and PE cells express GATA-6 (GATA6 binding protein) [3]. Although all mammalian embryos are thought to undergo the same two cell lineage segregations, and the roles of some critical transcription factors appear to be conserved [4], there are species-specific differences in the roles of certain transcription factors, the spatial pattern of cell lineage specification, and in the developmental stage at which cell lineage segregation takes place; for example, it occurs at an earlier embryonic age in mice (day 4.5, [5]) than in human (day 7, [6]), cattle (day 8, [7]) or pig (day 7, [8]) embryos. The process of cell lineage segregation has not been studied in depth in equine embryos after *in vivo* development, although Enders [9] suggested that PE cells migrated directly to line the TE at around day 8, without first participating in the formation of an obvious ICM. Aspects of cell lineage segregation have been examined more extensively in the context of the pluripotency of embryonic stem cells [10,11] or in *in vitro* produced (IVP) embryos, although these studies either lacked a marker to positively identify the pluripotent EPI cells [12] or focused almost entirely on EPI specification (using SOX-2) [13]. It has been shown that the pluripotent marker OCT-4/POU5F1 is unreliable for detecting equine EPI cells because it is not solely restricted to the ICM of horse embryos [11,12]. Furthermore, SOX-2 appears to be a better marker than OCT-4 because it specifically stains the EPI in IVP horse embryos [13]; CDX-2 and GATA-6 seem to be well conserved across species [4]. To better investigate possible differences in the timing and spatial distribution of cell lineage segregation between

equine IVP and *in vivo* derived (IVD) embryos it is imperative to use markers for each of the three cell lineages simultaneously.

Although the likelihood of pregnancy after the transfer of fresh [14] or frozen-thawed [15] equine IVP blastocysts exceeds 70%, this is approximately 15 to 20 % lower than after the transfer of fresh IVD blastocysts [16], suggesting that the developmental competence of IVP embryos is slightly lower than that of embryos that develop *in vivo*. In addition, the speed of *in vitro* embryo development affects embryo quality since day 7 or day 8 IVP blastocysts are more likely to yield a viable pregnancy than day 9 IVP blastocysts [15]. Although more slowly developing IVP embryos are therefore likely to be compromised in some way, it is not yet clear what the most important aberrations are [17]. In fact, assessing the quality of IVP equine embryos is challenging because they do not have a grossly visible blastocyst cavity and the ICM is not readily appreciated [18]. It is however possible that, while slowly developing IVP embryos do not have lower total cell numbers [17], they may have reduced numbers of cells in the ICM or EPI and, as a result, may fail to develop an embryo proper; this could contribute to lower pregnancy and higher early embryonic loss rates. Furthermore, even though *in vitro* culture conditions for equine embryos have improved markedly over time, as indicated by increased blastocyst production rates in clinical programs [19], they are still unable to completely mimic *in vivo* conditions. The importance of the *in vivo* environment for 'normal' specification of the different cell lineages was indicated by the loss of the unexpected OCT-4/POU5F1 staining of the TE cells of equine IVP embryos following a 2-3 period in the uterus of a mare [20]. In short, the effects of *in vitro* culture on the timing and pattern of early equine embryo cell fate decisions have not been examined in detail, despite their potential implications for subsequent embryo developmental competence. The aim of this study was to examine the influence of the conditions in which the embryo developed (IVD versus IVP), developmental stage (early blastocyst versus blastocyst: IVD), speed of *in vitro* embryo development (fast versus slow development: IVP) and environment (*in vitro* versus *in vivo*) for extended culture of IVP blastocysts on the pattern of expression of markers for the 3 cell lineages (CDX-2 for TE; SOX2 for EPI; and GATA-6 for PE) in equine embryos.

Materials and methods

In vivo derived embryos: collection, initial assessment and fixing

Animal procedures were approved by Utrecht University's Animal Experimentation

Committee (permit number: 1080020185164). *In vivo* embryos (n=6) were recovered by flushing the uterus of donor mares with lactated Ringer's solution, as described by Stout [21], 9 days after induction of ovulation with buserelin acetate (0.33µg/kg Suprefact®, IM: CHEPLAPHARM, Greifswald, Germany). One day after induction of ovulation, when the mares were in estrus with a large preovulatory follicle, they had been inseminated with semen from a fertile stallion; ovulation was confirmed by the emptying of the preovulatory follicle and replacement by a corpus hemorrhagicum which was detected by transrectal ultrasonography on the day after insemination. Recovered embryos were classified as early blastocysts (n=3) or blastocysts (n=3), as described by McCue [22]; early blastocysts had a thick zona pellucida, small blastocoel cavity and a barely visible capsule whereas blastocysts had a large blastocoel, a distinct ICM and a clearly discernible capsule between the trophectoderm and an attenuated zona pellucida. All embryos were fixed in 2% paraformaldehyde for 30 min at room temperature (RT; 19-21 ºC), washed twice in PBST (PBS containing 0.1% Triton X100) for 5 minutes, and then stored in PBST at 4 ºC until immunostaining.

In vitro produced embryos: production, culture and fixing

In vitro embryos were produced as described by Lazzari et al [23]. Briefly, immature oocytes were collected by transvaginal aspiration of antral follicles ≥ 5mm or by scraping follicles from post mortem ovaries, and shipped in H-SOF (HEPES buffered synthetic oviductal fluid [24]) to an assisted reproduction laboratory for *in vitro* maturation, intracytoplasmic sperm injection, and *in vitro* culture to the blastocyst stage. The time required (day of ICSI = day 0) for *in vitro* embryos to reach the blastocyst stage was recorded. All IVP blastocysts were slow-frozen and thawed as described by Lazzari et al [23]; after thawing, embryos were treated with pronase (0.5% in PBS) to remove the zona pellucida before 24 h culture in a modified SOF-IVC medium supplemented with bovine serum albumin (BSA) and amino acids [25], and containing 10% of a mixture (1:1) of fetal calf serum and serum replacement (KnockOut Serum Replacement, Life Technologies) at 38.5 ˚C in an atmosphere containing 5% CO_2 and 5% O_2. Five day 7 IVP blastocysts (fast development) were fixed to examine the expression of cell lineage markers, as were nine day 9 IVP blastocysts (slow development), to investigate whether the speed of *in vitro* development was associated with a different pattern of cell lineage marker expression. Additionally, day 7 IVP blastocysts were either cultured *in vitro* (n=5, without zona pellucida) or *in vivo* (n=3, with zona pellucida) for two more days. *In vitro* culture was carried out as described above. For *in vivo* culture, three

day 7 IVP blastocysts were transferred non-surgically into the uterus of recipient mares on day 4 after ovulation and recovered from the uterus by uterine lavage, as described above, 2 days later. All embryos were fixed and stored as described above until further processing.

Immunostaining

Fixed embryos were washed in fresh PBST and then permeabilized by incubating in PBS containing 1 % Triton X100 for 1 hour at RT. Non-specific binding was blocked by incubating the permeabilized embryos in PBST supplemented with 3% bovine serum albumin (BSA) and 5% normal goat serum (NGS) for 1 hour at RT. Next, the embryos were incubated with solutions of PBST (supplemented with 3% BSA and 5% NGS) containing the primary antibodies (1:500 dilution of mouse monoclonal antibody against CDX-2, M4392A-SUC, BiogeneX; and 1:250 dilution of rabbit polyclonal antibody against GATA-6, H-92, Santa Cruz) overnight at 4 ºC in a humidified chamber. After washing in PBST supplemented with 3% BSA three times for 10 minutes, the embryos were incubated with the secondary antibodies (1:250 Alexa Fluor 568-goat anti-mouse, A11031 Mol Probes; 1:250 Alexa Fluor 647-goat anti-rabbit, A21244 LifeTech) in PBST supplemented with 3% BSA and 5% NGS for 2 hours at RT. After washing three more times in PBST supplemented with 3% BSA for 10 minutes, the embryos were incubated with normal mouse IgG_1 (1:250 SC-3877, Santa Cruz) in PBST supplemented with 3% BSA and 5% NGS for 2 hours at RT. Following three 5 min washes as described above, embryos were incubated with SOX-2 (1:250 dilution of mouse monoclonal antibody against SOX-2, E-4, SC-365823 conjugated with Alexa Fluor 488, Santa Cruz) and Hoechst 33342 (1:500, B2261, Sigma) in PBST supplemented with 3% BSA and 5% NGS for 2 hours at RT. Finally, the embryos were mounted in a 5 µL droplet of antifade (Vectashield; Vector Laboratories) on glass slides (Superfrost Plus; Menzel).

Confocal imaging and image analysis

A Nikon A1R/STORM confocal microscope equipped with four lasers (405nm, Blue; 488nm, Green; 561nm, Red; and 647nm, Magenta) was used to assess the expression of Hoechst 33342 (all nuclei), SOX-2 (EPI), CDX-2 (TE) and GATA-6 (PE). The dichroic filter was a quad line laser filter (405/488/561/640) and the emission filters were 482/32, 515/30, 595/50 and 700/75 for Hoechst 33342, Alexa-Fluor 488 ™, Alexa Fluor 568 ™ and Alexa Fluor 647 ™, respectively. Z-stacks (1.1 µm thickness with top and bottom acquisition defined manually) were acquired using a 20X/0.75 NA (numerical aperture) air immersion lens (1000 µm working distance). Pinhole size was 26.82 µm and images (512x512 pixels)

were collected in the bidirectional mode with a pixel size of 0.65 µm. Image analysis was performed using Fiji image J and Imaris software version 8 (BitPlane). Individual image slices were processed for brightness and contrast using Fiji image J for graphical illustrations. All blastocysts were measured using Imaris (mean of two measurements from trophoblast perimeter to trophoblast perimeter). The total cell number (Hoechst 33342 positive nuclei), and total numbers of presumed TE (CDX-2 positive cells), PE (GATA-6 positive cells) and EPI (SOX-2 positive cells) were also counted using Imaris object spot detection module. Objects were filtered to contain mean intensities between minimum and maximum intensities (98-1277, 76-119, 70-1156 and 83-201) for blue (Hoechst 33342 positive nuclei), green (SOX-2 positive cells), red (CDX-2 positive cells) and magenta (GATA-6 positive cells) channels, respectively. Mean inter-EPI cell distances were measured using the Imaris spots-to-spots closest distance algorithm.

Statistical analysis

Shapiro-Wilk tests were used to assess the normality of the data. Differences in embryo size, total cell number, total numbers of TE, EPI and PE cells, and percentages of all cells classified as TE, EPI and PE cells were compared between day 7 IVD and IVP embryos using the Mann-Whitney test. Unpaired T tests with Welch's correction were used to detect differences in embryo size, total cell number, total numbers of TE, EPI and PE cells, and percentages of cells classified as TE, EPI and PE cells between day 7 (fast development) and day 9 (slow development) IVP blastocysts. The Mann-Whitney test was used to detect differences in embryo size, total cell number, total numbers of TE, EPI and PE cells between IVP embryos collected 2 days after transfer to a mare's uterus and IVP embryos cultured *in vitro* for 2 days. An IVP embryo without SOX-2 positive cells (collected 2 days after transfer to a mare's uterus) was excluded from the comparison of total EPI cell number. Statistical analysis was performed using GraphPad prism software version 8 (GraphPad Software, San Diego, CA, USA). Differences were considered statistically significant when $p < 0.05$; tendency 0.05-0.09. Data is presented as means ± SD (standard deviation).

Results

Expression of cell lineage markers in IVD early blastocysts (n=3) and blastocysts (n=3)

CDX-2 expression was exclusive to the TE of both IVD early blastocysts (Fig 1 A1) and blastocysts (Fig 1 B1), with no expression evident in cells positioned within the light microscopically-visible ICM. SOX-2 was expressed not only in the ICM, but was also co-

expressed with CDX-2 in the TE of early blastocysts (Fig 1 A2). This co-expression of SOX-2 in CDX-2 positive TE cells was almost completely lost in later blastocysts. In the later blastocysts, SOX-2 was expressed strongly in the presumed EPI (Fig 1 B2, B4). GATA-6 expression was visible in cells within the ICM of early blastocysts and also, co-expressed with SOX-2, at the periphery of the ICM (Fig 1 A3, A4). This co-expression of SOX-2 and GATA-6 was no longer evident in later blastocysts, where GATA-6 was expressed exclusively in the PE (Fig 1 B3, B4) and SOX-2 expression was only detected in the EPI (Fig 1 B2, B4). In IVD blastocysts, the PE was evident as a single cell layer lining the inner surface of the TE (Fig 1 B3, B4).

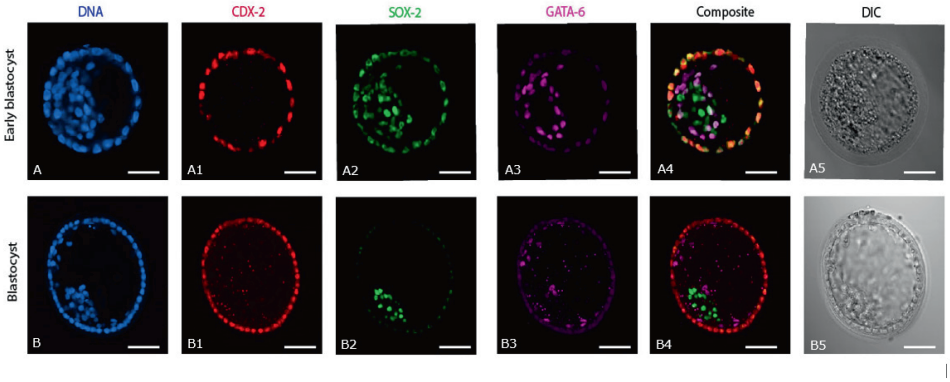

Figure 1. Expression of cell lineage markers (CDX-2, SOX-2 and GATA-6) in in vivo derived early blastocysts and blastocysts. *(A, B) DNA staining of all the nuclei. (A1, B1) expression of CDX-2. A2, B2) expression of SOX-2. (A3, B3) expression of GATA-6. (A4, B4) composite of CDX-2, SOX-2 and GATA-6. (A5, B5) DIC images of the respective early blastocyst and blastocyst. Scale bar = 50 µm.*

Expression of cell lineage markers in IVP Day 7 blastocysts (n=5)

CDX-2 was consistently expressed only in the TE of IVP blastocysts. (Fig 2 A1, B1, C1, D1). By contrast, SOX-2 expression varied between IVP blastocysts with regard to exact distribution (Fig 2 A2, C2) and the number of SOX-2 positive cells (Fig 2 A4, B4, C4, D4). Indeed, SOX-2 positive cells were scattered around the entire ICM, which extended over approximately half of the central 'cavity' of IVP blastocysts. In addition, SOX-2 was co-expressed either weakly (Fig. 2 B2, C2, D2) or strongly (Fig. 2 A2) with CDX-2 in the TE of three of 5 day 7 IVP blastocysts, although it was restricted to the presumptive EPI in the other two (Fig. 2 B2, B4, C2, C4). The distribution of GATA-6 expression was also variable in IVP blastocysts, although it was restricted to the PE of one of 5 embryos (Fig. 2 B3 B4, C3 C4), there was some co-expression of GATA-6 and CDX-2 in the TE of the remaining four (Fig. 2 A3, C3, D3).

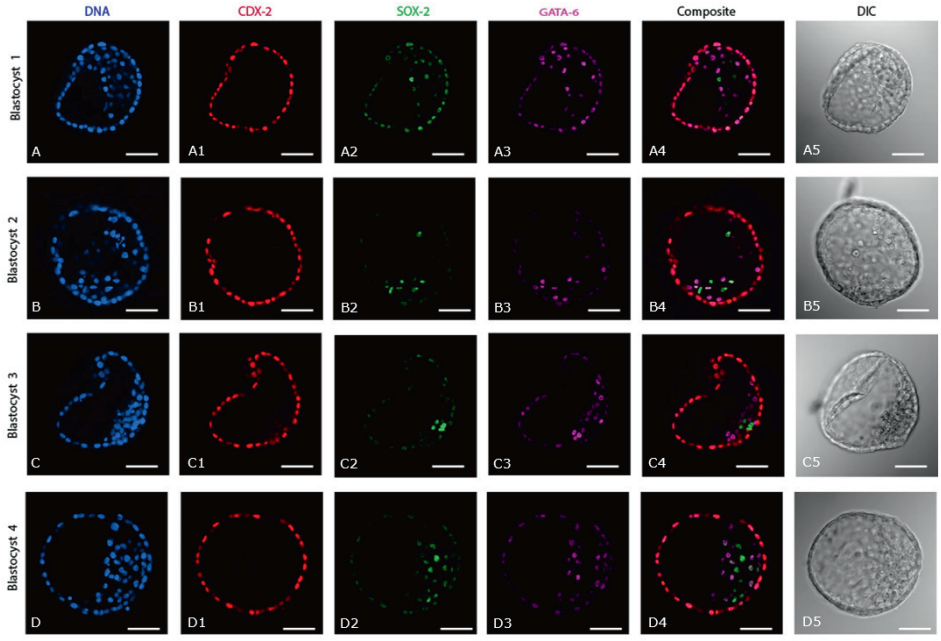

Figure 2. Expression of cell lineage markers (CDX-2, SOX-2 and GATA-6) in day 7 in vitro produced blastocysts. *(A, B, C,D) DNA staining of all the nuclei. (A1, B1, C1, D1) Expression of CDX-2. (A2, B2, C2, D2) Expression of SOX-2. (A3, B3, C3, D3) Expression of GATA-6. (A4, B4, C4, D4) composite of CDX-2, SOX-2 and GATA-6. (A5, B5, C5, D5) DIC images of the respective in vitro blastocysts. Scale bar = 50 µm.*

Differences in embryo size, total cell number and TE, PE and EPI allocation between day 7 IVD (n=3) and IVP (n=5) blastocysts

Although embryo size did not differ markedly between day 7 IVD (210±19 µm) and IVP blastocysts (184±9 µm), the total cell number was significantly higher in the IVD blastocysts (486±81 versus 317±21; IVD versus IVP) (Fig 3 A). While the total number of TE cells was also higher in IVD (395±54) than IVP blastocysts (264±34) (Fig 3 B), the percentage of cells classified as TE did not differ between then (82±3% and 83±5%, respectively). In contrast, neither the number nor the percentage of PE cells differed between IVD (52±23, 10±3%; respectively) and IVP (38±8, 12±3%) blastocysts. Similarly, while the number of EPI cells tended (p=0.05) to be higher in IVD (34±10) than IVP blastocysts (14±7), the percentages of EPI cells did not differ significantly (7±2% and 4±2%, respectively). On the other hand, the mean inter-epiblast cell distance was significantly higher in IVP blastocysts (52±6 µm) than in IVD blastocysts (35±3 µm) (Fig 3 C).

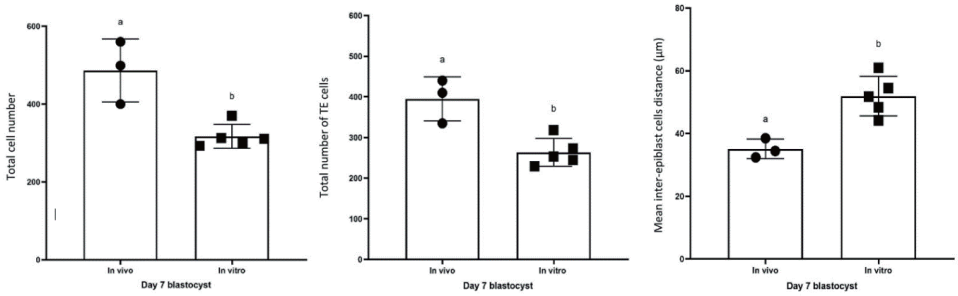

Figure 3. Differences between day 7 IVD and day 7 IVP blastocysts. *A) Total cell number, B) Total number of TE cells, C) Mean inter-epiblast cell distance. Error bars represents the standard deviation. Columns with different superscripts differ significantly $p<0.05$.*

Differences between day 7 (fast developing, n=5) and day 9 (slow developing, n=9) IVP blastocysts

As previously shown for day 7 IVP blastocysts, CDX2 expression was exclusive to the TE of IVP embryos that only reached the blastocyst stage after 9 days (Fig 4 A1, B1, C1, D1). The SOX-2 (Fig 4 C2, D2) and GATA-6 (Fig 4 C3, D3) positive cells in day 9 IVP blastocysts were spread over an even wider area than in day 7 IVP blastocysts (Fig 4 A2, B2 and A3, B3, respectively). SOX-2 or GATA-6 were co-expressed with CDX-2 in the TE of all day 9 IVP blastocysts (5/9 and 9/9, respectively: Fig 4 C2, C4, D4), and most day 7 IVP blastocysts (3/5 and 4/5 respectively: Fig 4 A2, A4). There were no significant differences in embryo size (184±9 vs 200±31µm), total cell number (317±31 vs 377±104), total TE cell number (264±34 vs 285±101) or total EPI cell number (14±7 vs 18±6) between day 7 (fast developing) and day 9 (slow developing) IVP blastocysts. Similarly, there were no differences in the percentages of TE (83±5% vs 75±10%) and EPI (4±2% vs 6±3%) cells between day 7 (fast developing) and day 9 (slow developing) blastocysts. By contrast, total PE cell number was significantly higher in day 9 (71±33) than day 7 (38±9) IVP blastocysts (Fig. 5 A), although the percentage of PE cells did not differ between them (19±10% vs 12±3%, respectively). However, the inter-epiblast cell distance was higher in day 9 (68±9 µm, slow developing) than day 7 (52±6 µm, fast developing) IVP blastocysts (Fig. 5 A).

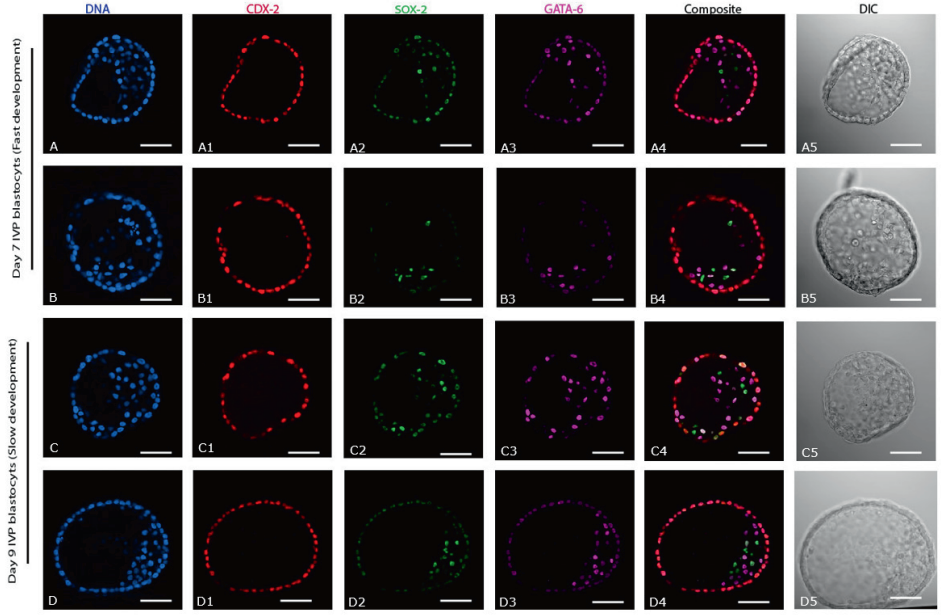

Figure 4. Expression of cell lineage markers (CDX-2, SOX-2 and GATA-6) in in vitro produced blastocysts; Day 7 (fast development and Day 9 (slow development). *(A, B,C,D) DNA staining of all the nuclei. (A1, B1, C1, D1) Expression of CDX-2. (A2, B2, C2, D2) Expression of SOX-2. (A3, B3, C3, D3) Expression of GATA-6. (A4, B4, C4, D4) composite of CDX-2, SOX-2 and GATA-6. (A5, B5, C5, D5) DIC images of the respective in vitro blastocysts. Scale bar = 50 µm.*

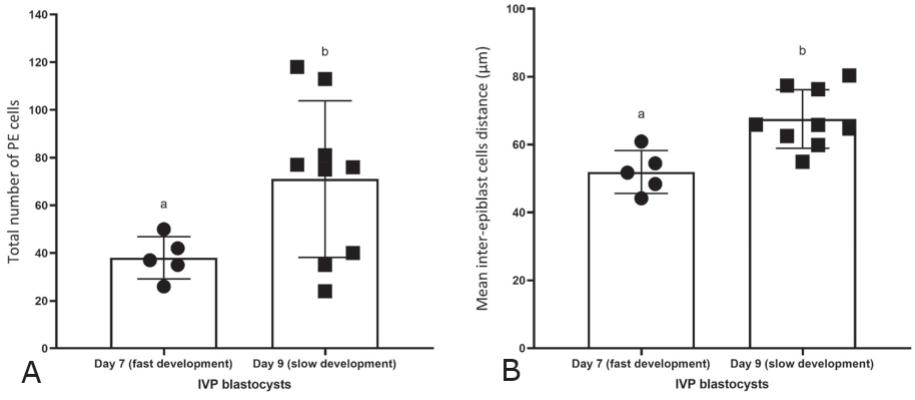

Figure 5. Differences between day 7 (fast developing) and day 9 (slow developing) IVP blastocysts. *A) Total number of PE cells. B) mean inter-EPI cell distance. Error bars represent the standard deviation. Different superscripts represent significant differences $p<0.05$.*

Effect of two days extra culture of day 7 IVP blastocysts in vitro (n=5) or in vivo (n=3)

Additional culture did not affect the expression of CDX-2, which remained restricted to the TE (Fig. 6 A1, B1, C1, D1, E1). However, whereas 2 days of additional culture *in vitro* had

no effect on the distribution of SOX-2 positive cells (scattered: Fig. 6 A2, B2), after 2 days in the uterus of a mare, the SOX-2 cells had compacted in 2 out of 3 embryos (Fig. 6 C2, D2). In the third IVP embryo collected 2 days after transfer to a mare's uterus, no SOX-2 positive cells were detected (Fig. 6 E2). After 2 days of additional *in vitro* culture, SOX-2 positive cells were still present in the TE, whereas SOX-2 staining had disappeared from the TE after 2 days of in *vivo* culture. As with SOX-2, GATA-6 expression was still present in the TE of day 7 IVP blastocysts cultured for an additional 2 days *in vitro* (Fig. 6 A3, B3). After 2 days *in vivo* development, the distribution of GATA-6 expression was variable (Fig.6 C3, D3), but it was less evident in TE cells. Embryo size (404±20 µm), total cell number (997±77), total TE cell number (827±47) and total PE cell number (103±11) were significantly higher in IVP embryos collected 2 days after transfer to a mare's uterus than in IVP embryos cultured *in vitro* for 2 days (186±26 µm, 350±133, 265±100 and 16±9, respectively). Total EPI cell number tended to be higher (p=0.09) in IVP embryos after 2 days in a mare's uterus than an *in vitro* culture (40±13 vs 11±6, respectively).

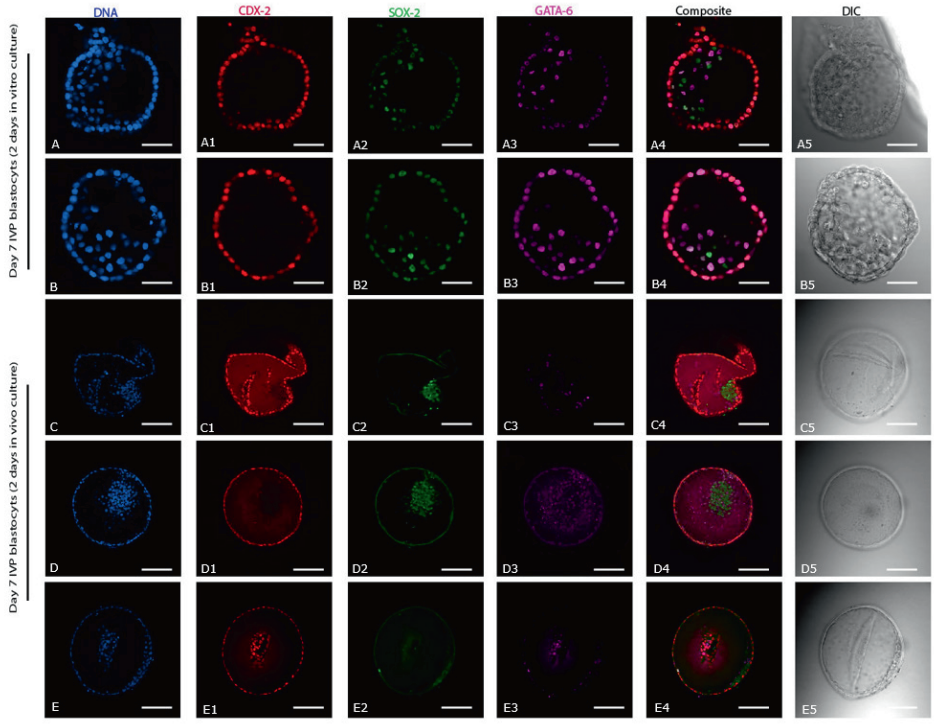

Figure 6. Expression of cell lineage markers (CDX-2, SOX-2 and GATA-6) in in vitro blastocysts; Day 7 cultured for an additional 2 days in vitro or in vivo. *(A, B, C, D) DNA staining of all the nuclei. (A1, B1, C1, D1) Expression of CDX-2. (A2, B2, C2, D2) Expression of SOX-2. (A3, B3, C3, D3) Expression of GATA-6. (A4, B4, C4, D4) composite of CDX-2, SOX-2 and GATA-6. (A5, B5, C5,*

D5) DIC images of the respective in vitro blastocysts. Scale bar = 50 µm (A, B) and 100 µm (C, D, E).

Discussion

This study compared the expression of markers for the first 3 cell lineages in IVD and IVP equine embryos. In IVD horse early blastocysts, the first cell lineage segregation (TE versus ICM) had been completed, and the second cell lineage differentiation (EPI versus PE) had been initiated. By the blastocyst stage, the second cell lineage decision had also been completed, and the EPI cells were much more compacted than at the early blastocyst stage. In comparison, IVP blastocysts lagged behind in development, as evidenced by a lower cell number, a less compacted ICM and, most obviously, because the second lineage differentiation was not complete in 3/5 of the day 7 IVP blastocysts. Moreover, the EPI cells in IVP blastocysts were intermingled with PE cells in a poorly compacted ICM, reminiscent of early stages of EPI:PE segregation in other species [26]. In IVP embryos that were slow to reach the blastocyst stage (9 rather than 7 days), compaction of the ICM and EPI was even more retarded. During extended culture, the environment (*in vivo* versus *in vitro*) had a marked impact on subsequent embryo development and cell differentiation. Day 7 IVP blastocysts cultured *in vitro* for 2 more days showed little or no progress in EPI organisation and compaction, whereas IVP blastocysts transferred to the uterus of a synchronized mare for 2 days were more developed (higher total cell number) and showed completion (or failure in one case) of the second cell lineage segregation (organization and compaction of EPI cells). These observations extend those of Choi et al. [12], although including a positive marker for EPI cells did allow a subtle refinement of their conclusion that the EPI and PE cells in equine embryos do not first aggregate together to form an ICM. In our study, in both IVD early blastocysts and IVP blastocysts, EPI and PE cells clustered together in an apparent ICM before the PE migrated to line the rest of the blastocoele cavity; the difference presumably arising in part from subtle differences in embryo developmental stage at the time of staining.

In mouse embryos, the first cell lineage segregation is considered to be completed by the morula stage, when CDX-2 is expressed solely by the TE [27]. In horse embryos, CDX-2 expression was already restricted to the TE of IVD early blastocysts, indicating that the first cell lineage segregation is completed at an earlier stage, e.g., the morula stage, and possibly prior to descent into the uterus. The second cell lineage division had not been completed in IVD early blastocysts, as indicated by co-expression of SOX-2 and GATA-6 at the periphery of the ICM. In IVD early blastocysts, SOX-2 was co-expressed with CDX-2 in the TE, a

phenomenon also reported in mouse early blastocysts, where it was suggested that SOX-2 co-expression plays a role in the establishment of the TE lineage [28,29]. Indeed, knocking out SOX-2 in two cell stage mouse embryos caused embryonic arrest characterized by the absence of CDX-2 expression [28]. In this respect, SOX-2 might also play a role in initial TE specification during early development of horse embryos.

Early differentiation and separation of EPI and PE was observed in *in vivo* horse early blastocysts in that GATA-6 positive cells encircled the SOX-2 positive cells. This cellular organization contrasted to mouse early blastocysts, in which EPI cells are intermingled with PE cells, often referred to as a 'salt and pepper' expression pattern [30]; the intermingling of PE and EPI we observed in IVP equine blastocysts therefore either emphasizes that they are at an earlier stage of development, or suggests a different (aberrant) spatial pattern of the second cell fate decision. In horse IVD blastocysts, the second cell lineage had been completed, since the three cell lineage markers (CDX-2, GATA-6 and SOX-2) were expressed separately in the presumptive TE, PE and EPI cells, respectively. This distinct expression of cell lineage markers in TE, PE and EPI at the blastocyst stage is similar to other species, including man, cow and pig [31], but is different to mouse [28,32] and goat [33,34] blastocysts (co-expression of SOX-2 with CDX-2 in the TE). Interestingly, a single cell layer of PE could be seen to line the inner surface of the TE, completing the yolk sac, as early as day 7 in IVD equine blastocysts, slightly earlier than previously observed by electron microscopy [9] and earlier than described in other large animal species including man, cow and pig (day 10) [4,31].

The dispersal of EPI cells, measurable as a greater mean inter-EPI cell distance, observed in IVP compared to IVD equine blastocysts (although total and relative EPI cell number were not different) suggests an impaired, or delayed, organization and compaction of the EPI in IVP blastocysts. This delay in EPI compaction might contribute to the reduced viability and developmental competence of IVP embryos compared to IVD embryos, as evidenced by the 15 to 20% lower pregnancy rate after transfer [35]. One possible impact of delayed EPI compaction may have been indicated by the failure to find any SOX-2 positive cells in of one of the 3 IVP embryos recovered 2 days after transfer to a mare's uterus; as will be discussed below, this embryo would almost certainly be non-viable. Similarly, IVP bovine blastocysts have been reported to suffer a higher incidence of defective embryonic lineage specification (particularly affecting the EPI), which was proposed to contribute to the 10-40% lower likelihood of pregnancy after transferring IVP than IVD bovine embryos to recipient cows

[36–38].

In addition to *in vitro* production *per se*, the second cell lineage segregation appears to be influenced by, or aberration in this segregation may contribute to, a slower rate of *in vitro* development because the SOX-2 positive cells in blastocysts that took 9 days to reach the blastocyst stage were even more scattered and the EPI less compact (higher inter-EPI cell distance) than in embryos that reached the blastocyst stage in 7 days. Even though the total and relative number of SOX-2 positive cells did not differ between day 9 (slow developing) and day 7 (fast developing) IVP blastocysts, it is possible that a delay in accumulating or specifying sufficient ICM and EPI cells, or indeed of specifying TE cells, explains the delayed formation of an appreciable blastocoele and TE layer, and contributes to the lower pregnancy rates after the transfer of slowly developing (day 9 or later) IVP blastocysts [15]. Moreover, it is tempting to speculate that the dispersed and uncompacted nature of the EPI in IVP blastocysts may predispose to the splitting of the EPI cells into two separate populations within the embryo, to form two separate EPIs. If so, this could explain the heightened risk of monochorionic-monozygotic twins observed after the transfer of IVP blastocysts (approximately 1%) [39]; a phenomenon that is encountered only rarely for embryos that develop to the blastocyst stage *in vivo* [40].

The importance of (micro)environmental cues for equine embryonic cell lineage specification was demonstrated by the marked effects of culturing IVP embryos for an additional 2 days in a mare's uterus, compared to a petri dish. Day 7 IVP blastocysts cultured *in vivo* for 2 days showed thinning of the zona, development of a capsule, and a marked increase in total cell number (997±77) accompanied by compaction of the ICM and/or EPI. By contrast, IVP blastocysts cultured for an additional 2 days *in vitro* showed few signs of further development, with only a modest increase in total cell number, no obvious compaction of the EPI and incomplete spatial segregation of SOX-2 and GATA-6 positive cells in the ICM. In this regard, uterine factors which promote embryo development and differentiation events, including EPI compaction, are presumably absent in *in vitro* culture. In the cow, embryokines such as insulin-like growth factor 1 and colony-stimulating factor 2 have been proposed to be key uterine factors that modulate and promote development of the embryo to later blastocyst stages [41], and may play a role in EPI specification and organization. In this respect, it would be interesting to investigate whether co-culture with endometrial cells, tissues or fluids or supplementation of *in vitro* culture system with putative embryokines would improve the in *vitro* development of equine embryos. Interestingly, as mentioned

previously, SOX-2 expression was completely absent in one of the day 7 IVP blastocysts cultured *in vivo* for 2 days, although expression of CDX-2 and GATA-6 was present. The authors hypothesize that this is an IVP embryo that has failed to specify an EPI. Transfer of such an embryo into the uterus of a mare could potentially result in a pregnancy, but presumably a vesicle that would fail to form an embryo proper, i.e. an anembryonic vesicle [42]. In this respect, a significant percentage (26%) of OPU-ICSI pregnancies lost after the first positive pregnancy scan are lost before formation of the embryo proper and/or recorded as anembryonic vesicles [43].

Conclusion

In conclusion, IVP horse blastocysts have a more dispersed EPI than IVD horse blastocysts with intermingling of EPI and PE cells. The greater dispersion may result from developmental delay, and is even more pronounced in slowly developing (day 9) IVP horse blastocysts. However, the EPI of IVP horse blastocysts compacts rapidly after transfer to the uterus of a recipient mare, which indicates that the uterine environment can normalize the developmental differences of IVP embryos. Overall, unraveling and comparing the intra- and extra-embryonic factors that affect the molecular mechanisms underlying cell commitment, and the inter-proteomic crosstalk between transcription factors that dictate cell fate, such as CDX-2-, SOX-2- and GATA-6, seems to be an important aspect of promoting improvement in the efficiency of generating ex *vivo*-derived high-quality blastocysts in equids and other mammalian species. This might also enhance *in vivo* developmental competence after intrauterine transfer of IVP-derived embryos propagated by advanced assisted reproductive technologies (ARTs) such as *in vitro* fertilization (IVF) based either on gamete co-incubation or intracytoplasmic sperm injection (ICSI) [44-47], and cloning based on somatic cell nuclear transfer (SCNT) [48-50].

Author Contributions: Conceptualization, M.U., T.A.E.S. and A.C.; data curation, M.U., V.F.C.S.; investigation, M.U., V.F.C.S.; methodology, M.U., V.F.C.S., M.B, S.C., C.G., G.L., M.R.V., T.A.E.S. and A.C.; software, M.U., M.R.V. and A.C.; supervision, M.R.V, T.A.E.S. and A.C.; Resources, T.A.E.S.; visualization, M.U., V.F.C.S., M.B., M.R.V., T.A.E.S. and A.C.; writing—original draft, M.U. and writing—review and editing, M.U., V.F.C.S., M.B., S.C., C.G., G.L., M.R.V., T.A.E.S. and A.C. All authors have read and agreed to the final version of the manuscript.

Funding: This work was supported by the Punjab Educational Endowment Fund (PEEF),

Punjab, Pakistan (PEEF/SSMS/18/222).

Institutional review board statement: Animal experiments were approved from Animal Welfare body (IvD) Utrecht (Approved work protocol 5164-2-01, Project number AVD 1080020185164).

Acknowledgments: The authors acknowledge the help of Jon de Rijk, Wilbert Beukens and Esther Akkerman with semen collection, and Bart Leemans and Leonie Arnold with mare management, embryo flushing and embryo transfer. Confocal images were acquired, and 3D image analysis was performed at the CCI (Centre for cellular Imaging) of the Faculty of Veterinary Medicine, Utrecht. The authors would like to thank Richard Wubbolts and Esther van 't Veld for their help and technical assistance. Veronica Flores da Cunha Scheeren was a PhD student at Department of Veterinary Surgery and Animal Reproduction, School of Veterinary Medicine and Animal Science, São Paulo State University (UNESP), Botucatu, Brazil and was supported by CAPES, Brazil (Financing code; 88882.433332/2019-01 and 88887.467895/2019-00).

Conflicts of Interest: The authors have no conflict of interest to declare.

Abbreviations: IVP, *in vitro* production; IVD, *in vivo* derived, TE, trophectoderm; ICM, inner cell mass; EPI, epiblast; PE, primitive endoderm; CDX-2, caudal-type homeodomain protein; GATA-3 , GATA-3 binding protein; SOX-2, SRY (Sex Determining Region Y) - box 2; NANOG, homeobox protein nanog; GATA-6, GATA6 binding protein; PBS, phosphate buffer saline; PBST, PBS containing 0.1 % Triton X100; H-SOF, HEPES buffered synthetic oviductal fluid; SOF-IVC, synthetic oviductal fluid-*in vitro* culture; BSA, bovine serum albumin, NGS, normal goat serum; RT, room temperature.

References

1. Cockburn, K.; Rossant, J. Making the Blastocyst: Lessons from the Mouse. *J. Clin. Invest.* **2010**, *120*, 995–1003, doi:10.1172/JCI41229.

2. White, M.D.; Zenker, J.; Bissiere, S.; Plachta, N. Instructions for Assembling the Early Mammalian Embryo. *Dev. Cell* **2018**, *45*, 667–679, doi:10.1016/j.devcel.2018.05.013.

3. Iqbal, K.; Chitwood, J.L.; Meyers-Brown, G.A.; Roser, J.F.; Ross, P.J. RNA-Seq Transcriptome Profiling of Equine Inner Cell Mass and Trophectoderm1. *Biol. Reprod.* **2014**, *90*, 1-9, doi:10.1095/biolreprod.113.113928.

4. Kuijk, E.W.; Du Puy, L.; Van Tol, H.T.A.; Oei, C.H.Y.; Haagsman, H.P.; Colenbrander,

B.; Roelen, B.A.J. Differences in Early Lineage Segregation between Mammals. *Dev. Dyn.* **2008**, *237*, 918–927, doi:10.1002/dvdy.21480.

5. Plusa, B.; Piliszek, A.; Frankenberg, S.; Artus, J.; Hadjantonakis, A.-K. Distinct Sequential Cell Behaviours Direct Primitive Endoderm Formation in the Mouse Blastocyst. *Development* **2008**, *135*, 3081–3091, doi:10.1242/dev.021519.

6. Niakan, K.K.; Eggan, K. Analysis of Human Embryos from Zygote to Blastocyst Reveals Distinct Gene Expression Patterns Relative to the Mouse. *Dev. Biol.* **2013**, *375*, 54–64, doi:10.1016/j.ydbio.2012.12.008.

7. Berg, D.K.; Smith, C.S.; Pearton, D.J.; Wells, D.N.; Broadhurst, R.; Donnison, M.; Pfeffer, P.L. Trophectoderm Lineage Determination in Cattle. *Dev. Cell* **2011**, *20*, 244–255, doi:10.1016/j.devcel.2011.01.003.

8. Zhi, M.; Zhang, J.; Tang, Q.; Yu, D.; Gao, S.; Gao, D.; Liu, P.; Guo, J.; Hai, T.; Gao, J.; et al. Generation and Characterization of Stable Pig Pregastrulation Epiblast Stem Cell Lines. *Cell Res.* **2022**, *32*, 383–400, doi:10.1038/s41422-021-00592-9.

9. Enders, A.C.; Schlafke, S.; Lantz, K.C.; Liu, I.K.M. Endoderm Cells of the Equine Yolk Sac from Day 7 until Formation of the Definitive Yolk Sac Placenta. *Equine Vet. J.* **2010**, *25*, 3–9, doi:10.1111/j.2042-3306.1993.tb04814.x.

10. Paris, D.B.B.P.; Stout, T.A.E. Equine Embryos and Embryonic Stem Cells: Defining Reliable Markers of Pluripotency. *Theriogenology* **2010**, *74*, 516–524, doi:10.1016/j.theriogenology.2009.11.020.

11. Desmarais, J.A.; Demers, S.-P.; Suzuki, J.; Laflamme, S.; Vincent, P.; Laverty, S.; Smith, L.C. Trophoblast Stem Cell Marker Gene Expression in Inner Cell Mass-Derived Cells from Parthenogenetic Equine Embryos. *REPRODUCTION* **2011**, *141*, 321–332, doi:10.1530/REP-09-0536.

12. Choi, Y.-H.; Ross, P.; Velez, I.C.; Macías-García, B.; Riera, F.L.; Hinrichs, K. Cell Lineage Allocation in Equine Blastocysts Produced in Vitro under Varying Glucose Concentrations. *REPRODUCTION* **2015**, *150*, 31–41, doi:10.1530/REP-14-0662.

13. Gambini, A.; Duque Rodríguez, M.; Rodríguez, M.B.; Briski, O.; Flores Bragulat, A.P.; Demergassi, N.; Losinno, L.; Salamone, D.F. Horse Ooplasm Supports in Vitro

Preimplantation Development of Zebra ICSI and SCNT Embryos without Compromising YAP1 and SOX2 Expression Pattern. *PLOS ONE* **2020**, *15*, e0238948, doi:10.1371/journal.pone.0238948.

14. Choi, Y.-H.; Hinrichs, K. Vitrification of in Vitro -Produced and in Vivo -Recovered Equine Blastocysts in a Clinical Program. *Theriogenology* **2017**, *87*, 48–54, doi:10.1016/j.theriogenology.2016.08.005.

15. Claes, A.; Stout, T.A.E. Success Rate in a Clinical Equine in Vitro Embryo Production Program. *Theriogenology* **2022**, *187*, 215–218, doi:10.1016/j.theriogenology.2022.04.019.

16. Cuervo-Arango, J.; Claes, A.N.; Stout, T.A.E. In Vitro-Produced Horse Embryos Exhibit a Very Narrow Window of Acceptable Recipient Mare Uterine Synchrony Compared with in Vivo-Derived Embryos. *Reprod. Fertil. Dev.* **2019**, *31*, 1904-1911, doi:10.1071/RD19294.

17. Ducheyne, K.D.; Rizzo, M.; Cuervo-Arango, J.; Claes, A.; Daels, P.F.; Stout, T.A.E.; de Ruijter-Villani, M. In Vitro Production of Horse Embryos Predisposes to Micronucleus Formation, Whereas Time to Blastocyst Formation Affects Likelihood of Pregnancy. *Reprod. Fertil. Dev.* **2019**, *31*, 1830-1839, doi:10.1071/RD19227.

18. Carnevale, E.M.; Metcalf, E.S. Morphology, Developmental Stages and Quality Parameters of in Vitro-Produced Equine Embryos. *Reprod. Fertil. Dev.* **2019**, *31*, 1758-1770, doi:10.1071/RD19257.

19. Stout, T.A.E. Clinical Application of in Vitro Embryo Production in the Horse. *J. Equine Vet. Sci.* **2020**, *89*, 103011, doi:10.1016/j.jevs.2020.103011.

20. Choi, Y.H.; Harding, H.D.; Hartman, D.L.; Obermiller, A.D.; Kurosaka, S.; McLaughlin, K.J.; Hinrichs, K. The Uterine Environment Modulates Trophectodermal POU5F1 Levels in Equine Blastocysts. *REPRODUCTION* **2009**, *138*, 589–599, doi:10.1530/REP-08-0394.

21. Stout, T.A.E. Equine Embryo Transfer: Review of Developing Potential. *Equine Vet. J.* **2010**, *38*, 467–478, doi:10.2746/042516406778400529.

22. McCue, P.M. Embryo Evaluation. In *Equine Reproductive Procedures*; Dascanio, J.J., McCue, P.M., Eds.; John Wiley & Sons, Inc: Hoboken, NJ, USA, 2014; pp. 169–172 ISBN 978-1-118-90439-8.

23. Lazzari, G.; Colleoni, S.; Crotti, G.; Turini, P.; Fiorini, G.; Barandalla, M.; Landriscina,

L.; Dolci, G.; Benedetti, M.; Duchi, R.; et al. Laboratory Production of Equine Embryos. *J. Equine Vet. Sci.* **2020**, *89*, 103097, doi:10.1016/j.jevs.2020.103097.

24. Tervit, H.R.; Whittingham, D.G.; Rowson, L.E.A. SUCCESSFUL CULTURE IN VITRO OF SHEEP AND CATTLE OVA. *Reproduction* **1972**, *30*, 493–497, doi:10.1530/jrf.0.0300493.

25. Lazzari, G.; Wrenzycki, C.; Herrmann, D.; Duchi, R.; Kruip, T.; Niemann, H.; Galli, C. Cellular and Molecular Deviations in Bovine In Vitro-Produced Embryos Are Related to the Large Offspring Syndrome1. *Biol. Reprod.* **2002**, *67*, 767–775, doi:10.1095/biolreprod.102.004481.

26. Zhu, M.; Zernicka-Goetz, M. Principles of Self-Organization of the Mammalian Embryo. *Cell* **2020**, *183*, 1467–1478, doi:10.1016/j.cell.2020.11.003.

27. Mihajlović, A.I.; Bruce, A.W. The First Cell-Fate Decision of Mouse Preimplantation Embryo Development: Integrating Cell Position and Polarity. *Open Biol.* **2017**, *7*, 170210, doi:10.1098/rsob.170210.

28. Keramari, M.; Razavi, J.; Ingman, K.A.; Patsch, C.; Edenhofer, F.; Ward, C.M.; Kimber, S.J. Sox2 Is Essential for Formation of Trophectoderm in the Preimplantation Embryo. *PLoS ONE* **2010**, *5*, e13952, doi:10.1371/journal.pone.0013952.

29. Mistri, T.K.; Arindrarto, W.; Ng, W.P.; Wang, C.; Lim, L.H.; Sun, L.; Chambers, I.; Wohland, T.; Robson, P. Dynamic Changes in Sox2 Spatio-Temporal Expression Promote the Second Cell Fate Decision through *Fgf4* / *Fgfr2* Signaling in Preimplantation Mouse Embryos. *Biochem. J.* **2018**, *475*, 1075–1089, doi:10.1042/BCJ20170418.

30. Schrode, N.; Saiz, N.; Di Talia, S.; Hadjantonakis, A.-K. GATA6 Levels Modulate Primitive Endoderm Cell Fate Choice and Timing in the Mouse Blastocyst. *Dev. Cell* **2014**, *29*, 454–467, doi:10.1016/j.devcel.2014.04.011.

31. Pérez-Gómez, A.; González-Brusi, L.; Bermejo-Álvarez, P.; Ramos-Ibeas, P. Lineage Differentiation Markers as a Proxy for Embryo Viability in Farm Ungulates. *Front. Vet. Sci.* **2021**, *8*, 680539, doi:10.3389/fvets.2021.680539.

32. Avilion, A.A.; Nicolis, S.K.; Pevny, L.H.; Perez, L.; Vivian, N.; Lovell-Badge, R. Multipotent Cell Lineages in Early Mouse Development Depend on SOX2 Function. *Genes Dev.* **2003**, *17*, 126–140, doi:10.1101/gad.224503.

33. Yu, X.; Zhao, X.; Wang, H.; Ma, B. Expression Patterns of OCT4, NANOG, and SOX2 in Goat Preimplantation Embryos from in Vivo and in Vitro. *J. Integr. Agric.* **2015**, *14*, 1398–1406, doi:10.1016/S2095-3119(14)60923-0.

34. HosseinNia, P.; Hajian, M.; Jafarpour, F.; Hosseini, S.M.; Tahmoorespur, M.; Nasr-Esfahani, M.H. Dynamics of The Expression of Pluripotency and Lineage Specific Genes in The Pre and Peri-Implantation Goat Embryo. *Cell J. Yakhteh* **2019**, *21*,194-203 doi:10.22074/cellj.2019.5732.

35. Cuervo-Arango, J.; Claes, A.N.; Stout, T.A. Effect of Embryo-Recipient Synchrony on Post-ET Survival of In Vivo and In Vitro-Produced Equine Embryos. *J. Equine Vet. Sci.* **2018**, *66*, 163–164, doi:10.1016/j.jevs.2018.05.058.

36. Santos, J.E.P.; Thatcher, W.W.; Chebel, R.C.; Cerri, R.L.A.; Galvão, K.N. The Effect of Embryonic Death Rates in Cattle on the Efficacy of Estrus Synchronization Programs. *Anim. Reprod. Sci.* **2004**, *82–83*, 513–535, doi:10.1016/j.anireprosci.2004.04.015.

37. Lucy, M.C. Reproductive Loss in High-Producing Dairy Cattle: Where Will It End? *J. Dairy Sci.* **2001**, *84*, 1277–1293, doi:10.3168/jds.S0022-0302(01)70158-0.

38. Wiltbank, M.C.; Baez, G.M.; Garcia-Guerra, A.; Toledo, M.Z.; Monteiro, P.L.J.; Melo, L.F.; Ochoa, J.C.; Santos, J.E.P.; Sartori, R. Pivotal Periods for Pregnancy Loss during the First Trimester of Gestation in Lactating Dairy Cows. *Theriogenology* **2016**, *86*, 239–253, doi:10.1016/j.theriogenology.2016.04.037.

39. Dijkstra, A.; Cuervo-Arango, J.; Stout, T.A.E.; Claes, A. Monozygotic Multiple Pregnancies after Transfer of Single in Vitro Produced Equine Embryos. *Equine Vet. J.* **2020**, *52*, 258–261, doi:10.1111/evj.13146.

40. McCue, P.M.; Thayer, J.; Squires, E.L.; Brinsko, S.P.; Vanderwall, D.K. Twin Pregnancies Following Transfer of Single Embryos in Three Mares: A Case Report. *J. Equine Vet. Sci.* **1998**, *18*, 832–834, doi:10.1016/S0737-0806(98)80333-X.

41. Hansen, P.J.; Tríbulo, P. Regulation of Present and Future Development by Maternal Regulatory Signals Acting on the Embryo during the Morula to Blastocyst Transition – Insights from the Cow. *Biol. Reprod.* **2019**, *101*, 526–537, doi:10.1093/biolre/ioz030.

42. Newcombe, J.R.; Cuervo-Arango, J. The Relationship Between the Positive

Identification of the Embryo Proper in Equine Pregnancies Aged 18-28 Days and Its Future Viability: A Field Study. *J. Equine Vet. Sci.* **2012**, *32*, 257–261, doi:10.1016/j.jevs.2011.09.068.

43. Claes, A.; Cuervo-Arango, J.; Broek, J.; Galli, C.; Colleoni, S.; Lazzari, G.; Deelen, C.; Beitsma, M.; Stout, T.A. Factors Affecting the Likelihood of Pregnancy and Embryonic Loss after Transfer of Cryopreserved in Vitro Produced Equine Embryos. *Equine Vet. J.* **2019**, *51*, 446–450, doi:10.1111/evj.13028.

44. Goszczynski, D.E.; Tinetti, P.S.; Choi, Y.H.; Hinrichs, K.; Ross, P.J. Genome activation in equine in vitro-produced embryos. Biol. Reprod. 2022, 106, 66–82, doi:10.1093/biolre/ioab173.

45. Frank, B.L.; Doddman, C.D.; Stokes, J.E.; Carnevale, E.M. Association of equine oocyte and cleavage stage embryo morphology with maternal age and pregnancy after intracytoplasmic sperm injection. Reprod. Fertil. Dev. 2019, 31, 1812–1822, doi:10.1071/RD19250.

46. Salamone, D.F.; Canel, N.G.; Rodríguez, M.B. Intracytoplasmic sperm injection in domestic and wild mammals. Reproduction 2017, 154, F111–F124, doi:10.1530/REP-17-0357.

47. Yao, Y.; Yang, A.; Li, G.; Wu, H.; Deng, S.; Yang, H.; Ma, W.; Lv, D.; Fu, Y.; Ji, P.; et al. Melatonin promotes the development of sheep transgenic cloned embryos by protecting donor and recipient cells. Cell Cycle 2022, 21, 1360–1375, doi:10.1080/15384101.2022.2051122.

48. Olivera, R.; Moro, L.N.; Jordan, R.; Luzzani, C.; Miriuka, S.; Radrizzani, M.; Donadeu, F.X.; Vichera, G. In Vitro and In Vivo Development of Horse Cloned Embryos Generated with iPSCs, Mesenchymal Stromal Cells and Fetal or Adult Fibroblasts as Nuclear Donors. PLoS One 2016, 11, e0164049, doi:10.1371/journal.pone.0164049.

49. Wiater, J.; Samiec, M.; Wartalski, K.; Smorąg, Z.; Jura, J.; Słomski, R., Skrzyszowska, M.; Romek, M.; Characterization of Mono- and Bi-Transgenic Pig-Derived Epidermal Keratinocytes Expressing Human FUT2 and GLA Genes – In Vitro Studies. Int. J. Mol. Sci. 2021, 22, 9683, doi:10.3390/ijms22189683.

50. Samiec, M.; Skrzyszowska, M. Biological transcomplementary activation as a novel and effective strategy applied to the generation of porcine somatic cell cloned embryos. Reprod. Biol. 2014, 14, 128–139, doi:10.1016/j.repbio.2013.12.006.

Chapter 6

General Discussion

Since the early 1990s, sport horse breeding in Europe has undergone a technological revolution, from a system dominated by natural mating to the current situation where artificial insemination is the norm, and an increasing proportion of pregnancies are produced by transfer of either flushed or *in vitro* produced embryos. Although the increased uptake of artificial breeding techniques has many potential advantages, as discussed in the general introduction, it also has significant potential disadvantages such as an increased number of opportunities for errors due to human error, which can include damage to the gametes or embryos during handling and storage. In addition, the more complex techniques involve circumvention of the natural processes involved in selecting fertile spermatozoa or oocytes. For example, intracytoplasmic sperm injection (ICSI) is currently the only commercially viable technique for producing equine embryos *in vitro*. However, ICSI bypasses the natural sperm selection methods which take place during the transit of spermatozoa through the female reproductive tract and even, although to a lesser extent, during conventional IVF. Since it is important to ensure that oocytes are fertilized with spermatozoa capable of giving rise to a viable embryo, *in vitro* sperm selection techniques have become an important part of the ICSI and IVF procedures. The techniques most commonly used to select 'high quality' spermatozoa are swim-up (SU), microfluidic (MF) sorting, and density gradient centrifugation (DGC). SU is currently the most common technique for sperm selection prior to ICSI but selects exclusively on the basis of sperm motility with no selection for DNA/chromatin integrity [1]. By contrast, MF has been reported to select spermatozoa that are not only motile but also more likely to have intact DNA, via rheotaxis or chemotaxis and thermotaxis (for review see [2]). In fact, MF systems are now optimized and used quite extensively for processing fresh human semen samples prior to IVF or ICSI [3]. On the other hand, equine ICSI almost always involves the use of cryopreserved semen and, in most cases, there is a preference to limit the amount of stored semen thawed (a small part of a 0.5 mL straw). As a result, in many cases ICSI has to be performed with a very limited number of viable spermatozoa, or sperm of poor post-thaw quality [4]. In **chapter 2**, a modified flotation DGC technique was developed using Opti-prep™ to select out high-quality spermatozoa from ejaculates of sub-fertile stallions, in particular stallions with unusually high percentages of spermatozoa with DNA damage. In a 3-layer system using 20% or 25% Opti-prep™ as an upper layer, morphologically normal, progressively motile spermatozoa with intact DNA were selected by virtue of their relatively high buoyancy, ascending up towards this upper layer during centrifugation such that they could be recovered from the interface between the upper and middle layers. Both a 20% and 25% upper layer proved to be suitable for

processing poor quality semen samples to select high-quality sperm. In this respect, 20% Opti-prep™ appeared to be more useful to process semen for insemination ,when higher sperm numbers are important, whereas 25% Opti-prep™ appeared to be more useful for ICSI because while the number of spermatozoa recovered was very low, the quality was high. Moreover, no increase in reactive oxygen species (ROS) production was detected in the recovered sperm; this had previously been reported [5] as a potential downside of the higher centrifugal forces (1000 *g*) used during modified floatation DGC. However, the modified floatation DGC method was optimized using fresh rather than frozen-thawed stallion semen. In the context of selecting the best possible sperm population for ICSI, it was therefore still important to compare the populations selected by MF and the modified flotation DGC techniques. To this end, a pilot study was performed using cryopreserved semen (n=3) to compare the effects of the MF and modified flotation DGC (20% Opti-prep™) techniques on semen quality parameters. The percentages of viable, acrosome-intact, morphologically normal, and progressively motile spermatozoa with intact DNA did not differ in the sperm populations recovered by MF and modified flotation DGC (Fig. 1). In fact, the only difference

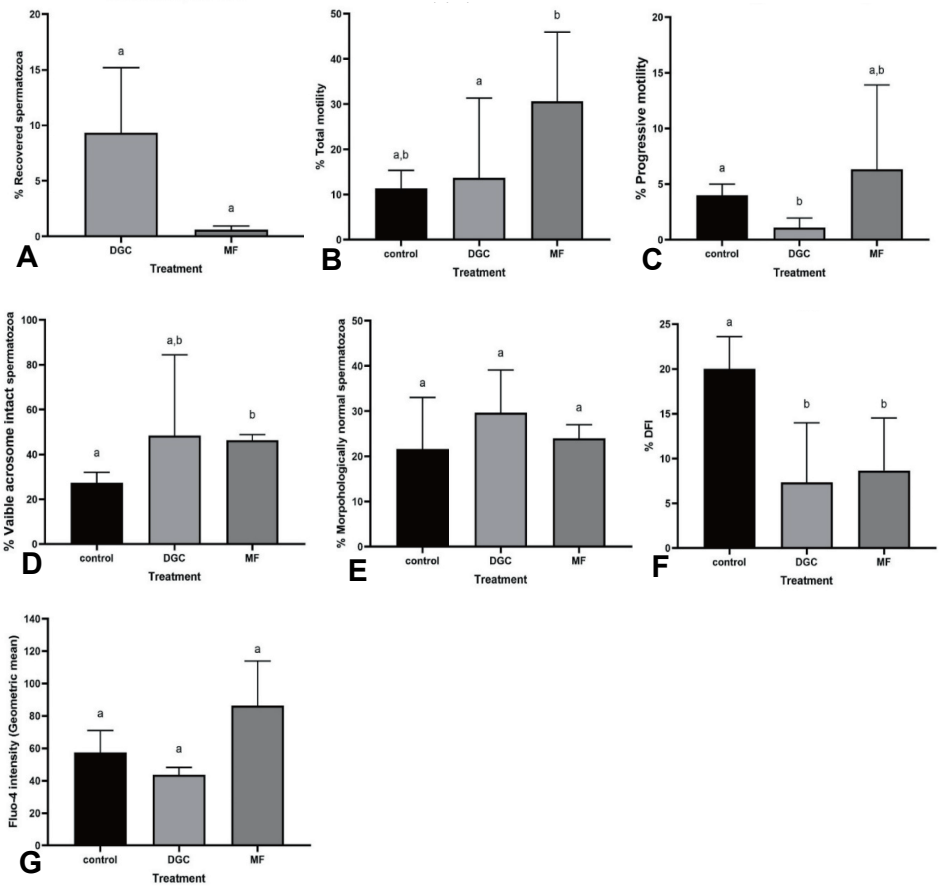

Figure.1 Semen quality parameters of frozen-thawed stallion semen before and after selection by modified flotation density gradient centrifugation (DGC) and Microfluidic (MF) sorting. *A) Percentage of spermatozoa recovered B) Percentage of motile spermatozoa (total) C) Percentage of progressive motile spermatozoa D) Percentage of viable, acrosome-intact spermatozoa E) Percentage of morphologically normal spermatozoa F) Percent DNA fragmentation Index (DFI; i.e. spermatozoa with damaged DNA) G) Fluo-4 intensity (geometric mean) – a measure of intracellular [Ca^{2+}].*

of motile spermatozoa recovered by MF (Fig. 1 C). Although both techniques preferentially selected spermatozoa with intact DNA, the magnitude of the impact of intact sperm DNA on cleavage and blastocyst rates or even embryo quality following ICSI is not yet known. However, it is also important to note that semen quality analysis after MF was laborious because of the very low number and concentration of spermatozoa recovered; this resulted in prolonged analysis times for both CASA and flow cytometric analysis. Another drawback of MF was that the low concentration of spermatozoa recovered necessitated an additional centrifugation step to concentrate the sperm cells after recovery. By contrast, the larger numbers of spermatozoa recovered by modified flotation DGC did not require any additional post-procedure steps. Another potential advantage of the modified flotation DGC is that it can readily be scaled up or down, e.g., to process low volumes (<500 µL) by preparing the gradient in a 2 mL Eppendorf tube. By contrast, MF is restricted to the size of chamber available, which in our case was 850 µl, which makes it unsuitable for processing fractions of a frozen 0.5 mL straw. Previous studies have also indicated that cryopreservation has a detrimental effect on phospholipase c zeta (PLC zeta; an oocyte activation factor) concentrations in human spermatozoa, and that DGC preferentially selected spermatozoa with a high PLC zeta content [6]. In this respect, it would be interesting to optimize the MF and modified floatation DGC methods to process frozen-thawed stallion semen samples shown to have a low ability to induce oocyte cleavage (e.g. re-frozen spermatozoa), to select a uniform population of high-quality spermatozoa and to measure the effects on both mean sperm PLC zeta content and the ability of the spermatozoa to trigger equine oocyte activation and *in vitro* embryo development.

In the horse breeding industry as a whole, AI with chilled stallion semen is still the most commonly used ART. Despite refinements in semen processing protocols and semen extenders, the recommendation to restrict transport or storage times for liquid semen to 24-48 h to prevent a fall-off in fertility has not changed and significantly limits applicability in some circumstances. In **chapter 3**, we investigated *in vitro* aging of stallion spermatozoa after prolonged storge (up to 96 h at 5 °C) by assessing basic semen quality parameters

alongside more advanced flow cytometric assays for changes in sperm activation status. The often-quoted minimum percentages of motile sperm consistent with a reasonable likelihood of pregnancy i.e., >35% total or progressive motility were maintained in most samples for 96 h and 72 h, respectively. Interestingly, the percentage of viable acrosome-intact spermatozoa remained high up to 96 h, despite a drop in sperm motility parameters, indicating either depletion of substrates required for motility or subcellular changes that could have impaired flagellar activity. In this respect, intra-cellular [Ca^{2+}] and plasma membrane fluidity increased over time up to 96 h, and this was reflected by a diminishing population of viable acrosome-intact spermatozoa with low plasma membrane fluidity and low intra-cellular [Ca^{2+}]. Previously, high intra-cellular [Ca^{2+}] was linked to failure of sperm binding to oviductal epithelial cells *in vitro* [7]. We hypothesize that an increase in intra-cellular [Ca^{2+}] after prolonged storage, as observed in **chapter 3**, may prevent binding of spermatozoa to oviductal epithelial cells *in vivo* and hamper the formation of a sperm reservoir in the mare's oviduct.

Recently, a successful IVF procedure for horses was reported by Felix et al, [8]; they used a 22 h *in vitro* incubation of freshly collected stallion spermatozoa in medium containing penicillamine, hypotaurine and epinephrine (PHE) to reliably fertilize *in vitro* matured oocytes during a 6 h co-incubation. However, cooled-stored semen subsequently incubated in identical conditions for a similar duration of time was not able to induce fertilization. It is tempting to speculate that the rise in intra-cellular [Ca^{2+}] or in sperm plasma membrane fluidity, both indicators of capacitation, could contribute to the failure of cooled stored semen to fertilize oocytes after a 22 h PHE incubation. In this respect (**chapter 3**), we found a 2-fold increase in intra-cellular [Ca^{2+}] after 24 h of cold storage without a significant change in plasma membrane fluidity compared to the starting point (time of semen dilution, 1 h; 15 ± 7%, viable, acrosome-intact spermatozoa with increased plasma membrane fluidity). A rapid change in intra-cellular [Ca^{2+}] during cold storage may limit the fertilizing potential of stallion spermatozoa *in vitro.* Therefore, it would be interesting to compare the effects of 22 h (and shorter) incubation of freshly-collected, cooled-stored and frozen-thawed semen in PHE-containing medium on indices of sperm activation and capacitation, such as membrane fluidity and the intra-cellular [Ca^{2+}], and on their ability to fertilize *in vitro* matured oocytes.

Given the difficulty of storing sperm in a liquid state for a prolonged period of time, a group in Australia recently developed a new semen extender designed to store stallion semen for up to seven days at ambient temperature [9]; clearly, the ability to reliably store sperm for a

number of days would be revolutionary for countries, or routes, where transport is unreliable and one needs to be certain that the semen is about to arrive before pharmacologically inducing ovulation in the mare. After 7 days of storage in this extender, semen quality was better preserved and a higher percentage of spermatozoa maintained motility after exposing them to capacitating conditions, than when semen was stored at 4 °C for seven days. In addition, a higher number of spermatozoa bound to heterologous zona pellucidae (from cattle oocytes) after storage at ambient temperature in the new extender than at 4 °C in a conventional extender [9]. While it is clearly most important to determine that the sperm stored at ambient temperature actually maintain adequate fertilizing capacity after prolonged storage, it would also be interesting to examine whether they somehow avoid the capacitation-like changes or *in vitro* aging that we observed during storage at 4 °C, i.e., increases in intra-cellular [Ca^{2+}] and membrane fluidity that probably limit the maintenance of fertilizing capacity.

Frozen-thawed semen also shows an increase in intra-cellular [Ca^{2+}], as part of a deterioration process often referred to as 'cryo-capacitation,' and which is proposed to be one of the reasons for the lower fertility of frozen-thawed compared to cooled-stored semen. In terms of sperm selection techniques, it is not known whether MF or DGC can select out spermatozoa with low intra-cellular [Ca^{2+}] post-thaw that would be more likely to retain fertilizing capacity. To this end, a preliminary experiment was performed to examine the effect of the two selection techniques on the intra-cellular [Ca^{2+}] in frozen-thawed stallion semen (n=3). Possibly in part because of the low number of samples compared, Fluo-4 intensity (an indicator of [Ca^{2+}] did not differ significantly in frozen-thawed stallion spermatozoa selected by MF compared to modified DGC (20% Opti-prep™) (Fig. 1G).

While selection of genetically superior stallions has been aided by all of the assisted reproductive technologies, selection of favourable female genetics has lagged behind considerably because embryo and oocyte technologies have taken much longer to develop to the extent that success rates were commercially viable. Even though embryo transfer has become increasingly popular since the early 2000s, more widespread implementation has been hampered by difficulties in developing treatments to induce multiple follicle development and ovulation in mares and in reliably cryopreserving embryos. In particular, cryopreservation of large (>300 μm in diameter) *in vivo* expanded blastocysts of the type normally collected when flushing horse embryos on day 7 or 8 after ovulation has historically been challenging because of their physical characteristics, namely the surrounding

glycoprotein capsule, a lower volume to surface area ratio and a relatively large volume of blastocoel fluid. In recent years, large *in vivo* produced expanded blastocysts have been successfully vitrified with [10] or without [11] blastocoel fluid aspiration. However, even though slow-freezing appears to be less damaging to small equine embryos than vitrification ([12], no information was available on the success of slow-freezing large *in vivo* expanded blastocysts following blastocoel puncture and aspiration. In **chapter 4**, we compared the impact of slow-freezing and vitrification on post-thaw/post-warming quality of large *in vivo* derived blastocysts collapsed by blastocoel aspiration prior to cryopreservation. Overall, slow-frozen large, aspirated blastocysts had lower embryo quality parameters than vitrified embryos after 24 h of post-thaw culture. This contrasted to earlier studies which reported that slow-freezing was less damaging to non-punctured large blastocysts than vitrification [12,13]. Equine embryos <300 µm can be successfully vitrified without puncturing the zona pellucida/capsule [14], and, recently, it was shown that equine embryos up to 550 µm can tolerate the vitrification process after they have been punctured, even without aspirating the blastocoele fluid [11]. Nevertheless, for equine embryos >550 µm, aspiration of as much fluid as possible is important for successful vitrification, and is done more efficiently using a micromanipulator rather than attempting to puncture manually with a needle. Although embryos up to 550 µm have been successfully vitrified after manual puncture with a microneedle [15], use of larger needles to puncture an embryo would be likely to irreparably damage the capsule, and thus, compromise the survival of the embryos *in vivo*. The disappointing results of slow-freezing of the large punctured blastocysts presented in **chapter 4** may, however, have resulted as a consequence of a cooling curve (-0.5 °C/min) that was not optimal for large expanded blastocysts, despite removing a large proportion of the blastocoel fluid (≥85%). The recent growth in popularity of IVEP via OPU and ICSI, has emphasized the advantages of cryopreserving embryos in terms of the efficiency of recipient mare management and use, and has stimulated increasing interest in cryopreserving flushed embryos. For OPU-ICSI, large numbers of embryos can be produced which can be most efficiently cryopreserved by slow-freezing, because this allows freezing and thawing of embryos in batches. If cryopreservation of punctured-expanded *in vivo* embryos were to become widespread, or successful techniques for superovulation become available, then it would similarly be useful to perform future studies to optimize the slow-freezing curve for *in vivo* expanded blastocysts of different sizes, because the technique is more suitable than vitrification when dealing with larger numbers of embryos. In the meantime, it is prudent to cryopreserve punctured-aspirated expanded blastocysts by vitrification.

The growth in equine IVEP necessitated estimations of the developmental stage of the IVP embryos, when they reach the blastocyst stage after 7-9 days of *in vitro* culture, in order to be able to select recipient mares at the optimal stage after ovulation. Having established that, a week after transfer, frozen-thawed equine IVP blastocysts had developed into embryonic vesicles of equivalent to day 11-12 *in vivo* pregnancies [16], it was apparent that IVP blastocysts behaved like day 5-6 *in* vivo embryos at the time they reached the blastocyst stage. This suggested a very different time-course of early embryonic development than seen *in vivo*, at least with respect to the first cell lineage segregation event. During early embryo development, the first cell lineage segregation event involves embryonic cells differentiating into trophectoderm (TE; express CDX-2) and inner cell mass (ICM) lines, and should be accompanied by blastocoele formation. Shortly afterwards, the second lineage segregation event would be expected and would involve the ICM differentiating further into epiblast (EPI, pluripotent cells; express SOX-2) and primitive endoderm (PE; express GATA-6). In **chapter 5**, we investigated the expression of cell lineage markers (CDX-2, SOX-2 and GATA-6) in both *in vivo* and *in vitro* produced embryos at the time that they developed a blastocoele. This revealed striking differences between *in vivo* and *in vitro* blastocysts with regard to the distribution of cells expressing the different lineage markers, in particular those expressing SOX-2 and GATA-6. The distribution of the various cell lineage markers was fairly uniform in the day 7 *in vivo* blastocysts with presumptive TE, EPI and PE expressing the appropriate cell markers, CDX-2, SOX-2 or GATA-6, respectively. By contrast, *in vitro* produced blastocysts that took 7 or 9 days to develop into blastocysts both exhibited much less obvious delineation of the distribution of SOX-2 and GATA-6 expressing cells. The presumptive EPI cells were more scattered in day 7 *in vitro* than *in* vivo blastocysts, and this more diffuse distribution was even more obvious in embryos that took 9 days to reach the blastocyst stage. These differences in the distribution of cells expressing the different lineage markers between *in vivo* and *in vitro* produced embryos suggest that current *in vitro* culture systems are suboptimal for supporting critical early cell differentiation events. This hypothesis was supported further by culturing day 7 *in vitro* produced blastocysts for an additional two days, either *in vitro* or *in vivo* (transferred into the uterus of a recipient mare). Interestingly, embryos transferred into the uterus developed to better resemble *in vivo* derived expanded blastocysts with a clearly delineated and compacted EPI. By contrast, embryos cultured for an additional two days *in vitro*, showed no changes in the distribution of cells expressing SOX-2 and GATA-6, which remained dispersed and interspersed. Indeed, the distance over which the EPI cells were spread was increased. Clearly, *in vitro* conditions

are not yet optimal for equine embryo development, and lead to delays in development and aberrations in cell lineage segregation. Given that IVP embryos that take even longer than 9 days to develop to the blastocyst stage are known to have reduced developmental capacity and, in particular, to more commonly succumb to early embryonic death [16], it was interesting to examine the distribution of cells expressing CDX-2, SOX-2 and GATA-6 in embryos that took more than 10 days to develop into a recognizable blastocyst. Figure 2 shows a day 11 and a day 13 blastocyst stained for CDX-2, SOX-2 and GATA-6. The two embryos

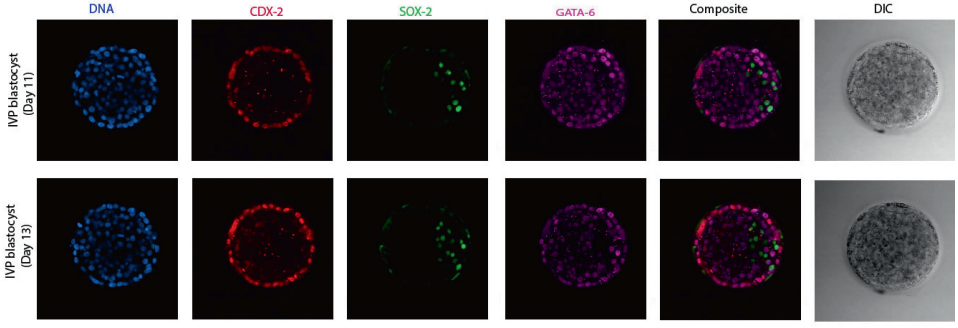

Figure.2 Expression of cell lineage markers (CDX-2, SOX-2 and GATA-6) in in vitro produced embryos that only reached the blastocyst stage after 11 or 13 days of culture. *(A1, B1) DNA staining of all the nuclei. (A2, B2) Expression of CDX-2. (A3, B3) Expression of SOX-2. (A4, B4) Expression of GATA-6. (A5, B5) Composite of CDX-2, SOX-2 and GATA-6. (A6, B6) DIC images of the respective in vitro blastocysts. Scale bar = 50 µm*

showed globally similar distributions of cells expressing the various lineage markers, with CDX-2 restricted to obvious peripheral TE cells in both blastocysts (Fig. 2 A2, B2). Interestingly, SOX-2 was expressed only in cells that had migrated to a restricted area of both blastocysts, presumably the ICM with a relatively compact presumptive EPI (Fig. 2 A3, B3). By contrast, expression of GATA-6 was observed in both presumptive PE cells and TE of both blastocysts (Fig. 2 A4, B4) indicating that the overly long period of *in vitro* development, >10 days, further compromised normal expression of cell lineage markers, especially GATA-6. In this respect, it would be interesting to investigate whether culturing IVP equine blastocysts in the presence of uterine tissue or fluids or factors (embryokines) may accelerate *in vitro* embryo development and lead to more *in vivo*-like patterns of cell lineage marker expression.

Of course, lower EPI cell number and aberrant distribution within IVP equine embryos (**chapter 5**) could be linked to reduced embryo viability, while more dispersed distribution

of the EPI cells could presumably predispose to the development of monozygotic twins, because the extended EPI would be more likely to split into two or more parts. One approach to rectify these aberrations would be to attempt to increase the EPI cell number in IVP blastocysts by culturing in the presence of factors that favour EPI cell specification. In the mouse, the EPI cell number increased when embryos were cultured in the presence of insulin, due to stimulation of the PI3K/GSK3 p53 pathway [17,18], while in bovine embryos incubation in the presence of Mek inhibitors led to a higher proportion of ICM cells developing into the EPI than the PE cell lineage [19]. Addition of insulin or Mek inhibitors to equine *in vitro* culture medium could also be tried to increase the EPI cell number in resulting blastocysts. IVP equine blastocysts showed intermingling of presumptive EPI and PE cells, similar to the 'salt and pepper' distribution of EPI and PE progenitors in day 3.5 mouse embryos [20] and day 7 bovine embryos [19], and this intermingling of presumptive EPI and PE cells was not resolved by increasing the duration of *in vitro* culture. In mouse embryos, GATA-6 in PE progenitors targets the Laminin and Dab2 genes, which initiate sorting of the two lineages (EPI and PE) by cellular adhesive function. Subsequently, the basal lamina (mainly consists of laminin) is formed, and separation of the two lineages is complete by day 4.5 [20]. The influence of GATA-6 expression on Laminin and Dab2 genes in equine blastocysts is not yet known. In murine embryonic stem cells, overexpression of GATA upregulated LamininB1 expression [21]. It is, therefore, tempting to speculate that stimulating GATA expression may activate Laminin in IVP equine blastocysts leading to a more rapid segregation of EPI and PE.

Two out of three IVP equine blastocysts transferred into a mare's uterus for 2 days showed separation of EPI from PE, emphasizing the importance of the uterine environment in stimulating the second cell lineage segregation and further development of the embryo. In the cow, smaller embryonic discs (EDs) have been reported in IVP-derived conceptuses compared to their *in vivo* counterparts [22], and a surprisingly high percentage (23-65%) of IVP-derived bovine conceptuses without an obvious ED has been reported in a number of studies [23–25]. It can be hypothesized that lower EPI cell numbers in IVP horse blastocysts would lead to sub-optimal ED development resulting in an anembryonic vesicle. In this respect, studying the next steps in development e.g. ED formation, the number of EDs (in case an EPI gives rise to two EDs), timing and appearance of gastrulation (the next major cell differentiation event) in a large number of IVP equine embryos transferred into the uterus

of mares and then flushed out, would provide valuable information on the next major events occurring during *in vivo* embryo development.

Future perspectives

In spermatozoa, intra-cellular [Ca^{2+}] concentration is regulated by several process including influx, efflux and regulation of the intra-cellular [Ca^{2+}] stores. CatSper, the sperm specific Ca^{2+} channel, and other Ca^{2+} channels control Ca^{2+} influx [26–28]. Ca^{2+}-ATPase and the Na^{+}/Ca^{2+} exchanger in the plasma membrane regulate Ca^{2+}-efflux [29,30]. Moreover, Ca^{2+}-ATPase and IP3-R, located in the outer acrosomal membrane, regulate the mobilization of intracellular Ca^{2+}, and participate in Ca^{2+}-influx and efflux across the acrosome [31,32]. Ca^{2+} uptake and release is also carried out by sperm mitochondria [33]. The redundant nuclear envelope, located in the spermatozoa's neck, serves as an additional Ca^{2+} store and also contains IP3R [34,35]. Maintaining precise intra-cellular [Ca^{2+}] concentrations is important for sperm motility, capacitation and the acrosome reaction. Prolonged storage of stallion semen caused an increase in intra-cellular [Ca^{2+}] over time that was inversely correlated with progressive and total motility (**chapter 3)**. In future studies, it would be interesting to investigate mechanisms to maintain a low intra-cellular [Ca^{2+}] concentration in stored stallion spermatozoa and to monitor the change in intra-cellular [Ca^{2+}] by live cell imaging technologies previously used to monitor intra-cellular [Ca^{2+}] concentration in mouse spermatozoa [36].

The aberrations in the second cell lineage segregation observed in *in vitro* produced (IVP) equine embryos, in particular the lack of compaction of the EPI, was resolved by a short period of development *in vivo* indicating the importance of uterine factors in stimulating the second cell lineage segregation. In this respect, it would be interesting to develop *in vitro* models that use endometrial cells to help steer a more normal preimplantation development of IVP equine embryos. An alternative approach would be to find candidate equine endometrial growth factors and embryokines involved in early *in vivo* equine embryo development (up to day 7 post ovulation) by studying the gene expression pattern of candidate embryokines in the oviduct and endometrium. In cattle, embryokines such as insulin-like growth factor 1 and colony-stimulating factor 2, have been proposed to be key uterine factors that modulate and promote the development of the embryo to the later blastocyst stages [37] and that may perform a role in EPI specification and organization. Testing of endometrial factors that act as embryokines for equine embryos would both enable the establishment of culture conditions able to support more *in vivo*-like development of

equine IVP embryos and might also allow prolonged *in vitro* culture (>10 days) of embryos to study the next events (ED formation and gastrulation) in development. In cattle, embryos have been cultured for 14 days *in vitro* on a gel to better study cell lineage segregation events [38] and increase our understanding of the regulation of these critical processes.

In conclusion, considerable advances have been made in the application of assisted reproductive technologies to horse breeding. While many of the techniques work well, there is still room for improvement in efficiency, user-friendliness and developmental competence of the embryos resulting from these techniques. This thesis has highlighted areas where improvement has already been achieved and others on which future research could focus.

References

1. Somfai, T.; Bodo, S.; Nagy, S.; Papp, A.; Ivancsics, J.; Baranyai, B.; Gocza, E.; Kovacs, A. Effect of Swim up and Percoll Treatment on Viability and Acrosome Integrity of Frozen-Thawed Bull Spermatozoa. *Reprod. Domest. Anim.* **2002**, *37*, 285–290, doi:10.1046/j.1439-0531.2002.00350.x.
2. Khodamoradi, M.; Rafizadeh Tafti, S.; Mousavi Shaegh, S.A.; Aflatoonian, B.; Azimzadeh, M.; Khashayar, P. Recent Microfluidic Innovations for Sperm Sorting. *Chemosensors* **2021**, *9*, 126, doi:10.3390/chemosensors9060126.
3. Leisinger, C.A.; Adaniya, G.; Freeman, M.R.; Behnke, E.J.; Aguirre, M.; VerMilyea, M.D.; Schiewe, M.C. Effect of Microfluidic Sperm Separation vs. Standard Sperm Washing Processes on Laboratory Outcomes and Clinical Pregnancy Rates in an Unselected Patient Population. *Reprod. Med.* **2021**, *2*, 125–130, doi:10.3390/reprodmed2030013.
4. Loomis, P.R.; Graham, J.K. Commercial Semen Freezing: Individual Male Variation in Cryosurvival and the Response of Stallion Sperm to Customized Freezing Protocols. *Anim. Reprod. Sci.* **2008**, *105*, 119–128, doi:10.1016/j.anireprosci.2007.11.010.
5. Aitken, R.J.; Clarkson, J.S. Significance of Reactive Oxygen Species and Antioxidants in Defining the Efficacy of Sperm Preparation Techniques. *J. Androl.* **1988**, *9*, 367–376, doi:10.1002/j.1939-4640.1988.tb01067.x.
6. Kashir, J.; Heynen, A.; Jones, C.; Durrans, C.; Craig, J.; Gadea, J.; Turner, K.; Parrington, J.; Coward, K. Effects of Cryopreservation and Density-Gradient Washing on Phospholipase C Zeta Concentrations in Human Spermatozoa. *Reprod. Biomed. Online* **2011**, *23*, 263–267, doi:10.1016/j.rbmo.2011.04.006.

7. Dobrinski, I. Intracellular Calcium Concentration in Equine Spermatozoa Attached to Oviductal Epithelial Cells in Vitro. *Biol. Reprod.* **1996**, *54*, 783–788, doi:10.1095/biolreprod54.4.783.
8. Felix, M.R.; Turner, R.M.; Dobbie, T.; Hinrichs, K. Successful in Vitro Fertilization in the Horse: Production of Blastocysts and Birth of Foals after Prolonged Sperm Incubation for Capacitation. *Biol. Reprod.* **2022**, *107*, 1551–1564.
9. Gibb, Z.; Clulow, J.R.; Aitken, R.J.; Swegen, A. First Publication to Describe a Protocol for the Liquid Storage of Stallion Spermatozoa for 7 Days. *J. Equine Vet. Sci.* **2018**, *66*, 37–40, doi:10.1016/j.jevs.2018.05.016.
10. Choi, Y.H.; Velez, I.C.; Riera, F.L.; Roldán, J.E.; Hartman, D.L.; Bliss, S.B.; Blanchard, T.L.; Hayden, S.S.; Hinrichs, K. Successful Cryopreservation of Expanded Equine Blastocysts. *Theriogenology* **2011**, *76*, 143–152, doi:10.1016/j.theriogenology.2011.01.028.
11. Wilsher, S.; Rigali, F.; Couto, G.; Camargo, S.; Allen, W.R. Vitrification of Equine Expanded Blastocysts Following Puncture with or without Aspiration of the Blastocoele Fluid. *Equine Vet. J.* **2019**, *51*, 500–505, doi:10.1111/evj.13039.
12. Hendriks, W.K.; Roelen, B.A.J.; Colenbrander, B.; Stout, T.A.E. Cellular Damage Suffered by Equine Embryos after Exposure to Cryoprotectants or Cryopreservation by Slow-Freezing or Vitrification: Cellular Damage Suffered by Equine Embryos during Cryopreservation. *Equine Vet. J.* **2015**, *47*, 701–707, doi:10.1111/evj.12341.
13. Tharasanit, T.; Colenbrander, B.; Stout, T.A.E. Effect of Cryopreservation on the Cellular Integrity of Equine Embryos. *Reproduction* **2005**, *129*, 789–798, doi:10.1530/rep.1.00622.
14. Pérez-Marín, C.C.; Vizuete, G.; Vazquez-Martinez, R.; Galisteo, J.J. Comparison of Different Cryopreservation Methods for Horse and Donkey Embryos. *Equine Vet. J.* **2018**, *50*, 398–404, doi:10.1111/evj.12777.
15. Wilsher, S.; Rigali, F.; Kovacsy, S.; Allen, W. (Twink) Successful Vitrification of Manually Punctured Equine Embryos. *Equine Vet. J.* **2021**, *53*, 1227–1233, doi:10.1111/evj.13400.
16. Claes, A.; Cuervo-Arango, J.; Broek, J.; Galli, C.; Colleoni, S.; Lazzari, G.; Deelen, C.; Beitsma, M.; Stout, T.A. Factors Affecting the Likelihood of Pregnancy and Embryonic Loss after Transfer of Cryopreserved in Vitro Produced Equine Embryos. *Equine Vet. J.* **2019**, *51*, 446–450, doi:10.1111/evj.13028.

17. Campbell, J.M.; Nottle, M.B.; Vassiliev, I.; Mitchell, M.; Lane, M. Insulin Increases Epiblast Cell Number of In Vitro Cultured Mouse Embryos via the PI3K/GSK3/P53 Pathway. *Stem Cells Dev.* **2012**, *21*, 2430–2441, doi:10.1089/scd.2011.0598.

18. Campbell, J.M.; Lane, M.; Vassiliev, I.; Nottle, M.B. Use of Insulin to Increase Epiblast Cell Number: Towards a New Approach for Improving ESC Isolation from Human Embryos. *BioMed Res. Int.* **2013**, *2013*, 1–7, doi:10.1155/2013/150901.

19. Kuijk, E.W.; van Tol, L.T.A.; Van de Velde, H.; Wubbolts, R.; Welling, M.; Geijsen, N.; Roelen, B.A.J. The Roles of FGF and MAP Kinase Signaling in the Segregation of the Epiblast and Hypoblast Cell Lineages in Bovine and Human Embryos. *Development* **2012**, *139*, 871–882, doi:10.1242/dev.071688.

20. Chazaud, C.; Yamanaka, Y.; Pawson, T.; Rossant, J. Early Lineage Segregation between Epiblast and Primitive Endoderm in Mouse Blastocysts through the Grb2-MAPK Pathway. *Dev. Cell* **2006**, *10*, 615–624, doi:10.1016/j.devcel.2006.02.020.

21. Fujikura, J.; Yamato, E.; Yonemura, S.; Hosoda, K.; Masui, S.; Nakao, K.; Miyazaki, J.; Niwa, H. Differentiation of Embryonic Stem Cells Is Induced by GATA Factors. *Genes Dev.* **2002**, *16*, 784–789, doi:10.1101/gad.968802.

22. Bertolini, M.; Beam, S.W.; Shim, H.; Bertolini, L.R.; Moyer, A.L.; Famula, T.R.; Anderson, G.B. Growth, Development, and Gene Expression by in Vivo- and in Vitro-Produced Day 7 and 16 Bovine Embryos. *Mol. Reprod. Dev.* **2002**, *63*, 318–328, doi:10.1002/mrd.90015.

23. Berg, D.K.; van Leeuwen, J.; Beaumont, S.; Berg, M.; Pfeffer, P.L. Embryo Loss in Cattle between Days 7 and 16 of Pregnancy. *Theriogenology* **2010**, *73*, 250–260, doi:10.1016/j.theriogenology.2009.09.005.

24. Loureiro, B.; Block, J.; Favoreto, M.G.; Carambula, S.; Pennington, K.A.; Ealy, A.D.; Hansen, P.J. Consequences of Conceptus Exposure to Colony-Stimulating Factor 2 on Survival, Elongation, Interferon-τ Secretion, and Gene Expression. *Reprod. Camb. Engl.* **2011**, *141*, 617–624, doi:10.1530/REP-10-0511.

25. Desmet, K.L.J.; Marei, W.F.A.; Richard, C.; Sprangers, K.; Beemster, G.T.S.; Meysman, P.; Laukens, K.; Declerck, K.; Vanden Berghe, W.; Bols, P.E.J.; et al. Oocyte Maturation under Lipotoxic Conditions Induces Carryover Transcriptomic and Functional Alterations during Post-Hatching Development of Good-Quality Blastocysts: Novel Insights from a Bovine Embryo-Transfer Model. *Hum. Reprod. Oxf. Engl.* **2020**, *35*, 293–307, doi:10.1093/humrep/dez248.

26. Ren, D.; Navarro, B.; Perez, G.; Jackson, A.C.; Hsu, S.; Shi, Q.; Tilly, J.L.; Clapham, D.E. A Sperm Ion Channel Required for Sperm Motility and Male Fertility. *Nature* **2001**, *413*, 603–609, doi:10.1038/35098027.

27. Cohen, R.; Buttke, D.E.; Asano, A.; Mukai, C.; Nelson, J.L.; Ren, D.; Miller, R.J.; Cohen-Kutner, M.; Atlas, D.; Travis, A.J. Lipid Modulation of Calcium Flux through CaV2.3 Regulates Acrosome Exocytosis and Fertilization. *Dev. Cell* **2014**, *28*, 310–321, doi:10.1016/j.devcel.2014.01.005.

28. Florman, H.M.; Jungnickel, M.K.; Sutton, K.A. Regulating the Acrosome Reaction. *Int. J. Dev. Biol.* **2008**, *52*, 503–510, doi:10.1387/ijdb.082696hf.

29. Breitbart, H.; Stern, B.; Rubinstein, S. Calcium Transport and Ca2+-ATPase Activity in Ram Spermatozoa Plasma Membrane Vesicles. *Biochim. Biophys. Acta BBA - Biomembr.* **1983**, *728*, 349–355, doi:10.1016/0005-2736(83)90505-9.

30. Rufo, G.A.; Schoff, P.K.; Lardy, H.A. Regulation of Calcium Content in Bovine Spermatozoa. *J. Biol. Chem.* **1984**, *259*, 2547–2552.

31. Dragileva, E.; Rubinstein, S.; Breitbart, H. Intracellular Ca2+-Mg2+-ATPase Regulates Calcium Influx and Acrosomal Exocytosis in Bull and Ram Spermatozoa1. *Biol. Reprod.* **1999**, *61*, 1226–1234, doi:10.1095/biolreprod61.5.1226.

32. Walensky, L.D.; Snyder, S.H. Inositol 1,4,5-Trisphosphate Receptors Selectively Localized to the Acrosomes of Mammalian Sperm. *J. Cell Biol.* **1995**, *130*, 857–869, doi:10.1083/jcb.130.4.857.

33. Pizzo, P.; Drago, I.; Filadi, R.; Pozzan, T. Mitochondrial Ca2+ Homeostasis: Mechanism, Role, and Tissue Specificities. *Pflüg. Arch. - Eur. J. Physiol.* **2012**, *464*, 3–17, doi:10.1007/s00424-012-1122-y.

34. Ho, H.-C.; Suarez, S.S. An Inositol 1,4,5-Trisphosphate Receptor-Gated Intracellular Ca2+ Store Is Involved in Regulating Sperm Hyperactivated Motility1. *Biol. Reprod.* **2001**, *65*, 1606–1615, doi:10.1095/biolreprod65.5.1606.

35. Ho, H.-C.; Suarez, S.S. Characterization of the Intracellular Calcium Store at the Base of the Sperm Flagellum That Regulates Hyperactivated Motility. *Biol. Reprod.* **2003**, *68*, 1590–1596.

36. Romarowski, A.; Sánchez-Cárdenas, C.; Ramírez-Gómez, H.V.; Puga Molina, L. del C.; Treviño, C.L.; Hernández-Cruz, A.; Darszon, A.; Buffone, M.G. A Specific Transitory Increase in Intracellular Calcium Induced by Progesterone Promotes Acrosomal Exocytosis in Mouse Sperm1. *Biol. Reprod.* **2016**, *94*, doi:10.1095/biolreprod.115.136085.

37. Hansen, P.J.; Tríbulo, P. Regulation of Present and Future Development by Maternal Regulatory Signals Acting on the Embryo during the Morula to Blastocyst Transition – Insights from the Cow. *Biol. Reprod.* **2019**, *101*, 526–537, doi:10.1093/biolre/ioz030.
38. Akizawa, H.; Saito, S.; Kohri, N.; Furukawa, E.; Hayashi, Y.; Bai, H.; Nagano, M.; Yanagawa, Y.; Tsukahara, H.; Takahashi, M.; et al. Deciphering Two Rounds of Cell Lineage Segregations during Bovine Preimplantation Development. *FASEB J.* **2021**, *35*, doi:10.1096/fj.202002762RR.

Chapter 7

Nederlandse samenvatting

Nederlandse samenvatting

Sinds het begin van de jaren ‘90 heeft de fokkerij van sportpaarden in Europa een technologische revolutie ondergaan. Oorspronkelijk werd de in de paardenfokkerij voornamelijk gewerkt met een natuurlijke dekking van de merrie door de hengst. Tegenwoordig is kunstmatige inseminatie (KI) van de merrie de norm. Het is mogelijk om gespoelde of in vitro geproduceerde (IVP) embryo’s over te zetten in draagmerries (via zogenaamde embryo transplantatie ofwel ET). Met KI en ET wordt een hoog drachtpercentage gerealiseerd. Hoewel deze nieuwere technieken veel voordelen bieden zoals besproken in de algemene inleiding, zijn er ook aanzienlijke nadelen. Zo bestaat er een grotere kans op een menselijke fout, waardoor er bijvoorbeeld schade kan ontstaan tijdens het behandelen en het bewaren opslaan van gameten of embryo’s. Bovendien worden bij deze meer complexe technieken, de natuurlijke processen omzeild, die betrokken zijn bij het selecteren van vruchtbare spermatozoa of eicellen. Momenteel is de intracytoplasmatische sperma-injectie (ICSI) de enige commerciële betrouwbare techniek voor het produceren van IVP paardenembryo's. ICSI, en in minder mate conventionele in vitro fertilisatie (IVF), omzeilen echter de natuurlijke sperma selectiemethoden die plaatsvinden tijdens het transport van spermatozoa door het vrouwelijke voortplantingsorgaan. In vitro sperma selectietechnieken zijn daarom een belangrijk onderdeel geworden van de ICSI- en IVF-procedures. Het is immers essentieel dat een eicel wordt bevrucht door een functioneel intacte spermacel. Alleen daardoor kan de bevruchte eicel zich verder ontwikkelen tot een gezond levend dier. De meest gebruikte technieken om spermacellen van 'hoge kwaliteit' te selecteren, zijn de swim-up techniek (SU), de microfluïdische sorterings techniek (MF) al dan niet in combinatie met een dichtheidsgradiënt-centrifugatie techniek (DGC). Zowel de SU als de MF selecteren de meest motiele spermacellen terwijl de DGC selecteert op goed gematureerde spermacellen (dat wil zeggen de spermacellen met de hoogste dichtheid).

Hoofdstuk 2 beschrijft de ontwikkeling van een aangepaste flotatie DGC-techniek met Opti-prep™ om spermacellen van hoge kwaliteit te selecteren van hengsten met verminderde vruchtbaarheid. Deze is in het bijzonder toegepast bij hengsten waar de spermacellen een hoog percentage met DNA-schade hebben. In een 3-laags systeem met 20% of 25% Opti-prep™ als bovenlaag, komen de morfologisch normale, progressief beweeglijke spermatozoa met intact DNA terecht in het grensvlak tussen de bovenste en middelste laag als gevolg van hun relatieve dichtheid, en komen na centrifugatie terecht in de bovenste laag..

Zowel de 20% als de 25% bovenlaag zijn geschikt voor het selecteren van hoge kwaliteit spermacellen uit een hengstensperma monster met een minder goede kwaliteit. De 20% Opti-prep™ is beter bruikbaar bij de verwerking van hengsten voor KI aangezien er bij de KI hogere spermacel-concentraties van belang zijn. Er komen namelijk meer spermacellen in de bovenlaag in vergelijking met de 25% Opti-prep™ . De 25% Opti-prep™ als bovenlaag blijkt juist weer bruikbaarder voor de selectie van hengstenspermacellen bij ICSI. Bij ICSI is niet het aantal geselecteerde spermacellen, maar alleen de allerhoogste selectie van een hoge kwaliteit van de spermacellen van belang. Bij de DGC van de 25% bovenlaag blijkt de aangepaste hogere centrifuge-stap (1000 *g*) geen toename te veroorzaken in de productie van reactieve zuurstofcomponenten (ROS) in het geselecteerde hengstensperma ten opzichte van de DGC van de 20% (1000 *g*) bovenlaag waar een lagere centrifugesnelheid wordt gebruikt.

In de paardenfokkerij is KI met verdund en gekoeld sperma de meest gebruikte voortplantingstechniek. Ondanks verbeteringen in spermaverwerkingsprotocollen en -verdunners, is het aanbevolen om de transport- of opslagtijden van verdund en gekoeld sperma te beperken tot 24-48 uur om een daling in de vruchtbaarheid er van te voorkomen. **Hoofdstuk 3** beschrijft onderzoek naar de veranderingen die plaats vinden in spermacellen van de hengst tijdens langdurige opslag (tot 96 uur bij 5°C). Naast de bepaling van spermakwaliteit met standaardparameters, zijn er ook met meer geavanceerde flowcytometrische analyses veranderingen in de activeringsstatus van de spermacellen bepaald. Een progressieve en totale beweeglijkheid van 35% van de spermacellen wordt als een minimum percentage gezien om een dracht tot stand te brengen. Deze waardes zijn in de meeste monsters geobserveerd na een bewaartijd van 72 en 96 uur. Het percentage levende, acrosoom-intacte spermacellen blijft hoog tot 96 uur, ondanks een afname in de bewegelijkheid. Dit kan enerzijds wijzen op een uitputting van metabole substraten die nodig zijn voor de beweeglijkheid, of anderzijds, op intracellulaire veranderingen die de flagellaire activiteit van spermatozoa verminderen. In de loop van de bewaartijd neemt het gehalte aan intracellulair Ca^{2+}-en de vloeibaarheid van de plasmamembraan toe. Daardoor neemt de populatie van levende, acrosoom-intacte spermacellen met een lage vloeibaarheid van de plasmamembraan en met een laag gehalte aan intracellulair Ca^{2+}-af.

Terwijl de selectie van genetisch superieure hengsten bespoedigd werd door alle geassisteerde voortplantingstechnologieën, is de selectie van waardevolle genetisch superieure merries aanzienlijk achtergebleven door gebrek aan de mogelijkheid op selectie van eicellen en embryo's. De embryo- en eiceltechnologieën zijn pas veel later ontwikkeld

voordat ze commercieel levensvatbaar werden. Hoewel ET sinds 2000 steeds populairder is geworden, is een wijdverspreide implementatie van selectie op eicellen en embryo's van het paard om verschillende redenen beperkt: Er zijn problemen bij het ontwikkelen van behandelingen die een meervoudige follikelontwikkeling en ovulatie induceren bij merries. Er zijn ook problemen bij het betrouwbaar invriezen van gespoelde embryo's uit de merrie. Ten derde, blijkt het invriezen van grote (>300 μm in diameter) geëxpandeerde blastocysten -die normaal gespoeld worden uit de uterus van merries op dag 7 of 8 na de ovulatie- , een uitdaging. De glycoproteïne capsule die dit soort blastocysten omringt, de lagere volume-oppervlakte verhoudingen van deze blastocysten alsmede het relatief grote vloeistof volume in de blastocoel zijn factoren die een potentieel negatieve invloed hebben op het invriezen van de grotere, gespoelde embryo's. Desondanks, zijn de afgelopen jaren grote, gespoelde geëxpandeerde blastocysten zowel zonder als na de verwijdering van de blastocoel-vloeistof met succes gevitrificeerd. Hoewel het langzaam invriezen van kleinere paardenembryo's minder schadelijk lijkt te zijn dan vitrificatie ervan, is er geen informatie beschikbaar over het succes van het langzaam invriezen van grote gespoelde geëxpandeerde blastocysten na punctie en aspiratie van het blastocoel vloeistof. **Hoofdstuk 4** beschrijft de vergelijking van de embryo kwaliteit na het langzaam invriezen met die van na het vitrificeren. Eerst is uit de grotere gespoelde blastocysten het blastocoelvocht verwijderd, waarna ze ofwel langzaam ofwel door vitrificatie werden ingevroren. Over het algemeen is, na het ontdooien, de embryo kwaliteit van deze grotere blastocysten slechter na langzaam invriezen dan na vitrificatie. Ondanks de verwijdering van een groot deel van de blastocoelvloeistof (≥85%), zijn de resultaten verkregen na het langzaam invriezen teleurstellend en mogelijk het gevolg van een suboptimale afkoelingscurve (-0,5 °C/min).

Bij IVP embryo's is het een vereiste dat het blastocyst stadium wordt bereikt en ook accuraat bepaald kan worden. De draagmerries die in het juiste en optimale hormonale stadium na de ovulatie zijn, worden voor de toepassing van ET geselecteerd. Ingevroren IVP blastocysten worden ontdooid en in de geselecteerde draagmerrie geplaatst. Na een week kan worden gemeten of deze blastocysten zich verder ontwikkeld hebben tot embryonale vrucht-blaasjes die vergelijkbaar zijn met de vruchtblaasjes van een natuurlijke dracht bij ongeveer 11 of 12 dagen. Echter de IVP blastocysten waren slechts ontwikkeld tot een stadium vergelijkbaar met dag 5-6 van in vivo embryo's. Dit suggereert een heel ander tijdsverloop van vroege embryonale ontwikkeling na IVP en ET in vergelijking tot een dracht na inseminatie met hengstensperma, althans tot aan de eerste cellijn segregatie. Tijdens deze

eerste cellijn segregatie differentiëren embryonale cellen in trofectoderm (TE; expressie van CDX-2) en een binnenste celmassa (ICM). Tevens gaat dit gepaard gaan met de vorming van de blastocoel of blastocyst-holte. Kort daarna (bij de tweede cellijn segregatie) gaat de ICM verder differentiëren in epiblast (EPI, pluripotente cellen; expressie van SOX-2) en primitief endoderm (PE; expressie van GATA-6). **Hoofdstuk 5** beschrijft de expressie van cellijn markers (CDX-2, SOX-2 en GATA-6) in zowel in vivo als IVP embryo's op het moment dat ze een blastocoel gaan ontwikkelen. Er zijn duidelijke verschillen tussen in vivo en in vitro blastocysten met betrekking tot de distributie van cellen die de verschillende markers tot expressie brengen met name in de SOX-2 en GATA-6 expressie. De verdeling van de markers was vrij uniform op dag 7 in de in vivo blastocysten waar TE, EPI en PE elk de te verwachten specifieke markers (respectievelijk CDX-2, SOX-2 of GATA-6) tot expressie brachten. De afbakening van cellen die SOX-2 en GATA-6 tot expressie brachten bleek veel minder duidelijk bij de IVP blastocysten die overigens ook 7 of 9 dagen nodig hadden om zich te ontwikkelen tot het blastocyst stadium. De vermoedelijke EPI-cellen zijn meer verspreid in dag 7 IVP blastocysten dan in vivo blastocysten, en deze meer diffuse distributie iss zelfs nog prominenter aanwezig in de IVP embryo's die 9 dagen nodig hadden om het blastocyst stadium te bereiken. De verschillen in de distributie van cellen die de verschillende markers tot expressie brengen tussen de in vivo en de in vitro geproduceerde embryo's, suggereren dat de huidige in vitro kweeksystemen suboptimaal zijn voor het ondersteunen van de cellijn differentiatie tijdens de vroege embryonale ontwikkeling. Een ondersteuning hiervoor komt uit het experiment waarin dag 7 IVP blastocysten twee extra dagen gekweekt werden, ofwel in vitro, ofwel in vivo (dus na overplaatsing naar de uterus van een draagmerrie). IVP embryo's die in de uterus zijn overgezet lijken meer op in vivo geëxpandeerde blastocysten en hebben een duidelijk afgebakende en compacter EPI. Daarentegen vertonen IVP embryo's die twee dagen extra in vitro werden gekweekt geen veranderingen in de distributie van cellen die SOX-2 en GATA-6 tot expressie brengen. Tevens is de afstand tussen de EPI-cellen groter dan bij blastocysten die twee extra dagen in de uterus waren geplaats. Het is daarom duidelijk dat in vitro omstandigheden nog niet optimaal zijn voor de ontwikkeling van paardenembryo's. Deze suboptimale condities leiden tot vertragingen in embryonale ontwikkeling en afwijkingen in de cellijn segregatie.

Toekomstperspectieven

In spermacellen worden de intracellulaire Ca^{2+} concentraties gereguleerd door verschillende processen waaronder de influx en efflux van Ca^{2+} en de regulering van de intracellulaire

Ca^{2+} voorraden. CatSper, het sperma specifieke Ca^{2+} kanaal en andere Ca^{2+} kanalen regelen de calcium instroom. Ca^{2+} ATPase en de Na^{+}/Ca^{2+} wisselaar in de plasmamembraan reguleren de Ca^{2+} influx en efflux. Bovendien reguleren Ca^{2+} -ATPase en IP3-R, gelegen in het buitenste acrosomale membraan, de mobilisatie van intracellulair Ca^{2+} en nemen ook deel aan Ca^{2+} instroom en efflux over het acrosoom membraan. De Ca^{2+} opname en afgifte wordt ook gereguleerd door de mitochondriën van de spermacel. Het overgebleven gedeelte van de kernenveloppe in de nek van de spermacel dient als een extra Ca^{2+}opslag en bevat ook IP3-R. Het handhaven van nauwkeurige intracellulaire Ca^{2+} concentraties is belangrijk voor de beweeglijkheid, de capacitatie en de acrosoom-reactie van spermatozoa. Langdurige opslag van hengstensperma op 5°C veroorzaakt een toename van intracellulair Ca^{2+} die omgekeerd gecorreleerd is met progressieve en totale beweeglijkheid (**hoofdstuk 3**). Het zou interessant zijn om in de toekomst te onderzoeken of er een mechanisme is dat in staat is lage intracellulaire Ca^{2+} concentratie te handhaven tijdens de langere opslag van hengstensperma. Het is daarbij van belang om de veranderingen in intracellulaire Ca^{2+} alleen te volgen in levende spermacellen met behulp van imaging technologieën die al toegepast zijn om de intracellulaire calcium concentratie te visualiseren in levende muizen spermacellen.

De afwijkingen in de tweede cellijn segregatie, zoals waargenomen in IVP paardenembryo's en dan met name het uitblijven van de aggregatie van EPI cellen, kan worden voorkomen door een kort verblijf van de IVP embryo in de baarmoeder van een draagmerrie. Dit suggereert het belang van baarmoederfactoren bij het stimuleren van de tweede cellijn segregatie. Het zou daarom interessant zijn om in vitro modellen te ontwikkelen die gebruik maken van endometriumcellen om een meer normale pre-implantatieontwikkeling van IVP-paardenembryo's te verkrijgen. Een alternatieve benadering zou zijn om groeifactoren en embryokines te vinden in het endometrium van de merrie die betrokken zijn bij de vroege ontwikkeling van paardenembryo's (tot dag 7 na de ovulatie). Dit zou o.a. kunnen door het expressiepatroon van kandidaat genen van embryokines in de eileider en het endometrium te bestuderen. Bij runderen zijn de insuline-achtige groeifactor 1 en de koloniestimulerende factor 2 die in de literatuur zijn voorgesteld als belangrijke embryokines die de ontwikkeling van het embryo moduleren en stimuleren. Deze factoren kunnen tevens een rol spelen in EPI-specificatie en -organisatie. Het testen en identificeren van endometriumfactoren, die fungeren als embryokines voor paardenembryo's, zou tot een verbetering kunnen leiden in de kweekomstandigheden waarin in vitro geproduceerde paardenembryo's meer zouden kunnen gaan lijken op in vivo embryo's. Tevens zou dit ook langdurige in vitro kweek van

embryo's (>10 dagen) mogelijk maken om andere gebeurtenissen (embryonale schijfvorming en gastrulatie) in embryonale ontwikkeling in vitro te bestuderen. Bij runderen zijn embryo's gedurende 14 dagen in vitro gekweekt op een gel om de cellijn segregatie beter te bestuderen en om kennis te verwerven in de regulatie van deze kritieke processen.

Kortom, er is aanzienlijke vooruitgang geboekt op het gebied van moderne voortplantingstechnologieën in de paardenfokkerij. Hoewel veel van de technieken redelijk goed beginnen te werken, is er ruimte voor verbetering in efficiëntie, gebruiksvriendelijkheid van deze technieken. Uiteindelijk zal de ontwikkelingscompetentie van de embryo's geproduceerd met deze technieken verbeteren. Het in dit proefschrift beschreven onderzoek geeft aan waar al verbetering is bereikt, maar geeft ook aan waar toekomstig onderzoek tot verdere optimalisatie zou kunnen leiden.

Appendices

Acknowledgements

In the Name of **ALLAH**, the Most Beneficent and the Most Merciful. I thank **ALLAH** for making my dream come true. During my PhD journey, many people played a significant role by helping and supporting me. I was lucky to have such a support from great people to make this thesis a reality.

I am proud and grateful to have you, **Professor Dr. Tom Stout**, **Dr. Anthony Claes** and **Dr. Marta de Ruijter-Villani**, as my supervisors. Thank you, Prof. Tom, for being critical, and for your kind comments and suggestion throughout my research and writing phase. Despite the limitations, I learnt a lot from you in the clinics. **Dr. Anthony**, thank you for being there and for your support. You always sparked courage in me and thank you for believing in me that I can do all those things. Thank you for teaching me all the research related stuff as well as about the clinical procedures. I really enjoyed our friday meetings and discussions about the research projects. I am really grateful and proud to have you as one of my teachers. **Dr. Marta**, thank you so much for your help and support to make my research and data analyses complete. Thank you for your help in streamlining the staining protocols, imaging and image analyses. I also thank **Dr. Heiko Henning** for supervising and helping me in my early years. I was really lucky to have such an amazing scientist and problem solving person around me. I know, I am short of words to describe how proud and grateful I am to have you all along my journey, and I really enjoyed working with you. I learnt a lot from all of you.

I am grateful to the horse reproduction clinics team for their help and support. Thank you, Soledad, Bart, Leonie, Jon, Wilbert and Esther, for all the help. It was always an immense joy to collaborate with you all and have a small chat. Specially, I always enjoyed the clinics day out and other fun activities with the whole team. I equally thank to the horse reproduction lab team, **Mabel**, **Claudia** and **Ainhoa**, for all the help and support in lab activities.

I am also thankful to the Farm Animal Health team, **Dr. Hilde**, **Leni**, **Christine** and **Kaylee** for their help and support. **Arend**, thank you for all the help during my research and it was always a boundless joy to have a discussion with you about research and other aspects of life. Thank you for your help in practicing the Dutch. I am also thankful to **Dr. Bart Gadella** for the discussion and suggestions about my research projects.

Over the years, I came to know a lot of people with whom I shared my office. I am grateful that I met so many wonderful young researchers over the years. **Nadia**, **Maxime**, **Jonna**, **Jiayi**, **Marleen** and many more, I thank you all for the great moments and chats in our office.

Richard and **Esther**, Thank you for your help and support during the confocal microscopy session and analyses.

I thank the Pakistani community here, specially, **Adnan** and **Ishtiaq** families for their support and help. I am also grateful to have wonderful **friends** back home in **Pakistan**, who are an important part of my life. **Rafi ullah**, **Zeeshan**, **Asher**, **Mohtashim**, **Tayyab**, **Ahmad**, **Ahsan**, **Zarak**, **Tahseen**, **Abdul Bari** and many more. I also thank **Mr. Henk** for being a nice landlord.

In the end, I am thankful to my **parents (Muhammad Zafar Ayub Khan and Khadija Zahra)** and **siblings (Hina Khan, Usman Khan and Sana Khan)** for the unconditional support and love. Without your support and prayers, it would have been difficult to go to a totally different country and pursue my dream.

About the author

Muhammad Umair was born on 14th of August 1990 in Muzaffargarh, Punjab province, Pakistan. After completing his basic education in Muzaffargarh, he started his undergraduate study as a DVM student in 2009 at the University of Veterinary and Animal Sciences (UVAS), Lahore, Punjab province, Pakistan. He obtained his DVM degree in 2014 and started his Master of Philosophy (M.Phil.) in theriogenology at Department of Theriogenology of UVAS in the same year. In his M.Phil., he did research on equine semen under the supervision of Dr. Mushtaq Ahmad and completed his M.Phil. in 2016. In 2018, he obtained a 4-year PhD scholarship from Punjab Educational Endowment Fund (PEEF), Punjab province, Pakistan and started his PhD under the supervision of Prof. Dr. Tom A.E. Stout, Dr. Anthony Claes and Dr. Marta Ruijter-Villani at the Department of Clinical Sciences, Faculty of Veterinary Medicine, Utrecht University, The Netherlands.

List of Publications

1.Umair, M.; Henning, H.; Stout, T.A.E.; Claes, A. A Modified Flotation Density Gradient Centrifugation Technique Improves the Semen Quality of Stallions with a High DNA Fragmentation Index. *Animals* **2021**, *11*, 1973. https://doi.org/10.3390/ani11071973

2.Umair, M, Claes, A, Buijtendorp, M, Cuervo-Arango, J, Stout, TAE, Henning, H. In vitro aging of stallion spermatozoa during prolonged storage at 5°C. *Cytometry*. 2023; 103(6): 479– 491. https://doi.org/10.1002/cyto.a.24712

3.Umair M, Beitsma M, de Ruijter-Villani M, Deelen C, Herrera C, Stout TAE, Claes A. Vitrifying expanded equine embryos collapsed by blastocoel aspiration is less damaging than slow-freezing. Theriogenology. 2023 May;202:28-35. doi: 10.1016/j.theriogenology.2023.02.028. Epub 2023 Mar 2. PMID: 36893660.

4.Umair M, Scheeren VFDC, Beitsma MM, Colleoni S, Galli C, Lazzari G, de Ruijter-Villani M, Stout TAE, Claes A. In Vitro-Produced Equine Blastocysts Exhibit Greater Dispersal and Intermingling of Inner Cell Mass Cells than In Vivo Embryos. Int J Mol Sci. 2023 Jun 1;24(11):9619. doi: 10.3390/ijms24119619. PMID: 37298570; PMCID: PMC10253440.

Conference abstracts

1. M Umair, M Beitsma, MD Ruijter-Villani, C Deelen, TAE Stout, A Claes, Slow-freezing is more damaging than vitrification to post-thaw quality of large equine embryos collapsed by blastocoele aspiration, Journal of Equine Veterinary Science, Volume 113, 2022, 103975, ISSN 0737-0806, https://doi.org/10.1016/j.jevs.2022.103975.
2. Muhammad Umair, Anthony N Claes, Verônica F da Cunha Scheeren, Mabel M Beitsma, Silvia Colleoni, Cesare Galli, Giovanna Lazzari, Marta de Ruijter-Villani, Tom A Stout, In vitro produced equine blastocysts exhibit dispersed ICM cell allocation, Journal of Equine Veterinary Science, Volume 125, 2023, 104681, ISSN 0737-0806, https://doi.org/10.1016/j.jevs.2023.104681.

Oral presentation

1. M Umair, M Beitsma, MD Ruijter-Villani, C Deelen, TAE Stout, A Claes, Slow-freezing is more damaging than vitrification to post-thaw quality of large equine embryos collapsed by blastocoele aspiration, 10th International Symposium on Equine Embryo Transfer and Technology (ISEET), Pisa, Italy.